Theoretical Design and Synthesis of Donor-Acceptor Conjugated Polymers for Photovoltaic and NLO Applications

Thesis submitted to

Cochin University of Science and Technology

in partial fulfilment of the requirements

for the award of the degree of

Doctor of Philosophy

in

Chemistry

Under the Faculty of Science

by

Jiby K. Gopinath

Department of Applied Chemistry

Cochin University of Science and Technology

Kochi – 22

July 2015

Theoretical Design and Synthesis of Donor-Acceptor Conjugated Polymers for Photovoltaic and NLO Applications

Ph.D. Thesis under the Faculty of Science

By

Jiby K. Gopinath
Research Fellow
Department of Applied Chemistry
Cochin University of Science and Technology
Kochi, India 682022
Email: jibyapril19@gmail.com

Supervising Guide

Dr. K. Sreekumar
Professor
Department of Applied Chemistry
Cochin University of Science and Technology
Kochi, India 682022
Email: drsreekumar@gmail.com

Department of Applied Chemistry
Cochin University of Science and Technology
Kochi, India 682022

July 2015

DEPARTMENT OF APPLIED CHEMISTRY
COCHIN UNIVERSITY OF SCIENCE AND TECHNOLOGY
KOCHI - 682022, INDIA

Dr. K. Sreekumar
Professor

Ph: 9447121530
E-mail: drsreekumar@gmail.com

Date: 30th July 2015

Certificate

This is to certify that the thesis entitled **"Theoretical Design and Synthesis of Donor-Acceptor Conjugated Polymers for Photovoltaic and NLO Applications"** submitted for the award of the Doctor of Philosophy of the Cochin University of Science and Technology, is a record of original research work carried out by Ms. Jiby K. Gopinath under my supervision and guidance in the Department of Applied Chemistry, Cochin University of Science and Technology, Kochi and further that it has not formed the part of any other thesis submitted previously for the award of any other degree/diploma.

Dr. K. Sreekumar
(Supervising Guide)

Declaration

I hereby declare that the thesis entitled **"Theoretical Design and Synthesis of Donor-Acceptor Conjugated Polymers for Photovoltaic and NLO Applications"** submitted for the award of the Ph. D Degree, is based on the original research work done by me under the guidance of Dr. K. Sreekumar, Professor, Department of Applied Chemistry, Cochin University of Science and Technology and further that it has not previously formed the basis for the award of any other degree.

Kochi-22
30/07/2015

Jiby K. Gopinath

Acknowledgement

Let me humbly express my heartful thanks to Dr. K. Sreekumar, my guide for his invaluable guidance, wise advises, constant encouragement and constructive criticism during my research work. Without his compassion, this thesis would not have materialized. I am highly thankful to Dr. N. Manoj, HOD, Department of Applied Chemistry and Dr. K. Girish Kumar, Former HOD, Department of Applied Chemistry for rendering all the necessary facilities for the research work. I am also grateful to Dr. P. V. Mohanan, my doctoral committee member, DAC, CUSAT for his support during this study. I record my sincere thanks to all the faculty members and non-teaching staff of the department for their timely help and co-operation during my research work.

I wish to express my sincere thanks to Dr. K. P. Vijayakumar, Department of Physics, CUSAT for allowing me to do photovoltaic studies in his lab. My special thanks to the Director, International School of Photonics, CUSAT for the Nonlinear Optical studies.

My heartful thanks to Dr. Mahesh Kumar and Ms. Sona Narayanan for helping me in solving Computational chemistry problems and also for their timely help during the last stages of my research work. I whole heartedly thank Mr. Mathew and Mr. Nideep, ISP, CUSAT for helping me to carryout NLO measurements. My sincere gratitude to Tittu, Department of Physics, for the Photovoltaic studies of the polymers. My heartful thanks to Anuja, Unni and Ammu, Analytical lab, for the Cyclic Voltammetric studies. I hereby acknowledge SCTIMST, Thiruvananthapuram and Remya, Department of Polymer Science and Rubber Technology, CUSAT for GPC Analysis of the polymers.

I always cherish the sincere support and warm friendship of my former colleagues, Dr. Rajesh Krishnan, Dr. Kannan, Dr. Mahesh Kumar, Dr. Anoop,

Dr. Mangala and Dr. Elizabeth. I am so grateful to all my labmates Ms Sherly, Ms. Smitha, Ms. Sinija, Ms. Anjali, Ms. Jisha, Ms. Sowmya Xavier, Ms. Anjaly Jacob, Ms. Jaimy, Ms. Letcy, Ms. Shaibuna for rendering their helping hand during difficult times and for their sincere friendship. I am really thankful to Dr. Priya and Dr. Navya for their valuable friendship and love.

My dear friends Dr. Reny, Dr. Cimi, Dr. Vidhya and Dr. Sandhya deserve special mention for their motivating friendship and moral support during the research days. I express my sincere thanks to Dr. Sandhya, Dr. Reshma, Ms. Bhavya, Dr. Laina, Ms. Soumya (AC), Ms. Divya, Ms. Jessica, Ms. Shanty, Ms. Bindu, Ms. Sneha , Ms. Honey, Ms. Soumya (PC) for their valuable friendship and support. I would like to thank all my friends in the Department of Applied Chemistry, Department of Physics and Department of Polymer Science and Rubber Technology for their help and care. I would like to acknowledge DST, (PURSE) and CUSAT for providing the financial support to carry out my research work. I am also thankful to Dr. Shibu, Dr. Adarsh and Mr. Saji, SAIF-STIC, CUSAT, for all Spectral analysis.

I am truly indebted to my loving parents, my brother Jini and his family for their love, prayers, patience and support. Words fall short in expressing my thanks to Binoj, my beloved husband, for his love, care, and inspiration. Without his constant support, this Ph. D. thesis would never be realized. At this moment, I remember with gratitude his entire family members for their whole hearted support to achieve this goal in my life.

Above all, I thank god for giving me this wonderful opportunity to do research.

Jiby. K. Gopinath

Preface

Polymers with conjugated π-electron backbone display unusual electronic properties such as low energy optical transition, low ionization potentials, and high electron affinities. The properties that make these materials attractive include a wide range of electrical conductivity, mechanical flexibility and thermal stability. Some of the potential applications of these conjugated polymers are in sensors, solar cells, field effect transistors, field emission and electrochromic displays, super-capacitors and energy storage. With recent advances in the stability of conjugated polymer materials, and improved control of properties, a growing number of applications are currently being explored. Some of the important applications of conducting polymers include: they are used in electrostatic materials, conducting adhesives, shielding against electromagnetic interference (EMI), artificial nerves, aircraft structures, diodes, and transistors.

Major objectives of the present study are:

1) Design of donor- acceptor low band gap polymers for photovoltaic and NLO applications using Density Functional Theory in the periodic boundary condition (PBC) formalism.
2) Synthesis of the designed polymers using direct arylation and Suzuki Coupling methods.
3) Explore the application of the conjugated polymers as active layer in photovoltaic devices.
4) Explore the third order NLO properties of the conjugated polymers.

The thesis is divided into six chapters

First chapter gives an idea about the fundamentals of conducting polymers, computationally driven material design of polymers, few polymerisation techniques used to synthesise conducting polymers, and about the basics of photovoltaics and Nonlinear optics.

Second chapter describes the synthesis and characterisation of monomers which are used for preparing the desired polymers. Detailed description of experimental procedures are also presented.

Third chapter is about the use of quantum chemical tools for the theoretical studies of the electronic and structural properties of monomers and polymers. On the basis of donor-acceptor strength of the monomers, polymers are designed and the electronic structure and band gap of these designed polymers are evaluated.

Fourth chapter describes the synthesis of the designed polymers via Suzuki and Direct arylation methods and the polymers are characterised by UV-Vis, NMR, PL Spectroscopic techniques, TG/DTG and Cyclic Voltammetry techniques. Detailed synthetic procedures and characterisation data are also mentioned in this chapter.

Fifth chapter is about the Photovoltaic and NLO applications of the synthesised polymers. Summary and conclusion of the work done is presented in the **sixth chapter.** References are given at the end of each chapter.

Contents

.....ꕥ.....

Chapter 1

INTRODUCTION

Contents

1.1 Introduction

Over the past few decades, research on π-conjugated systems has rapidly grown as a broad multidisciplinary field, and has progressively generated a rich synthetic chemistry in the more general context of functional π-conjugated systems. The real breakthrough in the field of conjugated organic conducting polymers took place after the discovery of metallic conductivity in crystalline polyacetylene films with dopants such as halogens during the collaborative research involving Shirakawa, MacDiarmid and Heeger in 1977.[1,2] As a class of materials, conducting polymers share several characteristics, including macromolecular character and electrical transport properties and found wide range of applications such as in

chemical and bio-sensors, field-effect transistors, light emitting devices, solar cells, super capacitors, actuators and separation membranes, etc.[3-11]

In the eighties, main goal in the field of conducting polymers was the addition of new properties such as solubility, hydrophilicity, or molecular recognition to the inherent electronic, optical or electrochemical properties. With the emergence of the concept of ''plastic, soft or flexible electronics,'' π-conjugated systems are no longer viewed as bulk materials which are produced on a massive scale. They are considered as organic semiconductors synthesized and employed at a much smaller scale. This has generated a quite different view of the chemistry of functional π-conjugated systems. The control and manipulation of quantities such as absorption and emission spectra, oxidation and reduction potentials or luminescence efficiency have become the new priority targets.[12]

To explain the electronic phenomena in these organic conducting polymers, new concepts including solitons, polarons and bipolarons have been proposed by solid state physicists. The bulk conductivity of conducting polymers should, in principle, consist of contributions from intra-chain, inter-chain and inter-domain electron transportations. Other factors include the orientation, crystallinity and purity of the conjugated polymers.[13]

Eventhough the process of doping enhances the conductivity in conjugated polymers; this itself is often the source of their chemical instability and poor processability. The possible elimination of doping in

preparing conducting polymers, while, still achieving high conductivity, is one of the original motivations for the need of low band gap polymers which are intrinsic conductors of electricity.[14-17] Various strategies are used for the band structure engineering of polymers like Ladder polymerisation (Fig 1.1), Copolymerisation, Donor-Acceptor polymerisation etc. Donor-Acceptor polymerisation technique provides a successful route in designing low band gap electrically conducting polymers. Various novel D-A polymers differing in the electron donating and electron accepting moieties have been successfully designed and investigated and are used as active layer in photovoltaic applications.[18]

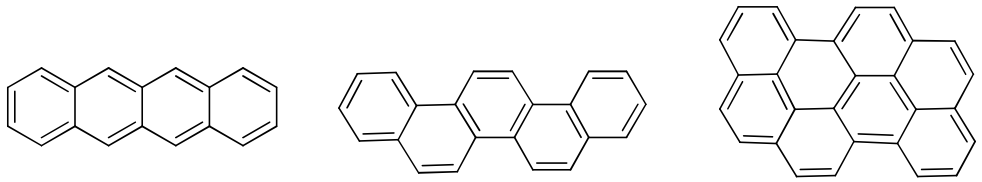

Fig. 1.1: Examples for Ladder polymers (a) polyacene, (b) polyphenanthrene, (c) polyacenacene

The methods of polymerisation also have profound effect on the conductivity of polymers. The methods are mainly divided into electrochemical and chemical polymerisations. The most common mechanism in electropolymerisation is that oligomers are formed in the close vicinity of the electrode and are deposited on the electrode. High molecular weight is obtained with monomers having large alkyl chains and are more highly

soluble and consequently have higher intermolecular conductivity. Stacking is partly prevented by the presence of large alkyl substituents. Unfortunately, lower stacking results in lower intermolecular conductivity. Hence there should be an optimal degree of substitution and size of substituents[19] (Fig 1.2).

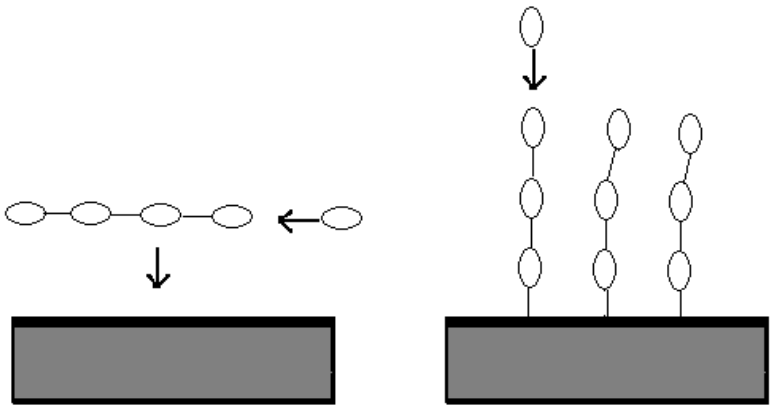

Fig. 1.2: Two mechanisms of electropolymerisation. (A) Deposition of oligomers on the electrode surface; (B) Growth of polymer chains on the surface.

The present thesis focuses on the theoretical design and synthesis of donor-acceptor conjugated polymers, their characterisation and applications in photovoltaic and third order nonlinear optics. This is motivated mainly by their promise of low cost, less toxic preparation methods and tunable optical properties. It was experimentally demonstrated and theoretically understood that many conjugated polymers possess extremely high third-order optical nonlinearity for various photonic applications like all-optical switching, image recognition, and optical limiting.[20-30]

1.2 Theoretical methods

Computationally driven molecular design has attracted increasing amount of research interest to accelerate the search for low band gap materials. This technique helps to explore new methodologies in pushing the efficiency further towards the theoretical limit. It is used to model a molecular system suitable for the intented use, prior to synthesizing that molecule in the laboratory and are often good enough to rule out unsuitable materials before synthesis. This is very useful, because, synthesizing a polymer could require months of labor and raw materials, and generate toxic waste. This method will provide valuable guidance and methodology for judicious material design of conjugated polymers for various applications with desirable macromolecular and electronic characteristics.[31]

A number of quantum chemical methods are available to determine the total energy to predict molecular structures such as *Ab initio* methods, Density functional methods, Semi-empirical and empirical methods, molecular mechanics, methods for solids, chemical dynamics and molecular dynamics. Among these methods, DFT is the most popular and versatile method available in Condensed-Matter Physics, Computational Physics, and Computational Chemistry. In the past, band gaps have been found by calculating the energy gaps of increasing oligomer lengths (n), then plotting the reciprocal oligomer length (1/n) as a function of the HOMO-LUMO gap (in eV) which require multiple calculations. Now PBC-DFT method is used

to find out the optimized geometry and electronic states of the polymers in single calculation in Guassian 09 quantum chemical codes.

Periodic Boundary Condition (PBC) has got several advantages when compared to the convensional 1/n method

a) It treats the polymer as a one-dimensional unit cell and calculations converge to find the lowest energy state and HOMO/ LUMO values

b) The major advantage of PBC is one calculation versus multiple calculations required for the 1/n method and as a result, calculation time could be saved compared to the 1/n method

c) Band gaps calculated by PBC-DFT method are in good agreement with experimental data.[32]

In order to get good agreement with experimental data, hybrid exchange correlation functional and 6-31G basic set was widely used. Recently Zhuang et al performed a systematic DFT and TD-DFT study on heteroatom effects of fluorene, nitrogen and chalcogen substitutions onto the donor and acceptor moieties of a thiophene-quinoxaline alternating polymer. They aimed to get an idea about how structural modifications to the conjugated backbone like the effect of extending pi-conjugation in the donor moiety can affect the molecular structure and electronic properties of a conjugated polymer.[33]

In another work, Bryan et al investigated the band structure and electronic properties of a series of vinylene-linked organic polymers by utilizing hybrid functionals with fully periodic boundary conditions (PBC) in conjunction with bond length alteration (BLA) and nucleus-independent chemical shift (NICS) calculations. Their results strongly emphasize that increasing the aromaticity of the polymer backbone does not ensure a low band gap. Instead, the destabilization of the ground state in the parent polymer towards the aromatic ↔ quinoidal level-crossing is a more effective way of lowering the band gap in conjugated systems[34] (Fig 1.3).

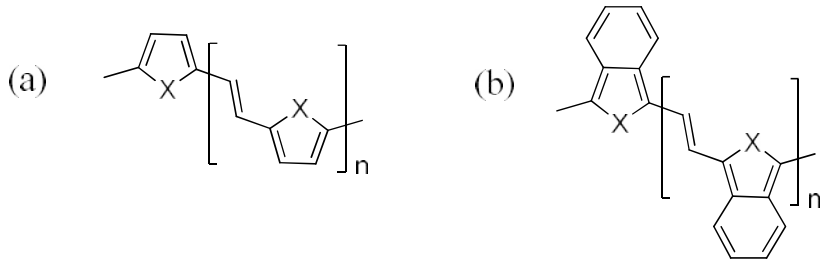

X = BCH_3, CH_2, NH, O, Se, PH_3, PCH_3O, SiH_2

Fig. 1.3: (a) Five-membered heterocyclic polymers and (b) benzannulated heterocyclic polymers. Here, vinylene linkage groups connect adjacent monomer units along the backbone chain.

On the basis of preliminary DFT calculations, Kamila et al designed and synthesised two xanthene based polymers, (2,7-bis(thiophen-2-yl)-9,9-dimethyl xanthene (a) and 2,7-bis(3-hexylthiophen-2-yl)-9,9-dimethylxanthene (b) that show a high degree of planarity. Electrochromism was observed for both polymers. The experimental data supported by density functional theory

modeling explain the influence of alkyl chain substitution on the properties of the investigated copolymers[35] (Fig 1.4).

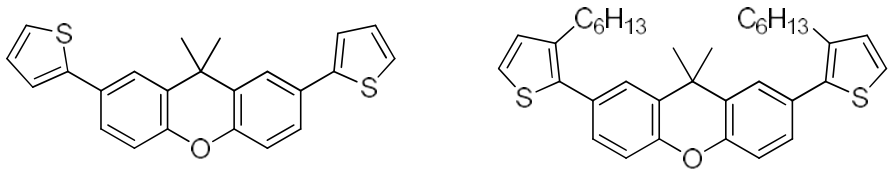

(a) (b)

Fig 1.4: Structure of 2,7-bis(thiophen-2-yl)-9,9-dimethylxanthene and 2,7-bis (3-hexylthiophen-2-yl)-9,9-dimethylxanthene

It was found that Heyd-Scuseria-Ernzerhof (HSE06) functional incorporating a screened Hartree Fock interaction is more computationally effective than the traditional hybrid functional B3LYP. [36, 37] In the present work, we have used B3LYP and HSE06 in combination with 6-31G basis set for calculating the optimized structure and electronic properties of D-A conjugated polymers.

1.3 Synthesis of conjugated polymers

Conjugated polymers are gaining a lot of interest due to their inherent functional properties and applications in plastic electronics. As a result, the number of synthetic methods for producing conducting polymers is continuously increasing. In addition to electrochemical[38-40] or chemical oxidative polymerizations,[41] transition metal-catalyzed cross-coupling reactions provide a particularly powerful synthetic strategy for Csp^2-Csp^2 and Csp-Csp^2 bond formation.[42] The most commonly employed transition-metal

catalysts are nickel or palladium based complexes. Palladium-catalyzed cross-coupling reactions are often used for conjugated polymer synthesis, including the Heck[43], Negishi[44], Stille[45], and Suzuki[46] coupling reactions. In 2010, the Nobel Prize in Chemistry was awarded jointly to Richard F. Heck, Ei-ichi Negishi and Akira Suzuki for their work on palladium-catalyzed cross-couplings in organic synthesis. Some of the coupling reactions are explained with examples.

1.3.1 Sonogashira coupling

The Sonogashira reaction is a cross-coupling reaction which employs a palladium catalyst to form a carbon–carbon bond between a terminal alkyne and an aryl or vinyl halide. Typically, the reaction requires anhydrous and anaerobic conditions, but new procedures have been developed where these restrictions are not important.

L. B. Sessions et al[47] synthesized alkyne-functionalized polymers and block copolymers by post polymerization modification of poly(4-bromostyrene) (PBrS) via palladium-catalyzed coupling with terminal alkynes (Scheme 1).

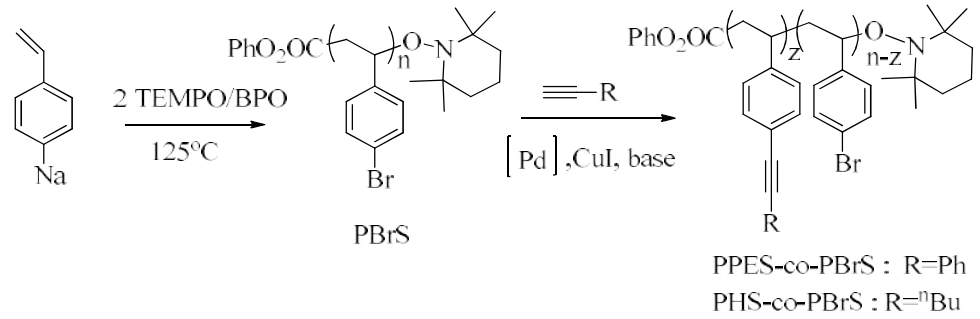

Scheme 1: Synthesis of alkyne-functionalized polymers

Recently, Morisaki and Chujo[48] have investigated through space π- π interaction as a new kind of polymer conjugation, by Sonogashira polymerization of [2.2] paracyclophane to yield a flexible polymer. This is not a conjugated system in the traditional sense, but maintains communication between segments via the cyclophane enforced π- π interactions and shows red shifted absorption characteristic of extended conjugation. (Scheme 2).

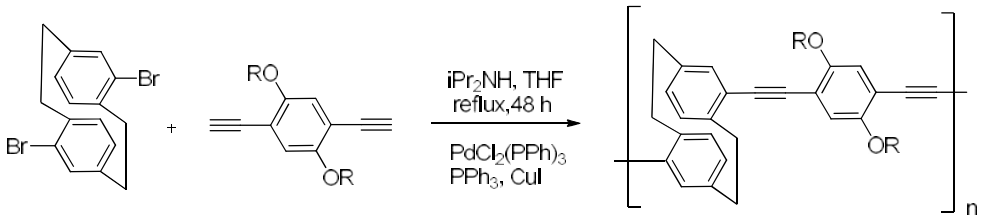

Scheme 2: Synthesis of paracyclophane based flexible polymer

1.3.2 Stille polymerisation

The Stille coupling is a versatile C-C bond forming reaction between stannanes and halides or pseudohalides, with very few limitations on the R-groups. The reaction has the advantage that it is run under neutral conditions making it even more tolerant of different functional groups than the Suzuki reaction. It can be used to synthesise a wide range of compounds including styrenes,[49] aromatic ketones[50] and biaryl derivatives.[51]

G. C. Schmidt[52] et al compared the semiconducting properties of a bithiophene-naphthalene diimide copolymer (PNDIT2) prepared by Ni-catalyzed chain-growth polycondensation and commercially available as Activink N2200 synthesized by Pd-catalyzed Stille polycondensation (Scheme 3).

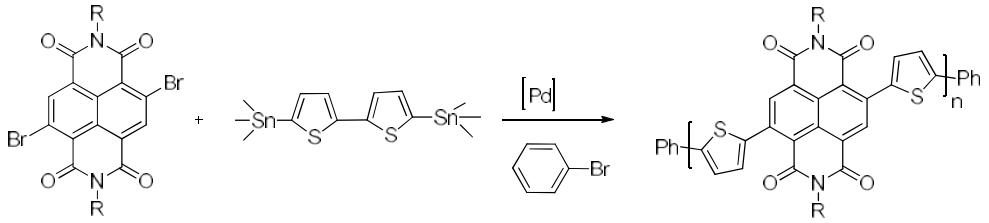

Scheme 3: Activink N2200

Recently Rumera et al[53] develop a novel and efficient route to synthesize thieno [3,4-c]pyrrole-4,6-dione (TPD) facilitating late-stage alkylation followed by copolymerization with alkylated bithiophene by Stille polymerization method (Scheme 4).

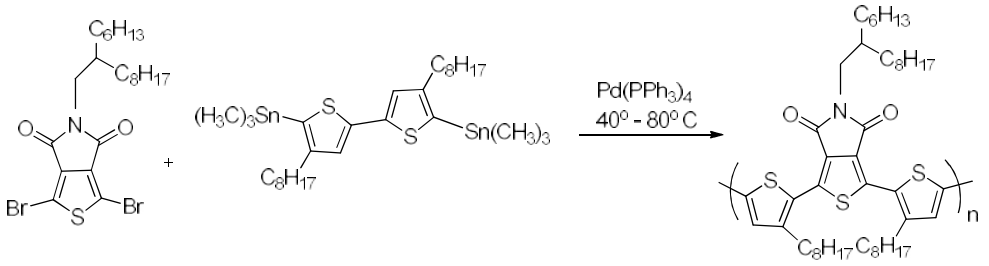

Scheme 4: Synthesis of thieno[3,4-c]pyrrole-4,6-dione based copolymer

1.3.3 Kumada coupling

Kumada Coupling was the first Pd or Ni-catalyzed cross-coupling reaction, developed in 1972[54(a)]. The coupling of Grignard reagents with alkyl, vinyl or aryl halides under Ni-catalysts is the method of choice for the low-cost synthesis of unsymmetrical biaryls. In the place of the halide reagent, pseudohalides can also be used, and the coupling has been shown to be quite effective using tosylate and triflate species in a variety of conditions.

Chavez et al[54(b)] reported an externally initiated living catalyst-transfer polymerization based on Ni(II)-catalyzed Kumada coupling of aromatic halogen substituted Grignard monomers. It is a highly efficient method for the controlled preparation of conjugated polymers such as polythiophenes and poly(*p*-phenylenes) (Scheme 5).

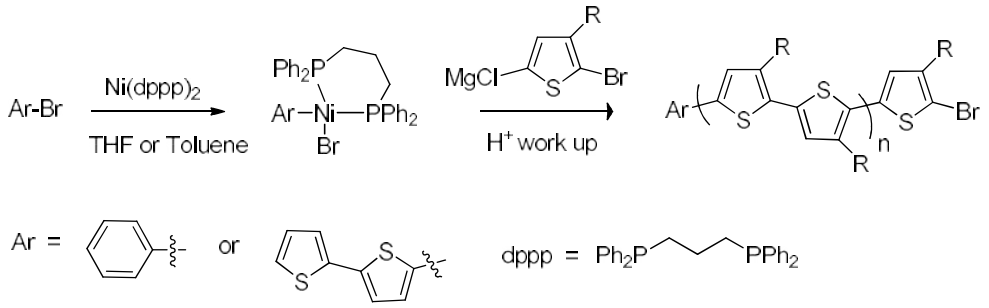

Scheme 5: Synthesis of Alkyl substituted polythiophenes

R. D. McCullough et al presented a method for the synthesis of structurally homogeneous and highly conductive 3-alkyl substituted polythiophenes [55] (Scheme 6).

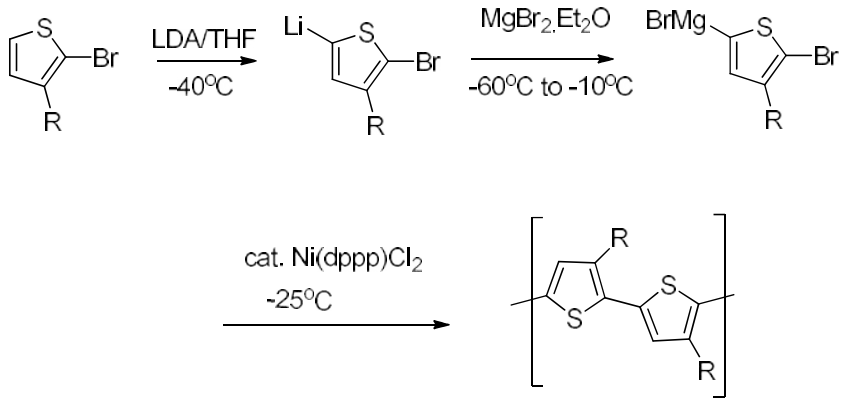

Scheme 6: McCullough method

1.3.4 Suzuki polymerisation

The Suzuki reaction is the Palladium catalyzed cross-coupling between organoboron compounds and organic halides leading to the formation of carbon-carbon bonds. The advantages of Suzuki coupling over other similar reactions are the availability of common boronic acids, mild reaction conditions, and the less toxic nature. It is easy to remove the inorganic by-products from reaction mixture. Being able to use water as a solvent, makes this reaction more economical, eco-friendly, and capable of using wide variety of water soluble reagents.

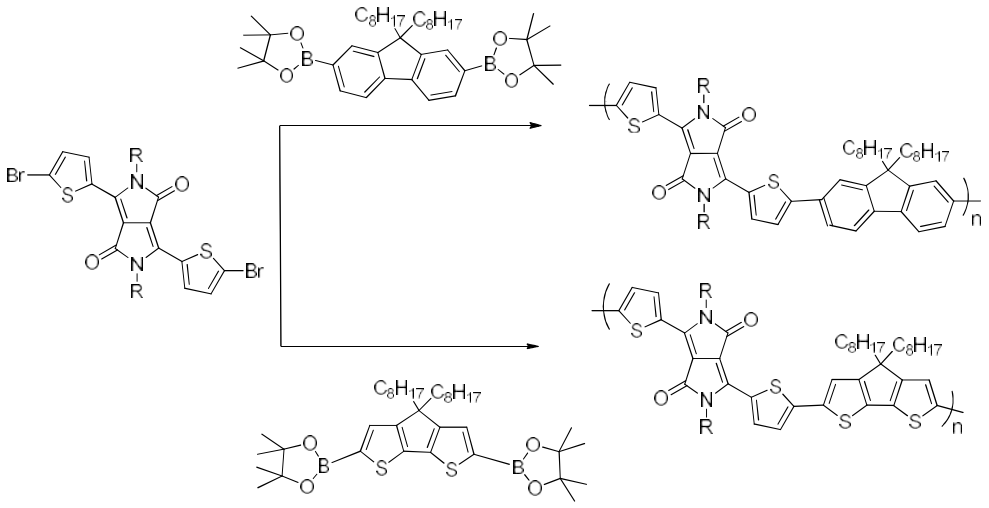

Catalyst – $Pd(PPh_3)/K_2CO_3(aq)$/aliquat 335 in toluene at 120^oC

Scheme 7: Synthesis of diketopyrrolopyrrole based polymers

A. P. Zoombelt et al synthesized new small band gap polymers with band gaps ranging from 1.24 to 1.77 eV incorporating diketopyrrolopyrrole units using Suzuki polymerization.[56] The polymers were applied as electron

donor in bulk heterojunction solar cells to give a power conversion efficiency of 1.7% (Scheme 7).

1.3.5 Direct arylation polymerisation

Coupling of aryl halides with catalytically activated C-H bonds provides a desirable and atom-economical alternative to standard cross-coupling reactions for the construction of new C-C bonds. Direct arylation is used to synthesise polymers that were previously difficult to prepare due to the instability of organometallic monomers. The major drawback of direct (hetero) arylation, however, is the lack of C-H bond selectivity which results in cross-linked material during polymerization reactions. Further fine-tuning of reaction conditions such as temperature and reaction time may suppress these unwanted side reactions. Alternatively, new monomers can be used where other reactive bonds are blocked, either sterically or by substitution with unreactive alkyl or halogen groups.

Direct arylation was also used to polymerise EDOT monomers substituted with different functional groups and the functional groups were tolerant to direct arylation conditions. The polymers were obtained in relatively moderate molecular weights.[57] Direct arylation provided entry into ProDOT and PEDOT polymers using several different reaction conditions that were amenable to a number of different functional groups (Scheme 8).

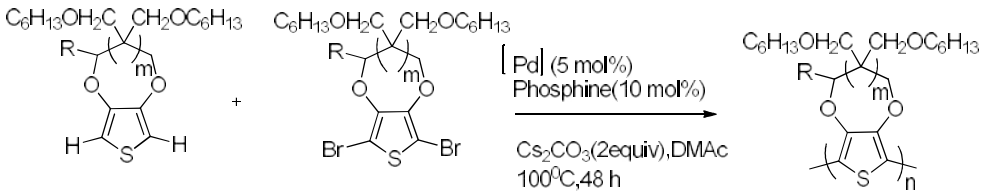

Scheme 8: An example for direct arylation polymerisation

In another report copolymerization of 4,4-bis(2-ethylhexyl)-4H-cyclopenta [2,1-b;3,4-b] dithiophene with dibromo benzothiadiazole via Direct arylation has been reported[58,59](Scheme 9).

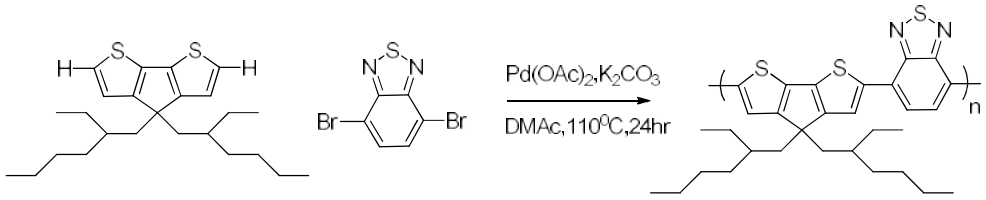

Scheme 9: Synthesis of cyclopenta[2,1-b;3,4-b]dithiophene based polymer

1.4 Photovoltaics

Photovoltaics (PVs), are increasingly recognized as one of the most promising and attractive methods for harvesting solar energy. Presently, PV modules based on crystalline silicon of high cost around $4 per watt dominate the commercial market. It is believed that this cost must decrease to $0.33 per watt for the widespread adoption of photovoltaics for electricity generation.[60] But to achieve costs that are truly competitive with fossil fuel energy sources, new technologies, often termed third generation PVs, must be developed.[61] Third generation solar cells (excitonic solar cells) are inexpensive, but moderately efficient. Organic photovoltaics (OPVs), dye

sensitized solar cells (DSSCs), and a few inorganic nanocrystal PVs are examples of excitonic solar cells.[62]

Solar cells made from organic semiconductors offer the potential to provide inexpensive solar power. OPVs can be divided into two general classes: devices based on organic small molecule semiconductors, and those based on polymer semiconductors. The former is generally processed by vapor deposition under high vacuum, while the latter is deposited from solution.[63, 64]

In 1958 D. Kearns and M. Calvin built the first organic thin film solar cell. They found that magnesium phthalocyanine disks coated with a thin film of air oxidized tetramethyl p-phenylenediamine shows the photovoltaic effect and this organic layer was sandwiched between two metal electrodes.[65] The potential created by the different work functions between the two conductors helps to split the exciton pairs. The photovoltaic properties are strongly dependent on the nature of the electrodes. But single layer organic solar cells do not work well. Because of very low dielectric constant of conjugated organic polymers and high coulombic forces between excitons, there were virtually no free charges formed in a pure polymer. So OPVs based on a single semiconductor have low quantum efficiencies (<1%), poor fill factor and low power conversion efficiencies (<0.1%). Another major problem with them is that the electric field is seldom sufficient to split the excitons. Often the electrons recombine with the holes without reaching the electrode.

In 1986, Tang first described a solution to this problem.[66] A thin-film, two-layer organic photovoltaic cell was fabricated from copper phthalocyanine and a perylene tetracarboxylic derivative. The two layers have different electron affinity and ionization energies, therefore electrostatic forces are generated at the interface between the two layers. Bi-layer cells split excitons much more efficiently than single layer photovoltaic cells. However, the donor and acceptor materials have to be in close proximity at the hetero-junction and are in the range of the exciton diffusion length, typically a few tens of nanometers. On the other hand, the thickness of the active layer should be comparable to the penetration length of the incident light, which is typically 80-200 nm. Thus both the exciton diffusion range and the poor shunt resistor can be improved. The bi-layer geometry guarantees directional photo-induced charge transfer across the interface. Since both types of charge carriers travel to their respective electrodes, the chances for recombination losses are significantly reduced. [67-70]

Although the Tang cell represented a major advance, a phenomenon known as the exciton diffusion bottleneck limited the efficiency of bilayer OPVs. However, because the exciton diffusion length is limited to about 10 nm, only excitons formed within this distance of the interface are likely to dissociate and contribute to the cell photocurrent. Excitons formed away from the interface simply recombine and are lost.[71] The solution to this problem was first described in 1995.[72] Instead of using two layers, the donor and acceptor materials are dissolved together and cast into a single mixed layer. OPVs utilizing these types of blends are known as bulk heterojunctions.

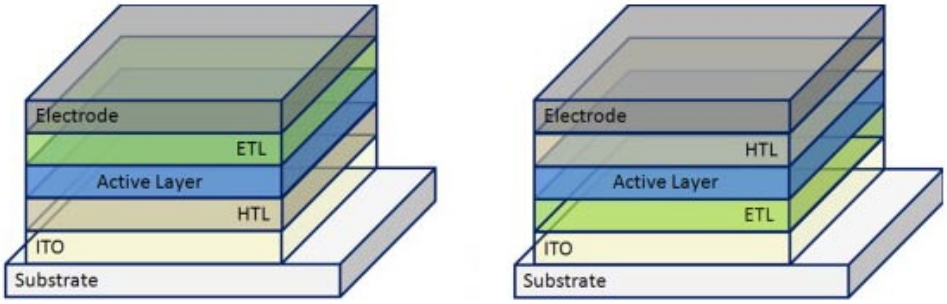

(a) (b)

Fig. 1.5: Different device architectures of bulk heterojunction solar cells. (a) Standard device design with the cathode on top of the device stack and (b) inverted device architecture with the cathode located on the transparent substrate.

Bulk heterojunction solar cells (figure 1.5) are built on a transparent substrate ITO (indium tin oxide) coated with a conductive and transparent electrode material. In the standard configuration, the ITO is coated with a hole transport layer (HTL) like PEDOT:PSS (poly(3,4-ethylenedioxythiophene) poly(styrene sulfonate)) or a thin oxide layer (e.g. MoO_3). On top of the HTL the photoactive layer, a blend of donor and acceptor material is coated followed by an optional electron transport layer (ETL) like zinc oxide or titanium dioxide and a low work function electrode. In the standard architecture, the top electrode is the cathode and calcium, barium or aluminum are applied for collecting the electrons generated in the photoactive layer. In the inverted architecture the transparent electrode coated on the substrate acts as the cathode. Both device architectures allow the preparation of high performance bulk heterojunction solar cells. The inverted design

offers processing advantages and shows improved ambient stability due to the absence of a low work function electrode[73] (Fig 1.5).

The first notable power conversion efficiencies (close to 3%) were obtained with a bulk heterojunction OPV utilizing a poly(phenylene vinylene) polymer known as MDMO-PPV as the donor and a soluble C_{60} derivative known as PCBM as the acceptor[74] (Fig 1.6).

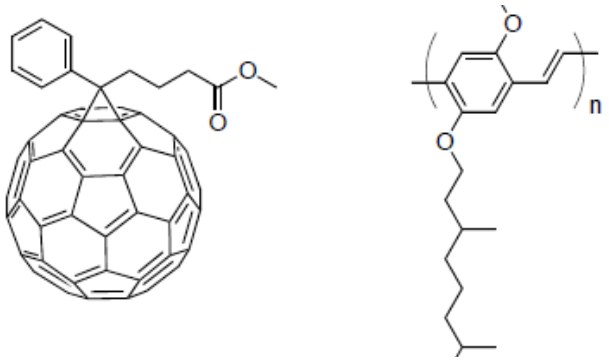

Fig. 1.6: Structure of PCBM and MDMO-PPV

Later it was discovered that, improved efficiencies could be achieved by replacing the MDMO-PPV donor with P3HT. Blends of P3HT and PCBM are now the best-studied bulk heterojunction pair. Maximum efficiencies for P3HT/PCBM cells are between 4 and 5%.[75] Efficiencies may continue to increase as polymer structures are further optimized and device architectures and processing conditions are improved.

J. S. Huang et al have described Förster resonance energy transfer-based heterojunction polymer solar cells that incorporate squaraine dye. The high

absorbance of squaraine in the near-infrared region broadens the spectral absorption of the solar cells and assists in increasing charge transport. They demonstrated a 38% increase in power conversion efficiency to reach 4.5% and opened up a new avenue for the development of high-efficiency polymer solar cells.[76]

Recently, efforts have been directed towards the development and understanding of soluble, non-fullerene, organic small molecules to fabricate bulk heterojunction (BHJ) solar cells. These efforts have been aimed at overcoming the inherent limitations of fullerene compounds such as the limited spectral breadth, air instability, and the typically higher production costs of fullerenes.[77(a)] B. Ebenhoch et al have reported the fabrication of solution-processed bulk heterojunction devices from subphthalocyanine (SubPc) units as the acceptor component and conventional polymeric donor materials such as MEH-PPV, P3HT and PTB7. Their results show that solution-processable SubPcs are promising alternatives to fullerenes for polymer solar cells[77(b)] (Scheme 10).

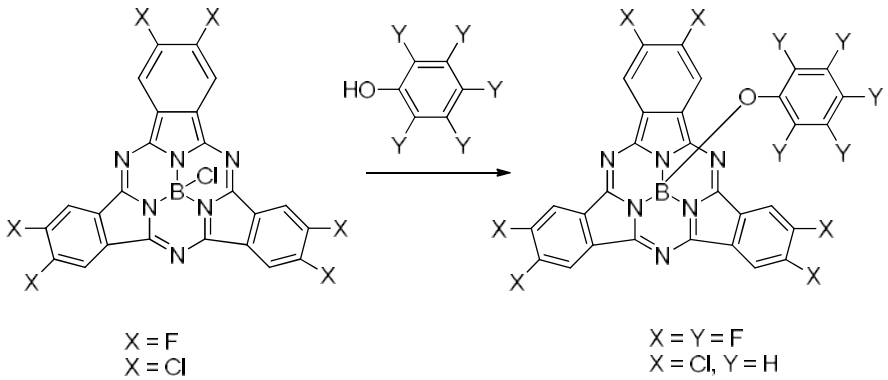

Scheme 10: Synthesis of Subphthalocyanine

In another work, Y. Liu et al have successfully demonstrated an integrated perovskite/bulk-heterojunction (BHJ) photovoltaic device for efficient light harvesting and energy conversion. They have efficiently integrated two photovoltaic layers, namely a perovskite film and organic BHJ film, into the device. The device structure is ITO/TiO_2/perovskite/ BHJ/MoO_3/Ag. Their result further suggests that the HTL(hole transporting layer) in traditional perovskite solar cell, even with good light absorption capability, cannot contribute to the overall device photocurrent, unless this HTL becomes a BHJ layer.[78]

In summary, bulk-heterojunction organic solar cells represent a promising technology which could be an important player in the future PV-market. Substantial research and development efforts are required to bring the technology to the necessary performance level.

1.4.1 Design and structural organization of π-functional materials for photovoltaic applications

1.4.1.1 Control of material properties

Generally, a conjugated polymer can be arbitrarily divided into three constituting components: the conjugated backbone, the side chains and the substituents.[79(a-e)] Fundamental material properties of organic electronic systems, such as conjugation length, light absorption, carrier mobilities, exciton dynamics, and processability, can be varied broadly through changes in molecular structure.

A first level of control is achieved by modulating the molecular structure of the π-functional system, including the pattern of its solubilizing side chains which improve the processibility of the polymer. Similarly, longer the conjugation length of the polymer, the smaller the band gap will be. The conjugation could be interrupted by torsion of the polymer backbone. For this reason, a planar conformation of the backbone is preferred for achieving a small band gap.[80, 81] The size of the solubilizing side chains was shown to affect the BHJ nanoscale morphology and OPV device performance. The degree of phase separation, microstructural order in crystalline fibers and carrier balance increase with increasing side-chain length. Branching and bulkiness of the solubilizing side chains appended to the π-conjugated backbone may substantially affect π-stacking distances and density of π-stacked backbones which are cited as determining factors governing charge transport in OPV's.[82] Polymer chain-end moieties influence the OPV device performance suggesting a significant variation in fill-factor (FF) and PCE. This has been attributed to both the introduction of carrier traps and possible chemical transformations which might occur as the device is operated. Substrate functionalization also affects the orientation of the polymer backbone relative to the substrate which influences the thin-film device performance. [83-85]

Another level of control is achieved by optimizing device architecture, material processing conditions, and the strategies that control thin-film

ordering. Processing conditions are as critical as material design, with material solubility impacting both material characterization and device optimization.[86-88] In order to bring OPVs one step closer to viable commercial application, parameters influencing device lifetime and cost-effective solutions will have to be implemented. In addition to these, challenges related to modest dielectric constants, small exciton diffusion lengths, and limited carrier mobilities inherent to organic electronics remain to be tackled.[89,90]

1.4.1.2 Band gap modulation

Band gap is a critical parameter determining the electronic, optical, redox, and electrical transport properties of a material. Tuning the band gap and the band edges will be of utmost importance in order to design new conjugated polymers for optoelectronic devices. Light-harvesting materials that have an optical gap between 1–2 eV are desired to maximize the solar cell efficiency.[91, 92] One well-established approach to obtain low band gap conjugated polymers is based on the strategy of donor–acceptor polymers, which forms strong interchain interactions that favor charge transport and also fine-tune the electronic structures of conjugated polymers, resulting in desired optoelectronic properties. In this approach, the energy levels and band gaps of conjugated polymers can be controlled by choosing appropriate donor and acceptor moieties, with the highest occupied molecular orbital (HOMO) energy level determined synergistically by the

donor and acceptor moieties and the lowest unoccupied molecular orbital (LUMO) energy level by the acceptor moiety.[93,94]

Decreasing the band gap of the donor material [(the HOMO level of the donor ($HOMO_{Donor}$) is raised or the LUMO level of the donor ($LUMO_{Donor}$) is lowered)] will broaden the absorption spectrum, making it possible to harvest more photons for charge generation. [95] Raising the HOMO level of the donor material will decrease the maximum value for V_{OC}, approximated by ($LUMO_{Acceptor}$ -$HOMO_{Donor}$). Lowering the LUMO level of the donor material will reduce the LUMO-level offset of the donor material to the acceptor material used. The $LUMO_{Donor}$ - $LUMO_{Acceptor}$ difference is considered to provide the driving force for exciton dissociation as well as to prevent recombination of photogenerated charges. A compromise is therefore needed to balance the band gap of the donor material and the favorable alignment of HOMO/LUMO energy levels of the donor material with respect to the acceptor material.[96,97] As a result, the effort to search for new electron donor polymers for OPVs is not merely directed to obtaining low band gaps, but also to controlling the band gap by tuning the HOMO and LUMO energy levels to their optimal positions. Furthermore, the design of efficient tandem solar cells requires a high V_{OC} or high J_{SC} in conjunction with a high PCE from the donor components, in order to maximize the overall performance. All of these require a better understanding of material design and device design.[98,99]

Recently, C. Chang et al synthesised selenophene-based low-band gap polymers. Their optoelectronic and photovoltaic properties and space-charge limited currents were compared with those of the related thiophene-based polymers. The band gaps of the Se-based derivatives were approximately 0.05–0.12 eV lower than those of their thiophene counterparts.[100(a)] (Fig1 7).

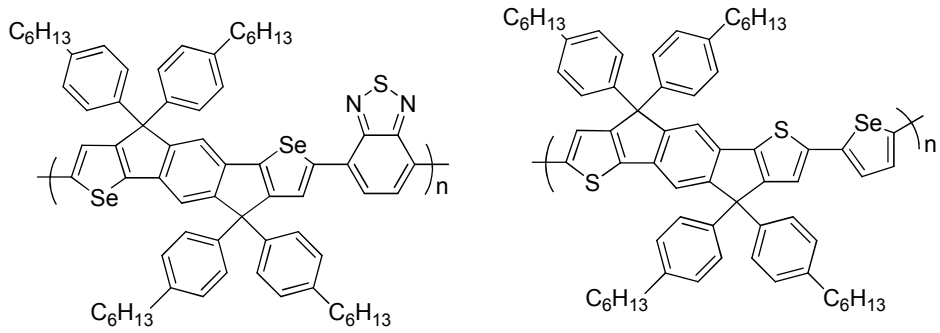

Fig. 1.7: Structure of selenophene based polymers

In another work, A. Patra et al prepared a series of new low-band-gap conjugated polymers via electropolymerization and solid-state polymerization. They introduced a new scheme for band gap control in conjugated polymers by replacing the sulfur atom with a selenium atom which has led to significant and predictable changes in the band gap of the polymers. This is due to the lower aromaticity of a selenophene ring compared to a thiophene ring. They achieved band gap control in very low band gap polymers through the use of different combinations of selenium and sulfur atoms in the main and peripheral rings.[100(b)] **(**Scheme 11**)**.

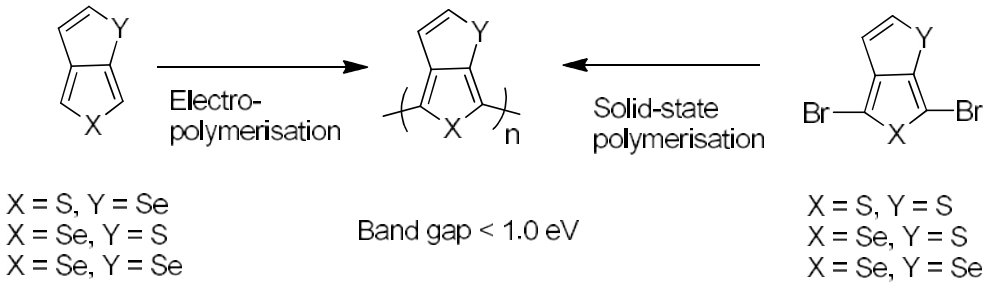

Scheme 11: Synthesis of low band gap polymers

S. Chang et al reported an alternative approach using nonvolatile, crystalline and conducting P3HT as an effective morphology control agent to enhance the efficiency of low band gap conducting polymer bulk heterojunction solar cells. Here the results indicate that favorable bi-continuous phase separation and appropriate domain size of each phase can be achieved to facilitate fast charge transport, and thus improve the power conversion efficiency of the solar cell. [100(c)]

1.5 Nonlinear optics

The past decade has witnessed a phenominal growth of research in the field of nonlinear optics in terms of basic physics as well as potential applications in optical information processing. Nonlinear optics is the study of phenomena that occur as a consequence of the modification of the optical properties of a material system by the presence of light. Although most of the nonlinear-optical phenomena require laser radiation, some classes of nonlinear-optical effects were known long before the invention of the laser. The most prominent ones include Pockels and Kerr electrooptic effects, [101]

as well as light-induced resonant absorption saturation, described by Vavilov.[102] The systematic studies of optical nonlinearities and the observation of a vast catalog of spectacular nonlinear optical phenomena became possible only with the advent of lasers.

One of its first applications was the very first nonlinear optical experiment, an SHG experiment, performed by Franken et al. in 1961[103(a)] (Fig.1.8). This work was followed by the discovery of a rich diversity of nonlinear optical effects, including sum-frequency generation, stimulated Raman scattering, self-focusing, optical rectification, four-wave mixing and many other nonlinear effects.

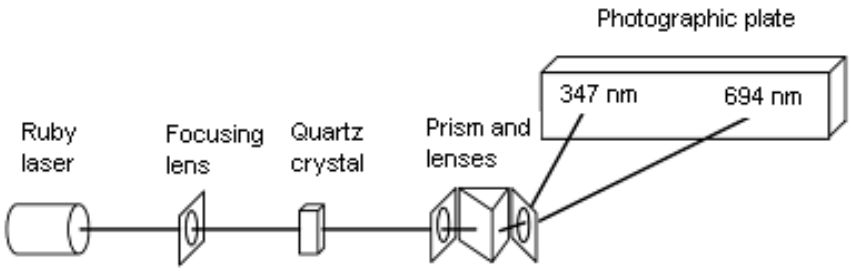

Fig. 1.8: Schematic diagram showing the arrangement for SHG in quartz crystal

Nonlinear-optical effects can be described within the general framework of macroscopic Maxwell equations which identify and classify nonlinear phenomena in terms of the nonlinear optical susceptibilities, nonlinear induced polarization and nonlinear-optical propagation effects. Whenever an external electric field is applied to matter, it induces or reorients dipole moments of atoms or molecules of the matter, resulting

in a nonzero average polarization of the material. If the applied electric field is not too large, the polarization is proportional to the field strength.[103(b)]

i.e, $P = \varepsilon_0 \chi^{(1)} E$ ... (1) where $\chi^{(1)}$ is the usual susceptibility of linear optics. Consequently, when the induced electron displacements in laser fields to be rather small; then a power series representation is used for the induced polarization as $P = \varepsilon_0(\chi^{(1)}E_1 + \chi^{(2)}E_2 + \chi^{(3)}E_3 + \ldots)$ .... (2) where $\chi^{(2)}$ and $\chi^{(3)}$ are referred to as Second and Third-order susceptibilities, respectively.

1.5.1 Nonlinear absorption

Absorption processes can be strongly nonlinear, particularly near atomic resonances. Increasing absorption can come from the introduction of multi-photon absorption at high intensity levels, whereas, reduced absorption comes from saturating the absorption line with high intensity light.

The absorption can be written as a function of intensity through $\alpha(I) = \alpha_o + \alpha_1 I + \alpha_2 I^2$ where α_o represents linear absorption, α_1 represents two-photon absorption, α_2 represents three-photon absorption, etc. The phenomenon of multi-photon absorption, where the absorption increases with intensity, is sometimes called reverse saturable absorption. Even though a material is transparent at low intensity, as the intensity grows, the absorption may increase. Two-photon absorption is the simultaneous

absorption of two photons in order to excite a molecule from one state to a higher energy electronic state and the energy difference between the lower and upper states of the molecule is equal to the sum of the energies of the two photons. It differs from linear absorption in that the atomic transition rate due to TPA (Two-photon absorption) depends on the square of the light intensity. This optical nonlinearity decreases the transmission of light as atoms or molecules absorb it while transitioning to higher levels. If the matrix elements allow it, these higher levels may return to the ground state by emitting fluorescence at twice the frequency of the input light. This multi-photon fluorescence has become a very important tool for biological applications.[104(a),(b)] A commercial example that demonstrates multi-photon absorption is the transparent glass cubes (or other shapes) that can be purchased with 3D images written inside.

Another important application of multi-photon absorption (or reverse saturable absorption) is optical limiting. This is defined as any process that limits the amount of light that can get through a material at high intensity. It has the potential application of protecting sensitive detectors and eyes from high power lasers. Wide varieties of organic and inorganic materials are being studied to achieve efficient optical limiting. The all-optical limiters rely on materials that exhibit one or more of the nonlinear optical mechanisms: two-photon absorption (TPA), excited state absorption (ESA), free carrier absorption, thermal defocusing and scattering, photorefraction,

nonlinear refraction and induced scattering. Coupling two or more of these mechanisms has also achieved enhancement in optical limiting, like self-defocusing in conjunction with TPA, TPA in one molecule with ESA in another molecule. [105(a)]

S. Chi et al reported a ternary mixture including a conjugated polymer electron donor, a fullerene electron acceptor and a plasticizer used for the fabrication of an optical quality, thick film of a MEH-PPV:PCBM:DOP blend ie, poly(2-methoxy-5-(2-ethylhexyloxy)-(phenylene vinylene)) (MEH-PPV), a C_{60} derivative (PCBM) and a plasticizer (1,2-diisooctylphthalate) (Fig 1.9) for optical limiting. These blend materials exhibited strong optical limiting characteristics in the near infrared region (750-900 nm), with broad temporal dynamic range spanning femtosecond to nanosecond pulse widths. [105(b)]

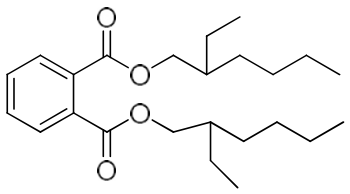

Fig. 1.9: Structure of 1,2-diisooctylphthalate

Saturable absorption occurring at wavelength close to resonance is given as $\alpha(I) = \alpha_o I_s/(I+I_s)$, where I_s is the saturation intensity. Saturable absorption has a number of practical applications, particularly for Q-switching and mode-locking lasers. Saturable absorbers are also useful

for nonlinear filtering outside laser resonators, which can clean up pulse shapes. Saturable absorption is particularly strong in semiconductor lasers at wavelengths just above the band edge.

1.5.2 Nonlinear scattering processes

In addition to transmission and absorption, light transmitted through materials can exhibit scattering. The linear elastic processes are Rayleigh and Mie scattering from density fluctuations in the medium. The non-elastic processes are Raman and Brillouin scattering. The nonlinear response caused by vibrations of a transparent optical medium to the light propagating through the medium is very fast, but not instantaneous.[105(c)] When these vibrations are associated with optical phonons, the effect is called Raman scattering, whereas acoustical phonons are associated with Brillouin scattering. The Raman interaction leads to two possible outcomes:

- the material absorbs energy and the emitted photon has a lower energy than the absorbed photon. This outcome is labeled Stokes Raman scattering.
- the material loses energy and the emitted photon has a higher energy than the absorbed photon. This outcome is labelled anti-Stokes Raman scattering (Figure1.10**)**.

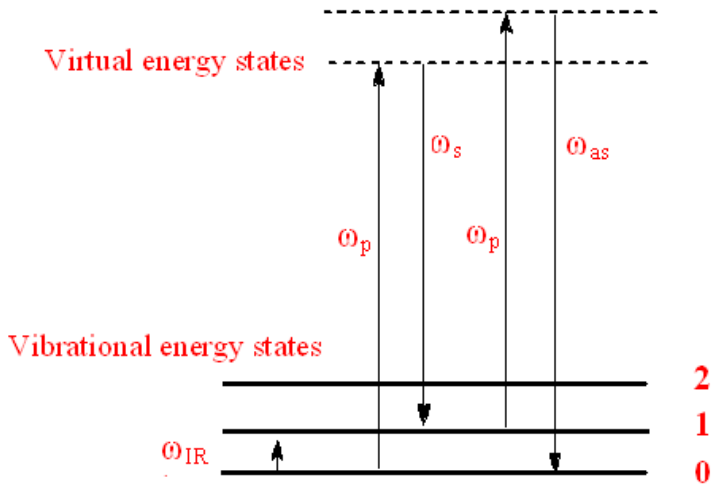

Fig. 1.10: Diagram for different linear and nonlinear optical processes. The optical processes depicted here are linear infrared, spontaneous Stokes and anti-Stokes scattering

The energy difference between the absorbed and emitted photon corresponds to the energy difference between two resonant states of the material and is independent of the absolute energy of the photon. When the intensity of the generated Stokes wave becomes sufficiently high, that wave may again act as the pump for a further Raman process. Apart from the Stimulated Raman scattering effect, there is also Spontaneous Raman scattering, caused by quantum effects.[106-109]

U. Gubler et al have explored an approach to substitute a linearly conjugated polymer in the backbone itself and evaluated the influence on the third-order nonlinear optical properties. They have determined the impact of various spacer groups (benzene, naphthalene, thiophene etc) on the

second-order hyperpolarizabilities of the resulting hybrid oligomers. Significant enhancements of the nonlinearities could be observed with a reduced red shift of the absorption spectra [110] (Fig 1.11**)**.

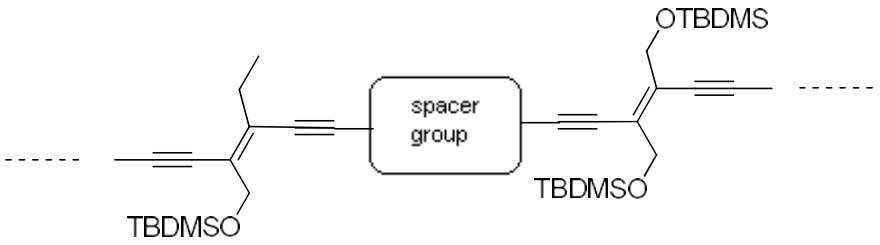

Fig. 1.11: An attractive method to modulate electron density distribution in conjugated oligomers and polymers is direct incorporation of functional groups (spacers) into the backbone

P. Poornesh et al reported measurements of the third-order nonlinear optical properties of a newly synthesized thiophene-based copolymer. The nonlinear transmission measurements were performed on the copolymer by employing the single beam Z-scan technique. The excited state absorption cross section σ_{exc}, was found to be larger than the ground state absorption cross section σ_g, indicating reverse saturable absorption (RSA) in the copolymer sample. Here, the copolymer seems to be a promising material for photonic device applications[111] (Fig 1.12).

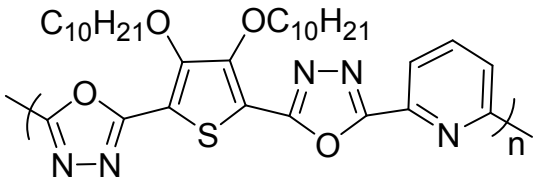

Fig. 1.12: Structure of the thiophene based copolymer

S Pramodini et al have presented the synthesis and characterization of third-order optical nonlinearity and optical limiting of the conducting polymers, poly (aniline-co-o-anisidine) and poly (aniline-co-pyrrole) (fig.1.13). The copolymers exhibited a reverse saturable absorption process and self-defocusing properties under the experimental conditions. Self-diffraction rings were also observed when exposed to the laser beam. The copolymers possess a lower limiting threshold and clamping level, which is essential to a great extent for power limiting devices. Therefore, copolymers of aniline emerge as a potential candidate for nonlinear optical device applications.[112]

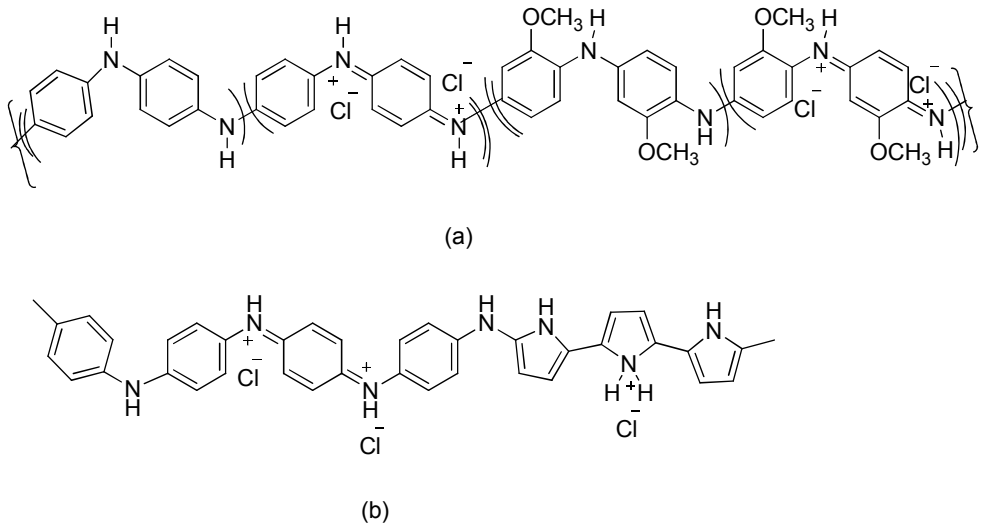

(a)

(b)

Fig.1.13: Molecular structure of (a) poly (aniline-co-o-anisidine) and (b) poly (aniline-co-pyrrole).

In another work, two copolymers of 3-alkylthiophene (alkyl = hexyl, octyl) and a thiophene functionalized with disperse red 19 (TDR19) as chromophore side chain were synthesized by oxidative polymerization. The

third-order nonlinear optical response of these materials was performed with nanosecond and femtosecond laser pulses using the third-harmonic generation (THG) and Z-scan techniques. From these experiments, it was observed that, although the TRD19 incorporation into the side chain of the copolymers was lower than 5%, it was sufficient to increase their nonlinear response in solid state. For instance, the third-order nonlinear electric susceptibility ($\chi(3)$) of solid thin films made of these copolymers exhibited an increment of nearly 60% when TDR19 incorporation increased from 3% to 5% [113] (Fig1. 14).

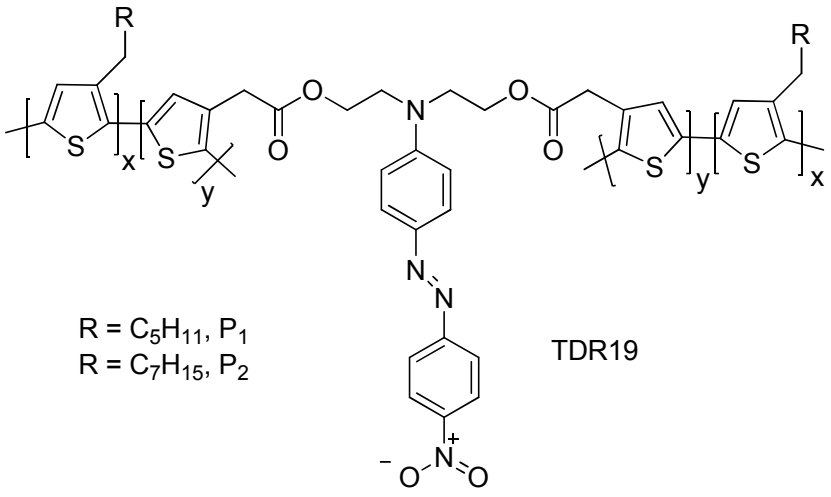

Fig.1.14: Structure of Copolymers P_1 and P_2

Over the past decade, polymeric materials have been identified as the materials of choice. Virtual electronic excitations are responsible for nonlinear optical effects in polymeric materials. Extended pi electron delocalisation along the backbone of the polymer chain gives rise to extremely

large polarisability. In addition to these, organic polymers have low dielectric constant, the possibility of structural modification, processibility, high optical damage thresholds, broad transparency ranges; can be polished and cost effective than those of inorganics. These advantages make organic polymers attractive candidates for nonlinear optical applications.

1.6 Aims and scope of the present study

- Design of donor- acceptor low band gap polymers for photovoltaic and NLO applications using Density Functional Theory in the periodic boundary condition (PBC) formalism.
- Synthesis of the designed polymers using direct arylation and Suzuki Coupling methods.
- Explore the application of the conjugated polymers as active layer in photovoltaic devices.
- Explore the third order NLO properties of the conjugated polymers.

References

[1] C. K. Chiang, C. R. Fincher, Y. W. Park, A. J. Heeger, H. Shirakawa, E. J. Louis S. C. Gau, and A. G. MacDiarmid, Phys. Rev. Lett. 1977, 39, 1098

[2] H. Shirakawa, E. J. Louis, A. G. MacDiarmid, C. K. Chiang, A. J. Heeger , J. Chem. Soc., Chem. Commun., 1977, 578.

[3] S. Li, C. Zhong, S. Dong, J. Zhang, X. Huang, C. Zhou, J. Lu, L. Ying, L. Wang, F. Huang, Y. Cao, Organic Electronics, 2014, 15, 850.

[4] M. D. Ho, D. Kim, N. Kim, S. M. Cho, H. Chae, Appl. Mater. Interfaces, 2013, 5, 12369.

[5] S. Hunder, J. Chen, T. D. Anthopoulos, Adv. Funct. Mater, 2014, 24, 5969.

[6] J. D. Smith, Prog. Polym. Sci., 1998, 23, 57.

[7] E. T. Kang, K. G. Neoh, K.L Tan, Prog. Polym. Sci., 1998, 23, 277.

[8] N. Gospodinova, L. Terlemezyan, Prog. Polym. Sci., 1998, 23, 1443.

[9] S. Palaniappan, A. John, Prog. Polym. Sci., 2008, 33, 732.

[10] S. Bhadra, D. Khastgir, N. K. Singha, J. H. Lee, Prog. Polym. Sci., 2009, 34, 783.

[11] A. Pud, N. Ogurtsov, A. Korzhenko, G. Shapoval, Prog. Polym. Sci., 2003, 28, 1701.

[12] J. Roncali, P. Blanchard, P. Fre`re, J. Mater. Chem., 2005, 15, 1589.

[13] L. Dai, J. Macromol. Sci., Rev. Macromol. Chem. Phys., 1999, 39, 273.

[14] A. K. Bakhshi, Annu Rep, Royal Soc Chem, Sec C, 1993, 89, 147.

[15] W. C. Chen, S. A. Jenekhe, Macromolecules, 1995, 28, 465.

[16] L. Kyungoon, A. Gregory, G. A. Sotzing, Macromolecules, 2001, 34, 5746.

[17] A. K. Bakhshi, D. J. Lathik, Solid State Commun, 1997, 101, 347.

[18] A.K.Bakhshi, B. Geethika, Electrically Conducting Polymers: Materials of Twenty First Century, J SCI IND RES, 2004, 63, 715.

[19] D. L. Wise, G. E Wnek, D. J. Trantolo, T. M. Cooper, J. D. Gresser, Electrical and Optical Polymer Systems, Marcel Dekker, Inc, New York, 1998.

[20] A. Breeze, A. Salomon, D. Ginley, B. Gregg. Photovoltaic Cells Based on Conducting Polymers and Perylene Diimides, NREL, Colorado, 2001.

[21] C. Halvorson, A. Hays, B. Kraabel, R. L.Wu, F. Wudl, A. J. Heeger, Science, 1994, 265, 1215.

[22] W. S. Fann, S. Benson, J. M. J. Madey, S. Etemad, G. L Baker, F. Kajzar, Phys. Rev. Lett, 1989, 62, 1492.

[23] C. Halvorson, D. Moses, T. W. Hagler, Y. Cao, A. J. Heeger, Synth. Met, 1992, 49, 49.

[24] C. Halvorson, T. W. Hagler, D. Moses, Y. Cao, A. J. Heeger, Chem. Phys. Lett, 1992, 200, 364.

[25] S. H Chi, J. M. Hales, C. F. Hernandez, S. Y. Tseng, J. Y. Cho, S. A. Odom, Q. Zhang, S. Barlow, R. R. Schrock, S. R. Marder, B. Kippelen, J. W. Perry, Adv. Mater., 2008, 20, 3199.

[26] R. H. Grubbs, C. B. Gorman, E. J. Ginsburg, J. W. Perry, S. R. Marder, ACS Symp. Ser., 1991, 455, 672.

[27] S. J. Chung, G. S. Maciel, H. E. Pudavar, T. C. Lin, G. S. He, J. Swiatkiewicz, P. N. Prasad, D. W. Lee, J. I. Jin, J. Phys. Chem. A, 2002, 106, 7512.

[28] S. V. Frolov, M. Liess, P. A. Lane, W. Gellermann, Z. V Vardeny, Phys. Rev. Lett, 2002, 78, 4285.

[29] M. A. Bader, G. Marowsky, A. Bahtiar, K. Koynov, C. Bubeck, H. Tillmann, H. Horhold, S. Pereira, J Opt Soc Am B, 2002, 19, 2250.

[30] M. Cha, N. S. Saricftci, A. J. Heeger, J. C. Hummelen, F. Wudl, Appl. Phys. Lett., 1995, 67, 3850.

[31] G. S. He, C. Weder, P. Smith, P. N. Prasad, IEEE J Quantum Electron, 1998, 34, 2279.

[32] C. Y. David, Computational Chemistry: A Practical Guide for Applying Techniques to Real-World Problems, John Wiley & Sons, Inc, New York, 2001.

[33] J. A. Schmidt, R. E. Koehn, T. M. Pappenfus, J. D. Alia, PBC-DFT : An Efficient Method to Calculate Energy Band Gaps of Conducting Polymers used in Solar Cells, University of Minnesota, Morris, 2010.

[34] W. Zhuang, A. Lundin, M. R. Andersson, J. Mater. Chem. A, 2014, 2, 2202.

[35] B. M. Wong , J. G. Cordaro, J. Phys. Chem. C, 2011, 115, 18333.

[36] K. Olech, R. Gutkowski, V. Kuznetsov, S. Roszak, J. Sołoducho, W. Schuhmann, ChemPlusChem , 2015, 80, 679.

[37] J. Heyd, G. E. Scuseria, M. Ernzerhof, J. Chem. Phys., 2006, 124, 219906.

[38] S. H . Vosko, L .Wilk, M. Nusair, Can J. Phys., 1980, 58, 1200.

[39] S. Sadki, P. Schottland, N. Brodie, G. Sabouraud, Chem. Soc. Rev, 2000, 29, 283.

[40] G. A . Sotzing, J. R. Reynolds, P . J. Steel, Adv Mater., 2004, 9, 795.

[41] R. J .Waltman, J. Bargon, Can. J. Chem., 1986, 64, 76.
(a) N .Toshima, S. Hara, Prog. Polym. Sci., 1995, 20, 155.

[42] Y. J. Cheng, T. Y. Luh, J. Organomet. Chem., 2004, 689, 4137.

[43] (a) T. Mizoroki, K. Mori, A. Ozaki, Bull. Chem. Soc. Jpn., 1971, 44, 581; (b) R. F. Heck, J. P. Nolley, J. Org. Chem., 1972, 37, 2320.

[44] (a) E. Negishi, A. O. King, N. Okukado, J. Org. Chem., 1977, 42, 1821; (b) A. O.King, N. Okukado, E. I. Negishi, J. Chem. Soc.-Chem. Commun., 1977, 683; (c) E. I. Negishi, Acc. Chem. Res., 1982, 15, 340.

[45] D. Milstein, J. K. Stille, J. Am. Chem. Soc., 1978, 100, 3636.

[46] (a) N. Miyaura, K. Yamada, A. Suzuki, Tetrahedron Lett., 1979, 20, 3437; (b) N. Miyaura, A. Suzuki, J. Chem. Soc., Chem. Commun., 1979, 866 ; (c) A. Suzuki, J. Organomet. Chem., 1999, 576, 147 ; (d) N. Miyaura, T. Yanagi, A. Suzuki, Synth.Commun., 1981, 11, 513.

[47] L. B. Sessions, B. R. Cohen, R. B. Grubbs, Macromolecules, 2007, 40 , 1926.

[48] Y. Morisaki, Y. Chujo , Prog. Polym. Sci., 2008, 33, 346.

[49] A. Nunez, B. Abarca, A. M. Cuadro, J. Builla, J. J. Vaquero,. J. Org. Chem. 2009, 74, 4166.

[50] G. Z . Zheng, Y. Mao, C. H. Lee, J. K . Pratt, J. R . Koenig, R. J. Perner, M. D. Cowart, G. A. Gfesser, S. McGaraughty, K. L. Chu, C. Zhu, H . Yu, K. Kohlhaas, K.M. Alexander, C.T Wismer, J. Mikusa, M. F. Jarvis, E.A. Kowaluk, A. O. Stewart, Bioorg. & Med. Chem. Lett., 2003, 18, 3041.

[51] A. F. Littke, L. Schwartz, G. C . Fu, J. Am. Chem. Soc. 2002, 124, 6343.

[52] G. C. Schmidt, D. Höft, K. Haase, A. C. Hübler, E. Karpov , R. Tkachov, M. Stamm, A. Kiriy, F. Haidu , D. R. T. Zahn, H. Yan, A. Facchetti, J. Mater. Chem. C, 2014, 2, 5149

[53] J. W. Rumera, K. L. H . Christine, I. Meagera, C. P. Yaua, Z. Huanga, C. B. Nielsena, S. E. Watkinsb, H. Bronsteinc, I. McCullocha, J. Org. Semiconductors, 2014 , 1, 30.

[54] (a) K. Tamao, K. Sumitani, M. Kumada, J. Am. Chem. Soc.,1972, 94, 4374.

(b) C. A. Chavez , J. Choi , E. E. Nesterov, Macromolecules, 2014, 47, 506.

[55] R. D. McCulloug, R. D. Lowe, J. Chem. Soc., Chem. Commun., 1992, 1, 70.

[56] A. P. Zoombelt, S. G. J. Mathijssen, M. G. R. Turbiez, M. M. Wienk, R. A. J. Janssen, J. Mater. Chem., 2010, 20, 2240.

[57] H. Zhao, C. Y. Liu, S. C. Luo, B. Zhu, T. H. Wang, H. F. Hsu, H. H. Yu, Macromolecules, 2012, 45, 7783.

[58] S. Kowalski, S. Allard, U. Scherf, ACS Macro Lett., 2012, 1, 465.

[59] S. W. Chang, H. Waters, J . Kettle, Z. R. Kuo, C. H. Li, C. Y. Yu, M . Horie, Macromol. Rapid Commun., 2012, 33, 1927.

[60] S. E. Shaheen, D. S. Ginley, G. E .Jabbour, MRS Bulletin, 2005, 30, 10.

[61] M. A. Green,. Physica E, 2002, 14, 65.

[62] I .Gur, N. A. Fromer, M. L .Geier, A. P. Alivisatos, Science, 2005, 310, 462.

[63] Y. Liang, Z. Xu, J. Xia, S. Tsai, Y. Wu, G. Li, C. Ray, L .Yu, Adv. Mater. 2010, 22, 135.

[64] P. Peumans, A. Yakimov, S. R. Forrest,. J. Appl. Phys., 2003, 93, 3693.

[65] D. Kearns, M. Calvin, J. Chem. Phys., 1958, 29, 950.

[66] C. W. Tang, Appl. Phys. Lett., 1986, 48, 183.

[67] S. R. Scully, M. D. McGehee, J. Appl. Phys., 2006, 100, 034907.

[68] (a) J. Brédas, J. E. Norton, J. Cornil, V. Coropceanu, Acc Chem. Res., 2009, 42, 1691.

(b) X. Zhu, Q. Yang, M. Muntwiler, Acc. Chem. Res., 2009, 42, 1779.

[69] V. D. Mihailetchi, J. Wildeman, P. W. M. Blom,. Phys. Rev. Lett., 2005, 94, 126602.

[70] Li. G. Shrotriya, V. Yao, Y. Huang, J. Yang, J. Mater. Chem. 2007, 17, 3126.

[71] K. M. Coakley, M. D. McGehee,. Chem. Mater. 2004, 16, 4533.

[72] (a) G. Yu, J. Gao, J. C. Hummelen, F. Wudl, A. J. Heeger, Science, 1995, 270, 1789.

(b) J. J. M. Halls, C. A. Walsh, N. C. Greenham, E. A. Marseglia, R. H Friend, S. C . Moratti, A. B. Holmes, Nature, 1995, 376, 498.

[73] M. C. Scharber , N. S. Sariciftci, Prog. Polym. Sci, 2013, 38, 1929.

[74] S. E. Shaheen, C. J. Brabec, N. S. Sariciftci, F. Padinger, T. Fromherz, J. C. Hummelen, Appl. Phys. Lett., 2001, 78, 841.

[75] (a) C. Yang, J. G. Hu, A. J. Heeger, J. Am. Chem. Soc., 2006, 128, 12007.

(b) W. Ma, C. Yang, X. Gong, K. Lee, A. J. Heeger, Adv. Funct. Mater., 2005, 15, 1617.

(c) G. Li. V. Shrotriya, J. Huang, Y. Yao, T. Moriarty, K. Emery, Y. Yang, Nat. Mater., 2005, 4, 864.

[76] J. Huang, T. Goh, X. Li, M. Y. Sfeir, E. A. Bielinski, S. Tomasulo, M. L. Lee, N. Hazari , A. D. Taylor, Nat. Photonic*s*, 2013, 7, 479.

[77] (a) A. F. Eftaiha, J. Sun, I. G. Hill , G. C. Welch**,** J. Mater. Chem. A**,** 2014, 2**,** 1201

(b) B. Ebenhoch, N. B. A. Prasetya, V. M. Rotello , G. Cooke, I. D. W. Samuel, J. Mater. Chem A, 2015, 3, 7345.

[78] Y. Liu , Z. Hong , Q. Chen , W. Chang , H. Zhou , T. Song , E. Young , Y. Yang , J. You G. Li , Y. Yang, Nano Lett., 2015, 15 , 662.

[79] (a) H. Zhou, L. Yang, W. You, Macromolecules, 2012, 45, 607 ;

(b) Z. G. Zhang, J. Wang, J. Mater. Chem., 2012, 22, 4178 ;

(c) H. J. Son, F. He, B.Carsten, L. P. Yu, J. Mater. Chem., 2011, 21, 18934 ;

(d) X. W. Zhan, D. B. Zhu, Polym. Chem., 2010, 1, 409 ;

(e) J. Roncali, Macromol. Rapid Commun., 2007, 28, 1761.

[80] (a) R. Hoffmann, C. Janiak, C. Kollmar, Macromolecules, 1991, 24, 3725

(b) C. Winder, N. S. Sariciftci, J. Mater. Chem., 2004, 14, 1077.

[81] C. Müller, E. Wang, L. M. Andersson, K. Tvingstedt, Y. Zhou, M. R. Andersson, O. Inganäs, Adv. Funct. Mater., 2010, 20, 2124.

[82] P. M. Beaujuje , J. M. J. Frechet, J. Am. Chem. Soc., 2011, 133, 20009.

[83] A. Salleo, R. J. Kline, D. M. DeLongchamp, M. L. Chabinyc, Adv. Mater. 2010, 22, 3812.

[84] R. J. Kline, M. D. McGehee, E. N. Kadnikova, J. S. Liu, J. M. J. Fréchet, M. F. Toney, Macromolecules 2005, 38, 3312.

[85] O. P. Lee, A. T . Yiu, P. M. Beaujuge, C. H. Woo, T. W. Holcombe, J. E. Millstone, J. D. Douglas, M. S. Chen, J. M. J. Fréchet, Adv. Mater. 2011, 23, 5359.

[86] J. Guo, Y. Liang, J. Szarko, B. Lee, H. J. Son, B. S. Rolczynski, L. Yu, L. X. Chen, J. Phys. Chem. B, 2010, 114, 742.

[87] J. M. Szarko, J . Guo, Y. Liang, B. Lee, B. S. Rolczynski, J . Strzalka, T. Xu, S. Loser, T. J. Marks, L .Yu, L. X. Chen, Adv. Mater., 2010, 22, 5468.

[88] K. M. Coakley, M. D. McGehee, Chem. Mater., 2004, 16, 4533.

[89] B. J. Kim, Y. Miyamoto, B. Ma, J. M. J. Fréchet, Adv. Funct. Mater., 2009, 19, 2273.

[90] J. A. Bartelt, Z. M. Beiley, E. T. Hoke, W. R. Mateker, J. D. Douglas, B. A. Collins, J. R. Tumbleston, K. R. Graham, A. Amassian, H. Ade, J. M. J .Fréchet, M. F. Toney, M. D. McGehee, Adv. Energy Mater., 2013, 3, 364.

[91] W. Shockley, H. J. Queisser, J. Appl. Phys., 1961, 32, 510.

[92] M. C. Scharber, N. S. Sariciftci, Prog. Polym. Sci., 2013, 38, 1929.

[93] (a) G. Dennler, M. C. Scharber, T. Ameri, P. Denk, K. Forberich, C. Waldauf, C. J. Brabec, Adv. Mater., 2008, 20, 579 ;

(b) G. Dennler, M. C. Scharber, C. J. Brabec, Adv. Mater., 2009, 21, 1323.

[94] M. C. Scharber, D. Wuhlbacher, M. Koppe, P. Denk, C. Waldauf, A. J. Heeger, C. L. Brabec, Adv. Mater., 2006, 18, 789.

[95] E. Bundgaard, F. C. Krebs, Sol. Energy Mater. Sol. Cells, 2007, 91, 954.

[96] R. A. J. Janssen, J. Nelson, Adv. Mater., 2013, 25, 1847.

[97] J. J. M. Halls, J. Cornil, D. A. dos Santos, R. Silbey, D. H. Hwang, A. B. Holmes, J. L. Bredas, R. H. Friend, Phys. Rev. B, 1999, 60, 5721.

[98] (a) G. Dennler, M. C. Scharber, C. J. Brabec, Adv. Mater. 2009, 21, 1323;

(b) J. You, L. Dou, K. Yoshimura, T. Kato, K. Ohya, T. Moriarty, K. Emery, C. C. Chen, J. Gao, G. Li, Y. Yang , Nat. Commun., 2013, 4, 1446.

[99] (a) T. Ameri, P. Khoram, J. Min, C. J. Brabec, Adv. Mater., 2013, 25, 4245 ; (b) L. Dou, J. You, Z. Hong, Z. Xu, G. Li, R. A. Street, Y. Yang, Adv. Mater., 2013, 25, 6642.

[100] (a) C. Chang, C. Chen,H. Chou, C. Liao, S. Chan, C. Cheng, J. Polym. Sci. A Polym. Chem., 2013, 51, 4550

(b) A. Patra, Y. H. Wijsboom, G. Leitus, M. Bendikov, Chem. Mater., 2011, 23, 896 ;

(c) S. Chang, H. Liao, Y. Shao, Y. Sung, S. Hsu, C. Ho, W. Su, Y. Chen, Mater. Chem. A, 2013, 1, 2447

[101] R. W. Boyd: Nonlinear Optics, 2nd edn. Academic, San Diego, 2003.

[102] S. I. Vavilov: Microstructure of Light ,USSR Acad. Sci., Moscow, 1950

[103] (a) P. A. Franken, A. E. Hill, C. W. Peters, G. Weinrich, Phys. Rev. Lett., 1961 7,118.

(b) F. Träger, Handbook of Lasers and Optics, Springer, Germany, 2012.

[104] (a) S. A. Ponomarenko, Fundamentals of Nonlinear Optics, Springer, Berlin, 2007;

(b) R. DeSalvo, A. A .Said, D. J. Hagan, E. W. V. Stryland, M. S. Bahae, IEEE J Quantum Electron, 1996, 32, 1324.

[105] (a) J. D. Bhawalkar, G. S. He and P. N. Prasad, Rep. Prog. Phys., 1996, 59**,** 1041.

(b) S. H. Chi, J. M. Hales, M. Cozzuol, C. Ochoa, M. Fitzpatrick, J.W. Perry Opt. Express*,* 2009*,* 17, 22062.

(c) R. Dekker, N. Usechak, M. Forst, A. Driessen, J. Phys. D: Appl. Phys., 2007 40, R249.

[106] (a) N.V. Kamanina, A.H. Reshak, P. Y. Vasilyev, A. I. Vangonen, V. I . Studeonov, Y. E. Usanov, J. Ebothe, E. Gondek, W. Wojcik, A. Danel. Physica E, 2009, 41, 391.

[107] Y. R. Shen, N .Bloembergen, Phys. Rev A, 1965, 137, 1787.

[108] D. Chen, S. Qin, S. He, Opt. Express, 2007, 15, 930.

[109] M. Troccoli, A. Belyanin, F. Capasso, E. Cubukcu, D. L. Sivco, A.Y Cho, Nature, 2005, 433, 845.

[110] U. Gubler, S. Concilio, C. Bosshard, I. Biaggio, P. Gunter, Appl. Phys. Lett., 2002, 81, 2322.

[111] P. Poornesh, P.K. Hegde, M.G. Manjunatha, G. Umesh , A.V. Adhikari, POLYM. ENG. SCI., 2009, 49, 875.

[112] S. Pramodini, Y. N. Sudhakar, M. SelvaKumar, P. Poornesh, Laser Physics. 2014, 24, 045408.

[113] M. Castillo, A. Juárez, M. Rodríguez, J. Uribe, G. Ortiz, M. Rodríguez, J. Maldonado, J. Álvarez, V. Barba, Int. J. Polym. Sci., 2015, 1.

…..ൟ…..

Chapter 2

SYNTHESIS AND CHARACTERISATION OF MONOMERS

Contents

Conjugated polymeric systems attract research communities worldwide because, they constitute a new class of materials which bind together desired semiconducting properties with mechanical flexibility and in some cases, biocompatibility. Such a practical combination is not observed in metals, inorganic semiconductors or non-conjugated saturated polymers. The advent of conducting polymers has created new opportunities for fundamental studies in solid-state physics. This type of materials constitute another fascinating crossover of chemistry and physics. Herein, we present the synthesis and characterization of monomers which are used for preparing the desired conjugated polymers. Detailed description of experimental procedures are presented.

2.1 Introduction

There has been substantial research effort to tackle the energy shortage, one of the greatest issues in the twenty first century and to look for new sources of energy.[1,2] The direct conversion of light into electricity has been achieved via inorganic solar cells, based on the photovoltaic effect, but come with a high manufacturing cost.[3,4] More recently, a new form of low cost solar cells based on organic semiconductors has emerged, which offer the potential for light weight, mechanically flexible and easy to process.[5] For a conjugated polymer to fit in organic photovoltaic solar cell, it should possess favourable physical and chemical properties, i.e., it should possess large absorption coefficient; low band gap; high charge mobility; favourable blend morphology; environmental stability; suitable HOMO/ LUMO level and solubility for achieving reasonable device efficiency.[6-10]

In order to harvest as much solar spectrum as possible, several structures of promising building blocks for potential high performance materials were developed. The control of band gap of π-conjugated systems has been in the centre of the synthetic chemistry of functional π-conjugated polymers for more than twenty years. Various structural factors affect the magnitude of band gap of a material, like bond length alteration, resonance effect, planarity, the introduction of electron-withdrawing or electron-releasing substituents and intermolecular interactions.[11,12]The insertion of double bonds between aromatic rings represent a simple and straightforward way of reducing ΔE.[13] Covalent rigidification of π-conjugated systems represents an efficient strategy for

band gap control and opens interesting perspectives for applications in photonic systems such as nonlinear optics, light-emitting devices or solar cells. [14]

Introduction of electron-releasing or electron-withdrawing groups represents the most immediate way to tune the HOMO and LUMO energy levels of a conjugated system. Electron-withdrawing groups induce a decrease of the HOMO level which results in a stabilization of the neutral state of the system.[15,16] H. Cha et al have investigated the molecular packing structures of two conjugated polymers based on alkoxy naphthalene, one with cyano-substituent and one without, to determine the effects of electron-withdrawing cyano-groups on the performance of bulk-heterojunction solar cells. A bulk-heterojunction device fabricated with the cyano-substituted polymer: $PC_{71}BM$ blend has a higher V_{OC}, a higher fill factor (FF) and a lower short circuit current J_{SC} than that of the noncyano-substituted polymer: $PC_{71}BM$ blend. Thus, the cyano-substitution of conjugated polymers may be an effective strategy for optimizing the domain size and crystallinity of the polymer: $PC_{71}BM$ blend, and for increasing V_{OC} by tuning the HOMO and LUMO energy levels of the conjugated polymer (Fig 2.1). But the introduction of cyano groups leads to a strong decrease of solubility, which must be taken into account when designing the target system.[17] Variation of the substituent on the aromatic unit in the main chain represents an effective way to perturb molecular orbitals or tune the solubility.

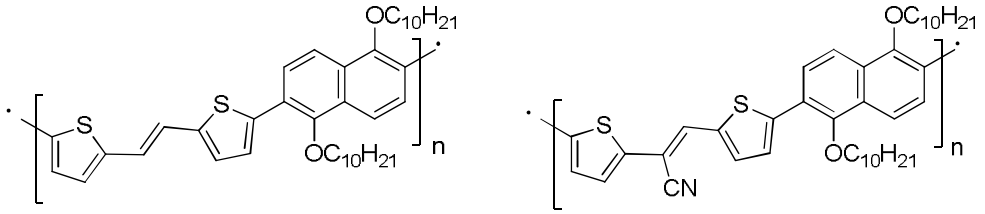

Fig. 2.1: Structures of two conjugated polymers based on alkoxy naphthalene, one with cyano-substituent and one without, to determine the effects of electron-withdrawing cyano groups on the performance of bulk-heterojunction solar cells

Introduction of electron-donor groups to a conjugated system produces an increase of the HOMO level, generally accompanied by a reduction of ΔE. Linear alkyl chain enhances the long-range order in the polymer, through lipophilic interactions between the alkyl chains, this effect being particularly important in regioregular polymers.[18-20] Strong electron donors such as alkoxy or alkylsulfanyl groups produce a large increase of the HOMO level. The conversion of a polyaromatic chain into a conjugated system with an enhanced quinoid character (fused heterocycles like fluorene, carbazole, quinoxaline etc) is one of the most efficient approaches for band gap reduction. A major drawback of some of these fused systems lies in their limited stability, which has led several groups to combine them with more stable building blocks to obtain multicyclic precursors.[21-24]

In addition to the energy level tuning, the polymer solubility also affects the physical properties of the polymer, such as processibility, phase behaviour, structural order and charge transport properties. Branched alkyl chains are more effective than their linear counterparts for inducing solubility, but affect the π-π interaction, and the charge carrier mobility.

Large sized alkyl chains will lengthen π-π stacking distance and reduce carrier mobility .[25-29] Bridging atoms that connects two aromatic rings also play a unique role in high performance materials.[30]

2.2 Common building blocks for conducting polymers

Ethylene (double bond) is a commonly adopted spacer or bridge in conjugated polymers. Introduction of vinylene spacers between aromatic units helps to reduce the torsional angle thereby lowering the band gap of the conducting polymer. Another advantage of vinylene and ethylenic bond between the rings is to impart restricted rotation of the rings due to the cis or trans configuration of the double bond.[31,32] Further lowering of the band gap has been achieved by placing an electron withdrawing cyano group on one of the vinyl carbons that helps in stabilizing the quinoidal state. V. Seshadri et al reported that conjugated polymers with band gaps of 1.2 eV were prepared from two isomeric monomers consisting of thieno[3,4-b]thiophene and cyanovinylene units.[33(a)] In another work, H. Padhy synthesized two β-cyanothiophene vinylene based polymers containing cyclopentadithiophene (CPDT-CN) and dithienosilole (DTS-CN) units. The effects of the bridged atoms (C and Si) and cyanovinylene groups on their thermal, optical, electrochemical, charge transporting, and photovoltaic properties were investigated[33(b,c)] (Fig 2.2**)**.

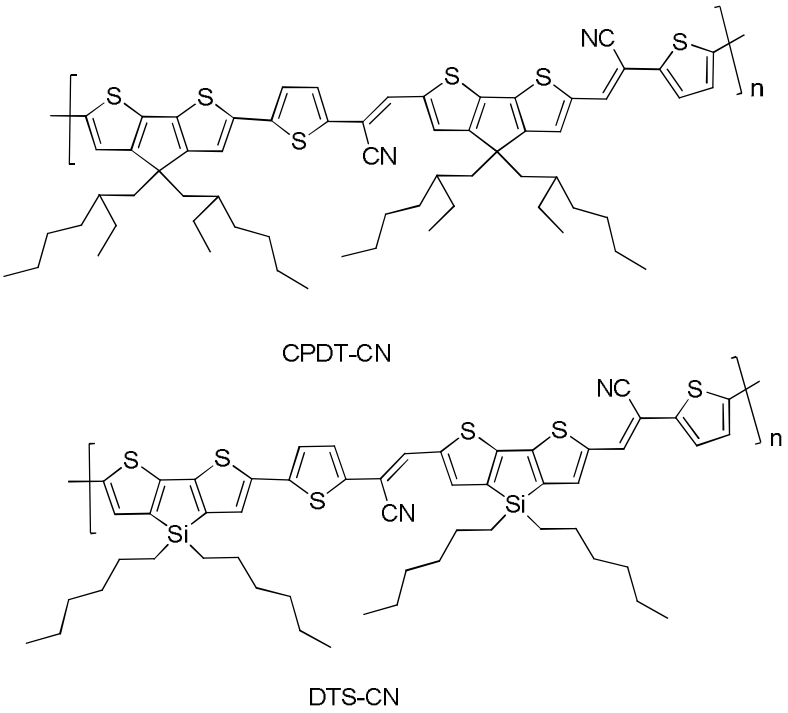

Fig. 2.2: Structure of two β-cyanothiophene vinylene based polymers

Benzene ring is the most fundamental building block for polymer solar cell materials whereby they can be coupled via single bonds as in PPP or fused to ribbons such as in poly (n)acenes. Poly (*p*-phenylene) shows poor solubility in common organic solvents which limits its application in organic electronics. Introduction of alkyl or alkoxyl chain on the backbone will increase the solubility.[34 (a)] Poly(phenylene vinylenes) (PPV) based polymers were one of the first semiconducting polymer species investigated for BHJ application.

T. Kietzke et al reported polymer blend solar cells with an external quantum efficiency of more than 30 % and a high overall energy conversion efficiency (ECE) of up to 1.7 % using a blend of M3EH−PPV (poly[2,5-dimethoxy-1,

4-phenylene-1,2-ethenylene-2-methoxy-5-(2-ethylhexyloxy)−(1,4-phenylene-1,2-ethenylene)]) (Fig.2.3) and CN−ether−PPV (poly[oxa-1,4-phenylene-1,2-(1-cyano)ethenylene-2,5-dioctyloxy-1,4-phenylene-1,2-(2-cyano) ethenylene- 1, 4-phenylene]).[34(b)]

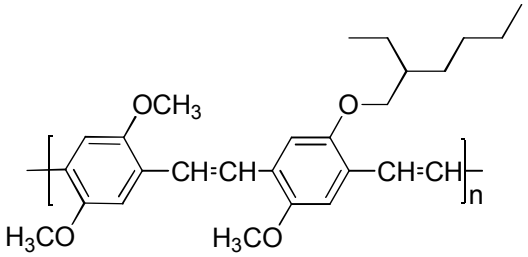

Fig.2.3: Structure of M3EH−PPV

Introducing acetylenic groups into the PPV structure form PPE-PPV showing outstanding optoelectronic properties and has successfully been used in solar cells. N. Tore et al incorporated silver nanoparticles in the active layer of anthracene containing poly(p-phenylene-ethynylene)-alt-poly(p-phenylene vinylene): phenyl-C61-butyric acid methyl ester) based bulk hetrojunction solar cells and found that the power conversion efficiency and also the life time of the cell were improved.[34(c)]

Thiophene has become one of the most commonly used building blocks in organic electronics due to its excellent optical and electrical properties as well as exceptional thermal and chemical stability.[35] Solubilizing moieties attached to the ring structure increases the solubility of polythiophenes. The band gap of the polythiophene can also be tuned by inductive and/or mesomeric effect from the heteroatom containing substitution. Of particular interest today are copolymers incorporating thiophene based fused rings, which allow high carrier mobilities or high efficiencies. Using a design strategy

similar to that used for regiosymmetric P3ATs,various kinds of rings have been successfully incorporated in polythiophene backbones.[36] Two frequently encountered thiophene-based conjugated polymers in literature are poly(3,4-ethylenedioxy thiophene) poly(styrene sulfonate) (PEDOT-PSS,) in conducting and hole transport layers for organic light emitting diodes (OLEDs) and PSCs and regioregular poly(3-hexylthiophene) (P3HT) as a hole transporting material in organic field effect transistors (OFETs) and PSCs [37] (Fig 2.4).

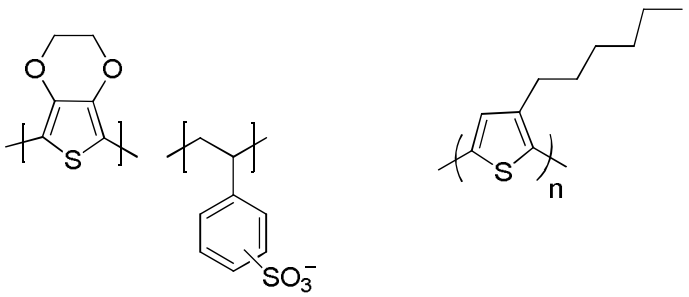

(a) (b)

Fig.2.4: Structure of (a) PEDOT-PSS and (b) P3HT

Fluorene based polymers have been widely explored as organic electronic material in the field of OLED, OFET and PVs due to their high photoluminescence quantum yield, high thermal and chemical stability, good film-forming properties and good charge transport properties. Polyfluorene, however, has a band gap of ~3.0 eV, which limits its application in solar cells. Therefore, fluorene is normally copolymerized with electron withdrawing moieties to construct polymers with band gap =2.0 eV. Palladium catalysed cross-coupling reaction is normally adopted for the polymerization due to the ease of halogenation at the 2,7-position of fluorene unit.

C. E. Song et al synthesized a set of novel conjugated polyfluorene copolymers, poly[(9,9'-didecylfluorene-2,7-diyl)-co-(4,7'-di-2-thienyl-2',1', 3'-benzothiadiazole-5, 5-diyl)-co-(pyrene-1,6-diyl)] via Pd(II)-mediated polymerization. The field effect carrier mobilities and optical, electrochemical, and photovoltaic properties of the copolymers were systematically investigated [38, 39] (Scheme 1).

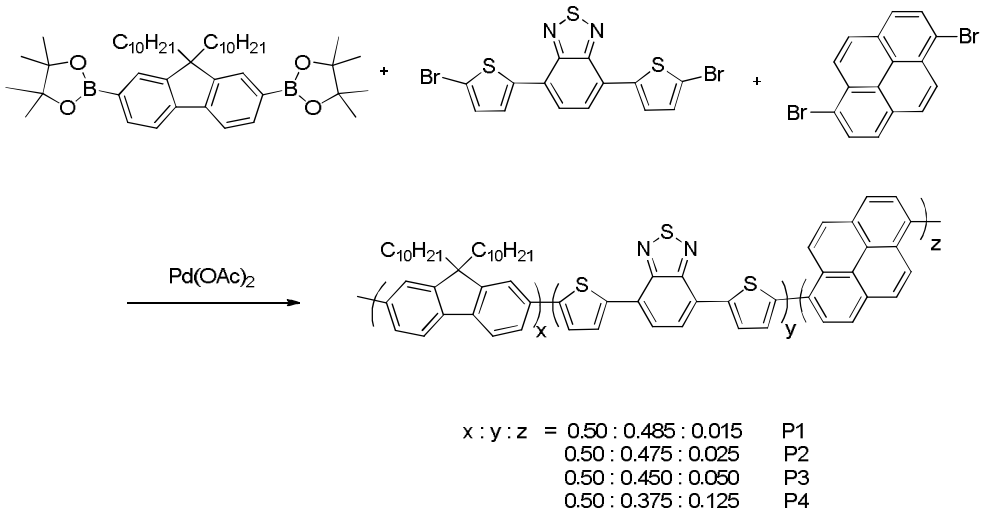

x : y : z = 0.50 : 0.485 : 0.015 P1
0.50 : 0.475 : 0.025 P2
0.50 : 0.450 : 0.050 P3
0.50 : 0.375 : 0.125 P4

Scheme 1: Synthesis of the copolymers

Fused heterocycles represent an important class of building blocks to achieve either low band gap or high carrier mobility depending on the orientation of the fused ring to the polymer main chain. They are one of the most frequently studied classes of organic materials due to their highly conjugated π-bonding systems, chemical stability, and tunable electronic properties. The fused system tends to favour the quinoidal mesomeric structure, resulting in the band gap being as low as 1.0 eV. Monomers with fused rings like carbazole, cyclopentadithiophene are useful building blocks to prepare low band gap polymers due to their coplanarity[40-50] (Fig 2.5).

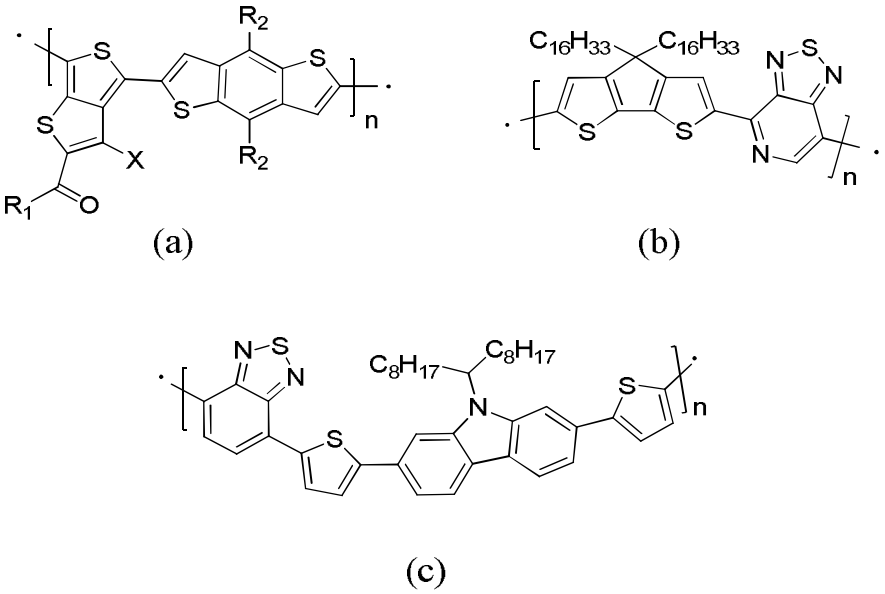

Fig. 2.5: Chemical structures of selected fused heterocycle-based polymers

Z. Feiz et al reported the first synthesis of a fused germaindaceno-dithiophene monomer and its polymerization with 2,1,3-benzothiadiazole by Suzuki polycondensation. The bridging hetero atom has also been shown to have a significant effect on the crystallinity of the polymer. The crystalline polymers demonstrated higher charge carrier mobilities ideal for a number of applications including bulk heterojunction solar cells. The improved crystallinity has been rationalised on the basis of the longer C–Ge bond length compared to the C–C bond, which changes the geometry of the fused ring allowing stronger π-π interactions to occur.[51]

2.3 Results and discussion

2.3.1 Synthesis of monomers

One of the monomers, benzene-1,4-diboronic acid used in polymer synthesis was obtained from Sigma Aldrich and used without further

purification. All the other monomers were synthesized on the basis of reported procedures and were characterized by spectroscopic techniques. HPLC grade solvents were used for the synthesis of monomers.

2.3.1.1 Synthesis of fluorene based monomers

2,7-Dibromofluorene[52] (M1) was prepared by the bromination of 9H - Fluorene. The dibromofluorene was treated with 1-bromooctane in the presence of KOH and a phase transfer catalyst in DMSO to give 2,7-dibromo-9,9-dioctyl fluorene[53] (M2). The above product was treated with n-butyl lithium and 2-isopropoxy-4,4,5,5-tetramethyl-1,3,2-dioxaborolane in dry THF at -78°C to form 2,7-bis(4,4,5,5-tetramethyl-1,3,2-dioxaborolan-2-yl)-9,9-dioctylfluorene[54] (M3) (Scheme 2). The ^{1}H NMR spectrum of M3 showed multiplets at δ 0.59-2.05 due to alkyl protons. It showed multiplets at δ 7.73-7.83 due to aromatic protons.

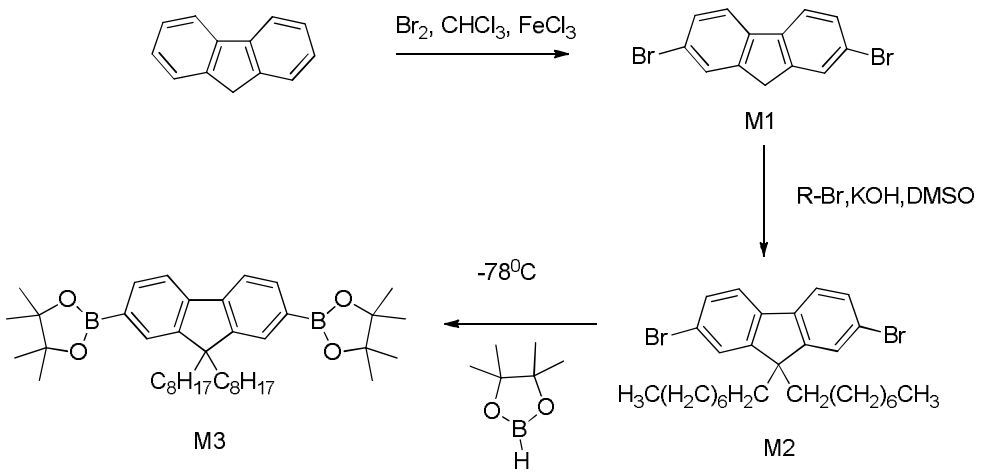

Scheme 2: Synthesis of fluorene based monomers

In another reaction 2,7-dibromofluorene (M1) on air oxidation in the presence of KOH in THF gave 2,7-dibromofluorenone[55] (M4). The synthetic route for the preparation of the compounds is presented in (Scheme 3). The ^{1}H NMR spectrum of M4 showed multiplets at δ 7.28-7.66 due to aromatic protons.

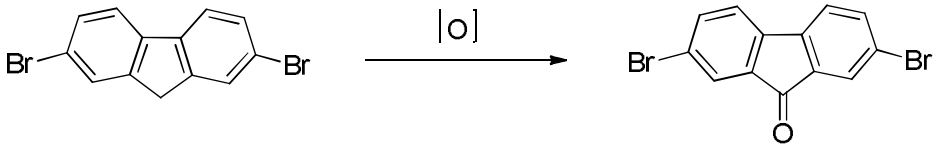

M4

Scheme 3: Synthesis of 2,7-dibromofluorenone

2.3.1.2 Synthesis of quinoxaline based monomers

A solution of 3,6-dibromo-1, 2-phenylenediamine on refluxing with acenaphthene quinone in ethanol and few drops of acetic acid gives 5,8-dibromoacenaphthyl quinoxaline (M5) as the product. 5,8-Dibromo-2,3-diphenyl quinoxaline (M6) was formed when 3,6-dibromo-1,2-phenylenediamine was treated with benzil. 10,13-dibromodibenzo[a,c]-phenazine (M7) was prepared by refluxing 3,6-dibromo-1,2-phenylene-diamine with phenanthrene-9,10-dione in ethanol/ acetic acid.[56] (Scheme 4). The ^{1}H NMR spectrum of all quinoxaline based monomers showed multiplets in the aromatic region.

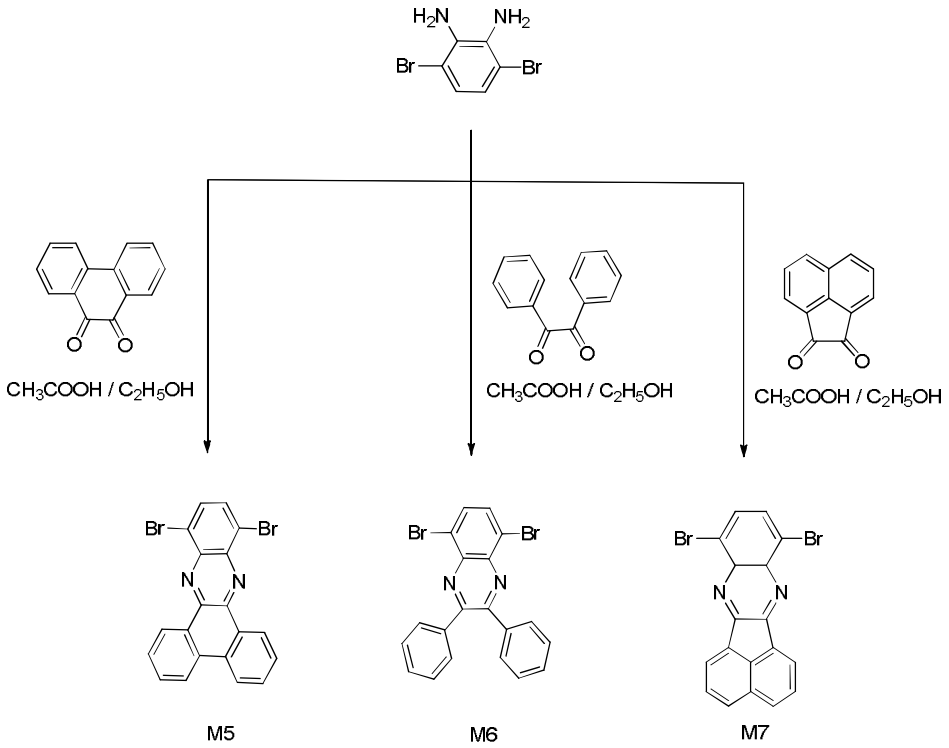

Scheme 4: Synthesis of quinoxaline based monomers

2.3.1.3 Synthesis of thiophene based monomers

In the synthesis of 3,4-dimethoxy thiophene [57](M8), first step involves the condensation of diethyl thiodiglycolate and diethyloxalate to give the 3,4-dihydroxythiophene dicarboxylic ester followed by methylation using freshly prepared dimethyl sulphate. This was followed by the hydrolysis of the ethyl ester with conc.HCl to form 3,4-dimethoxythiophene 2,5-dicarboxylic acid. Finally, the above product was decarboxylated at 160^{o}C to obtain the 3,4-dimethoxy thiophene as dark coloured liquid which was purified with column chromatography to yield a colourless liquid as the final product **(**Scheme 5). The ^{1}H NMR spectrum of dimethoxythiophene showed a

singlet at δ 3.8 due to methoxy hydrogens and another singlet at δ 6.2 due to aromatic hydrogens.

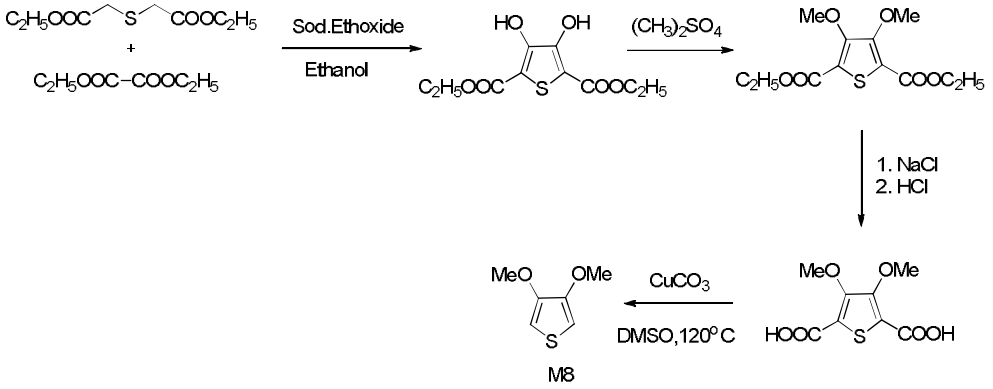

Scheme 5: Synthesis of 3,4-dimethoxy thiophene

3,4-dihexyl-2,5-dibromothiophene[58] was prepared by bromination of 3,4-dihexylthiophene with NBS in chloroform/acetic acid. The synthetic route for the preparation of the compounds is presented in Scheme 6.The ^{1}H NMR spectrum of the compound M9 showed multiplets at δ 0.89-2.51 due to aromatic protons.

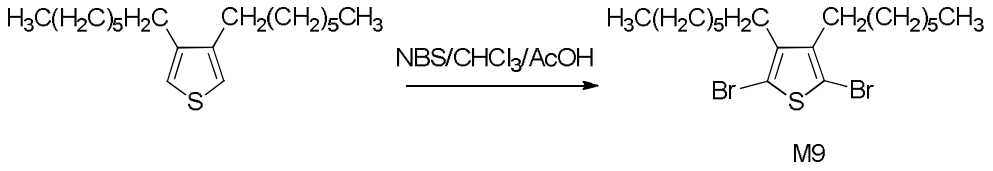

Scheme 6: Synthesis of 3,4-dihexyl-2,5-dibromothiophene

2.3.1.4 Synthesis of cyanovinylene based monomers

2,3-bis(4-bromophenyl)acrylonitrile[59](M10) was prepared by adding a solution of NaOH in ethanol to a mixture of 4-bromophenylacetonitrile and 4-bromobenzaldehyde in ethanol .

3-(4-bromophenyl)-2-(5-bromothiophen-2-yl) acrylonitrile (M11) was prepared by using 4-bromophenyl acetonitrile and 2-bromothiophene-5-aldehyde.2,2'-(thiophene-2,5-diyl)-bis-(3-(4-bromophenyl) acrylonitrile) (M12) was formed by treating 4-bromophenyl acetonitrile and 2,5-thiophene dialdehyde (Scheme 7). The ^{1}H NMR spectrum of the cyanovinylene compounds showed multiplets in the aromatic region and signals corresponding to the vinyl protons.

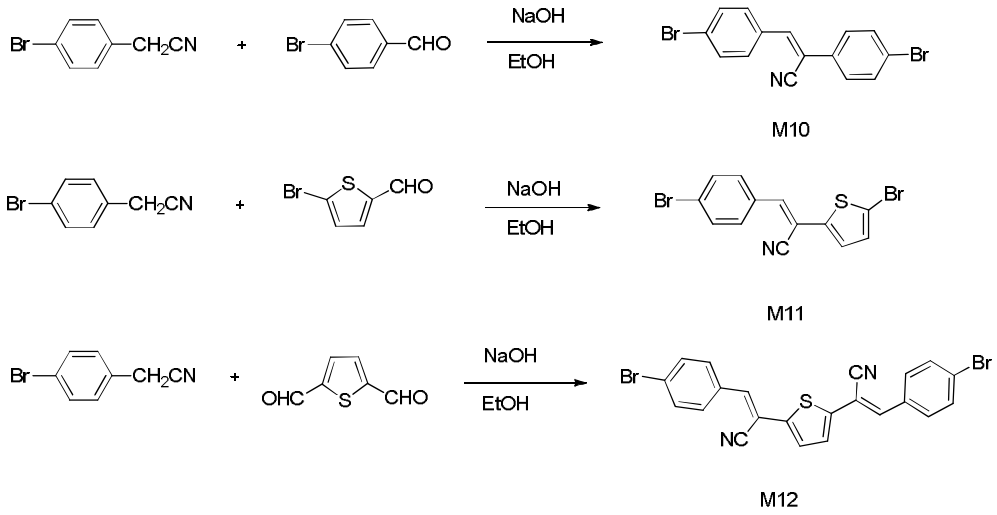

Scheme7: Synthesis of cyanovinylene based monomers

2.3.1.5 Synthesis of 3,6-Dibromo-N-(2-ethylhexyl)carbazole

3,6-Dibromo-N-(2-ethylhexyl) carbazole[60] (M13) was prepared by treating a solution of 3,6-dibromocarbazole with potassium carbonate and 2-ethylhexylbromide. The synthetic route for the preparation of the compounds is presented in (Scheme 8). The ^{1}H NMR spectrum of the compound M13 showed multiplets at δ 7.23-8.17 due to aromatic protons. The spectrum of M13 showed multiplets at δ 0.85-2.01 due to aliphatic protons. It also showed another multiplet around δ 4 due to –N-CH – protons.

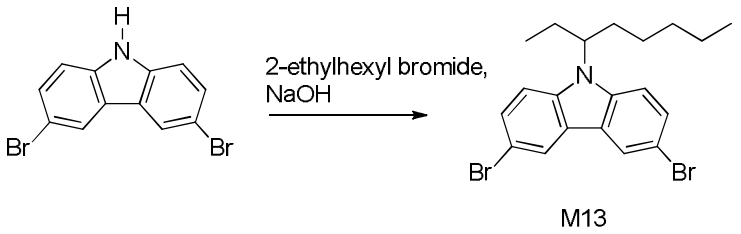

M13

Scheme 8: Synthesis of 3,6-Dibromo-N-(2-ethylhexyl)carbazole

2.3.1.6 Synthesis of 4,7-Dibromo-5,6-bis(decyloxy)benzo[c][1,2,5]oxadiazole

1,2-Bis(decyloxy)benzene was synthesised from catechol by treating it with 1-bromooctane and NaOH which was then nitrated with HNO_3. Next step involves the cyclisation of 1,2- dinitro-4,5-bis(decyloxy) benzene to form 5,6-bis(decyloxy)benzo[c][1,2,5]oxadiazole which was then brominated with bromine in acetic acid to form 4,7-Dibromo-5,6-bis(decyloxy)benzo [c][1,2,5]oxadiazole[61](M14) (Scheme 9). The ^1H NMR spectrum of the compound M14 showed multiplets at δ 0.9 - 1.8 due to aliphatic protons. The spectrum showed multiplets at δ 4.2 due to protons attached to alkoxy group.

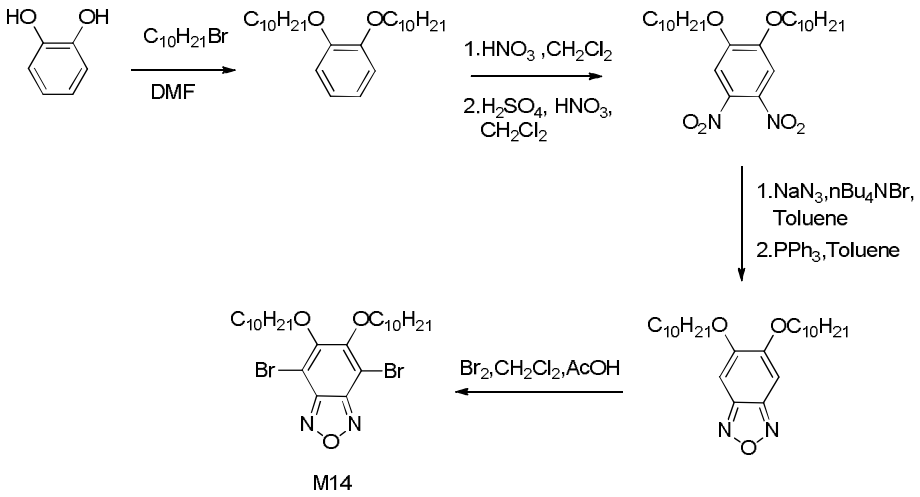

M14

Scheme 9: Synthesis of 4,7-Dibromo-5,6-bis(decyloxy)benzo[c][1,2,5]oxadiazole

2.4 Experimental procedure

2.4.1 Synthesis of fluorene based monomers

2.4.1.1 2,7-Dibromofluorene (M1)

To a solution of 9H-fluorene (6 g, 36 mmol), iron (III) chloride (92 mg, 1.6 mmol) in $CHCl_3$ (100 mL) at 0°C, 4 mL bromine was added drop by drop. The mixture was stirred for 12 h. After the reaction, it was poured into 50 mL water. The precipitate was washed with $NaHCO_3$ and $NaHSO_3$ solution. The organic layer was extracted with $CHCl_3$. The organic layer was dried over anhydrous magnesium sulphate. After filtration, the solvent was removed using rotary vacuum evaporation, and the residue was recrystallized from ethanol resulting in white crystalline product. Yield: 75%. M.P:161-166°C. ^{1}H NMR (400 MHz, $CDCl_3$): δ 7.66 (s, 2H), 7.60-7.59 (d, 2H), 7.51-7.49 (d, 2H), 3.87 (s, 2H).

2.4.1.2 2, 7-Dibromo-9,9-dioctyl-9H-fluorene (M2)

KOH solution (10mL, 50 %) and 1-Bromooctane (5.60 g, 29.0 mmol) was added drop wise to a mixture of 2,7-dibromo-9H-fluorene (3.88g, 12.0 mmol), tetrabutyl ammonium bromide (0.0225 g, 0.0975 mmol) in DMSO (50.0 mL) under N_2 atmosphere. The reaction mixture was stirred at 80°C for 2 days. The mixture was poured into H_2O (500 mL). The organic layer was extracted with dichloromethane. The combined organic layer was dried over anhydrous $MgSO_4$. The solvent was removed under reduced pressure. The crude product was purified by recrystallization from hexane to yield colourless crystals. Yield: 89%. M.P: 59-63 °C. ^{1}H NMR (400 MHz, $CDCl_3$), δ: 7.51 (s, 2H), 7.45 (m, 4H), 1.90 (m, 4H), 1.25-0.86 (m, 24H),

0.83 (t, 6H).^{13}C NMR ($CDCl_3$, 100 MHz), ppm: 153.2, 139.8, 131.2, 126.2, 122.3, 121.1, 46.4, 41.8, 31.7, 29.6, 29.0, 23.9, 22.8, 14.1. MS m/z : 548.4.

2.4.1.3 2,7-Bis(4,4,5,5-tetramethyl-1,3,2-dioxaborolan-2-yl)-9,9-dioctylfluorene(M3)

To a stirred solution of 2,7-dibromo-9,9-dioctyl fluorene (5.0 g, 9.1 mmol) in THF (70 ml) at -78°C was added drop wise n-butyl lithium in hexane (7.6 ml, 2.5 M, 19 mmol) at -78°C. The mixture was warmed to 0°C for 15 min and cooled back to -78°C. 2-isopropoxy-4,4,5,5-tetramethyl-1,3,2-dioxaborolane (4 g, 21.5 mmol) was added rapidly to the solution. The resulting mixture was warmed to room temperature and stirred for 24 h. The mixture was poured into water and extracted with diethyl ether. The organic extract was washed with brine and dried over magnesium sulphate. The solvent was removed under reduced pressure, and the crude product was purified by column chromatography, eluting with 2% ethyl acetate and hexane to give 2,7-bis(4,4,5,5-tetramethyl-1,3,2-dioxaborolan-2-yl)-9,9-dioctylfluorene as a pale yellow solid. Yield: 65%. ^{1}H NMR (400 MHz, $CDCl_3$), δ: 7.83 (d, 2H), 7.76 (s, 2H), 7.73 (d, 2H), 2.05 (m, 4H), 1.44 (s, 24H), 1.25-1.09 (m, 24H), 0.82 (t, 6H). MS m/z: 642

2.4.1.4 2,7-dibromofluorenone(M4)

Into a 100mL three-necked flask equipped with a mechanical stirrer, a snorkel and an air condenser were fitted, 2, 7-dibromo-9-fluorene (1.620 g, 5 mmol), KOH (0.280 g, 5 mmol) and THF (15 mL) were added. The reaction mixture was stirred at room temperature while the solution was kept lower than the snorkel, and air was introduced for 5 min every 30 min to ensure that there was sufficient oxygen with minimal loss of solvent. At

the completion of the reaction, the reaction mixture was filtered to remove KOH and the filtrate was concentrated to obtain the crude product.

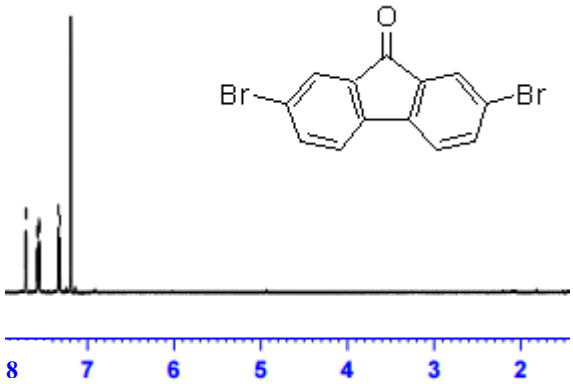

The crude product was washed with water (3 * 100 mL) and dried to give 2,7-dibromofluorenone as a yellow solid, Yield: 98%. M.P: 203-205°C. ^{1}H NMR (400 MHz, $CDCl_3$), ppm : 7.66 (dd, 2H), 7.52 (dd, 2H), 7.28 (s, 2H). ^{13}C NMR ($CDCl_3$, 100 MHz), ppm : 191.1, 142.4, 137.7, 135.4, 128.0, 123.5, 122.0. Elemental Analysis calculated for $C_{13}H_6Br_2O$: C, 46.20; H, 1.79. Found C, 46.44; H, 1.81.

2.4.2 Synthesis of quinoxaline based monomers

2.4.2.1 5,8-Dibromoacenaphthyl quinoxaline (M5)

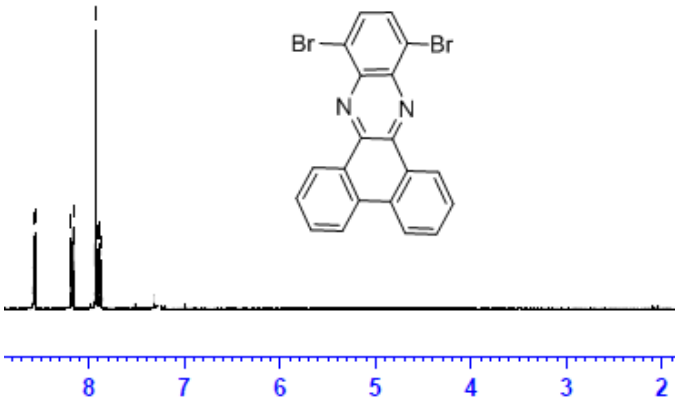

A solution of 3,6-dibromo-1, 2-phenylenediamine (0.15 g, 0.56 mmol) and acenaphthenequinone (0.10 g, 0.55 mmol) in ethanol (20 mL) and few drops of glacial acetic acid was heated to reflux for 1h, and cooled to 0°C. The precipitate formed was separated by filtration and washed with ethanol to afford 5,8-dibromoacenaphthyl quinoxaline as light yellow solid. Yield: 75%. ^{1}H NMR (400 MHz, $CDCl_3$), δ : 8.54 (d, 2H), 8.15 (d, 2H), 7.92 (s, 2H), 7.89-7.86 (m, 4H)

2.4.2.2 5,8-Dibromo-2,3-diphenyl quinoxaline (M6)

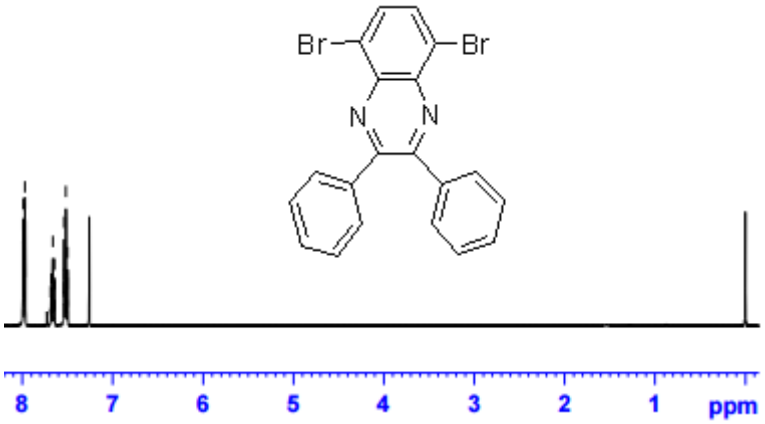

A solution of 3,6-dibromo-1, 2-phenylenediamine (1.0 g, 3.8 mmol) and benzil (0.80 g, 3.8 mmol) in ethanol (40 mL) and few drops of glacial acetic acid was heated to reflux for 1h, and cooled to 0°C. The precipitate formed was isolated by filtration and washed with ethanol to afford 5, 8-dibromo-2,3-diphenyl quinoxaline as light yellow solid. Yield: 80%. M. P: 221°C. ^{1}H NMR (400 MHz, $CDCl_3$), δ: 7.92 (s, 2H), 7.64 (m, 4H), 7.37 (m, 6 H). ^{13}C NMR ($CDCl_3$, 100 MHz), ppm : 123.7, 128.4, 129.6, 130.2, 133.1, 137.9, 139.4, 154.14. GC-MS: m/z=439.9

2.4.2.3 10,13-Dibromodibenzo[a,c]phenazine(M7)

A solution of 3,6-dibromo-1,2-phenylenediamine (1.03 g, 3.9 mmol) and phenanthrene-9,10-dione (0.81 g, 3.9 mmol) in 42 mL ethanol/ acetic acid (20:1) was heated to reflux for 2 h, and cooled to 0°C. The precipitate formed was isolated by filtration and washed with ethanol to afford 10, 13-dibromodibenzo [a,c] phenazine as yellow solid. Yield: 78%. M.P: 317 °C.^{1}H NMR ($CDCl_3$): δ 9.48 (dd, 2 H), 8.57 (dd, 2 H), 8.04 (s, 2H), 7.87-7.83 (dt, 2 H). ^{13}C NMR ($CDCl_3$, 100 MHz), ppm : 123.1, 124.2, 127.3, 128.4, 129.6, 131.3, 132.7, 132.9, 143.5.GC-MS: m/z = 437.9

2.4.3 Synthesis of thiophene based monomers

2.4.3.1 Diethyl thiodiglycolate

In a 500 mL round bottom flask, thiodiglycolic acid (100 g, 0.666 mol) was dissolved in dry ethanol (250 mL) and conc. sulphuric acid (10 mL) was added drop wise to it. The resulting mixture was refluxed for 24 h. The excess methanol was evaporated and the residue was dissolved in ethyl acetate, washed with saturated sodium bicarbonate solution until the aqueous layer was neutral. The organic layer was dried over sodium sulfate and the solvent was removed on a rotary evaporator to afford a light yellow liquid. Yield: 89%. M.P: 69-72 °C. ^{1}H NMR (400 MHz, $CDCl_3$), δ: 4.2 (q, 4H), 3.4 (s, 4H), 1.4 (t, 6H).

2.4.3.2 3,4-Dimethoxy-2,5-dicarbethoxythiophene

A solution of 10.5 g of sodium metal in 100 mL of dry ethanol was cooled at 0–5°C. To this, a solution of 26.7 g of diethyl thiodiglycolate and 26.7 g of diethyl oxalate was added and stirred. The temperature was maintained at 0°C. The sodium salt was precipitated as a yellow solid. The

reaction was completed by heating the reaction mixture to reflux for 2 h. After cooling, the solid was filtered and dried. The sodium salt of diester (15 g, 54.3 mmol) was taken in 65 mL of freshly distilled dimethyl sulfate and the mixture was heated at 100°C for 1 h. The excess dimethyl sulfate was distilled at low pressure and the crude product was dissolved in ethyl acetate (100 mL) and washed with cold 5% NaOH solution (50 mL). The organic layer was extracted and dried over sodium sulfate and solvent was evaporated to afford the compound as a pure light yellow solid. Yield: 64%. ^{1}H NMR (400 MHz, $CDCl_3$), δ: 4.1 (q, 4H), 3.9 (s, 6H), 4.1 (q, 4H), 1.2(t, 6H).

2.4.3.3 3,4-Dimethoxy thiophene-2,5-dicarboxylic acid

In a 100 mL round bottom flask 3,4-dimethoxy-2,5-dicarbethoxy thiophene (9 g, 34.6 mmol) was taken and 10% NaOH (50 mL) was added to it. The mixture was refluxed for 1 h. The reaction mixture was cooled to room temperature and conc. HCl was added to it with stirring. The precipitate thus formed was collected in a Buchner funnel and dried in an oven to give the above product as a white solid. Yield: 84%. ^{1}H NMR (400 MHz, $CDCl_3$), δ: 10.2 (s, 2H), 4 (s, 6H)

2.4.3.4 3,4-Dimethoxythiophene(M8)

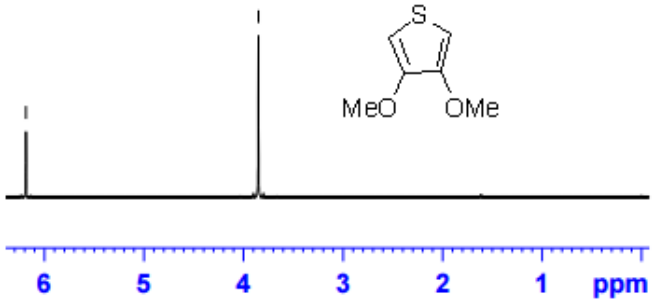

A 100 mL dry three necked round bottom flask was charged with 3,4-dimethoxy thiophene-2,5-dicarboxylic acid (9 g, 43.3 mmol), copper chromite (0.56 g, 4% mol) and dry quinoline (30 ml). The mixture was heated at 160°C for 4 h under argon atmosphere. The reaction mixture was vacuum distilled and the pink liquid obtained was dissolved in 50 mL of ethyl acetate and washed repeatedly with 5% HCl and water. The organic layer was dried over anhydrous Na_2SO_4, filtered and the solvent was evaporated to give a crude brown coloured liquid. The crude compound was purified by column chromatography using silica gel as the adsorbent and eluting using ethyl acetate/ petroleum ether mixture (v/v) to afford the product as colourless liquid, Yield: 56 %. B.P.110°C (17 bar). ^{1}H NMR (400 MHz, $CDCl_3$), δ: 6.2 (s, 2H), 3.8 (s, 6H). ^{13}C NMR ($CDCl_3$, 100 MHz), ppm : 57, 36, 96, 35, 147, 90. MS (EI); m/z= 144

2.4.3.5 3,4-Dihexyl-2,5-dibromothiophene (M9)

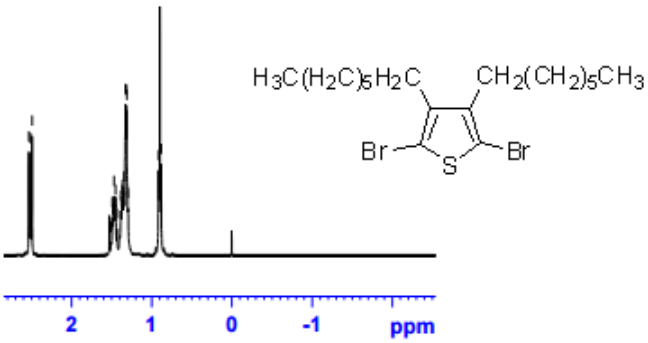

In a round-bottom flask, 3,4-dihexylthiophene (3.2 g, 12 mmol) and a mixture of chloroform/acetic acid 50:50 (50 mL) were stirred and kept at 30°C; NBS (4.48 g, 25.2 mmol) was slowly added. After complete addition, the reaction mixture was refluxed for 15–20 min, cooled to room

temperature and diluted with an equal volume of water, the chloroform layer was separated and washed (3 times) with sodium carbonate solution and once with water. The dibromo derivative was obtained as yellowish oil. Yield: 90 %. ^{1}H NMR (400 MHz, $CDCl_3$), δ: 2.51(t, 4H), 1.31 (m, 20H), 0.89(t, 6H).

2.4.4 Synthesis of Cyanovinylene based monomers

2.4.4.1 2,3-Bis(4-bromophenyl)acrylonitrile (M10)

4-Bromophenylacetonitrile (1.96 g, 10 mmol) and 4-bromobenzaldehyde (1.85 g, 10 mmol) were dissolved in ethanol (50 mL). To the mixture was added drop wise a solution of NaOH (50 mg) in ethanol (30 mL) under nitrogen atmosphere. The reaction mixture was stirred at room temperature for 1h. The product was obtained as a white precipitate. It was filtered, and washed with water to give a white powder.Yield: 91%. ^{1} H NMR ($CDCl_3$): δ 7.77 (d, 2H), δ 7.62-7.52 (m, 6H), 7.45 (s, vinylic proton).

2.4.4.2 3-(4-bromophenyl)-2-(5-bromothiophen-2-yl) acrylonitrile (M11)

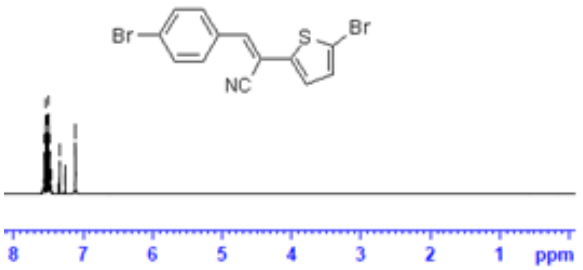

4-Bromophenylacetonitrile (1.96 g, 10 mmol) and 2-bromothiophene-5-aldehyde (1.91 g, 10mmol) were dissolved in 50 mL of dry ethanol under nitrogen atmosphere in 100 mL three-necked round-bottomed flask. A

mixture of 50 mg of sodium hydroxide and 30 mL of dry ethanol was added slowly, and the crude product was precipitated in the reaction mixture. The reaction mixture was stirred for 1 h at room temperature, and the precipitate was filtered and washed with water. A yellow powder was obtained. Yield: 85%. ^{1}H NMR (400 MHz, $CDCl_3$), δ: 7.8 (s, vinylic proton), 7.2 (d, 2H), 7.42-7.4 (m, 4H).

2.4.4.3 2,2'-(thiophene-2,5-diyl)-bis-(3-(4-bromophenyl) acrylonitrile) (M12)

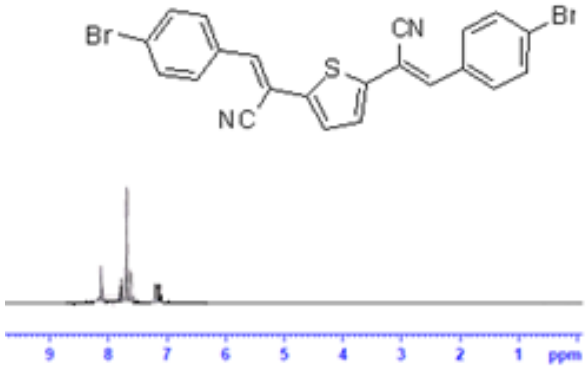

4-Bromophenylacetonitrile (1.96 g, 10 mmol) and 2,5-thiophene dialdehyde (0.70 g, 5 mmol) were dissolved in 50 mL of dry ethanol under nitrogen atmosphere in 100 mL three-necked round-bottomed flask. A mixture of 50 mg of sodium hydroxide and 30 mL of dry ethanol was added slowly, and the crude product was precipitated in the reaction mixture. The reaction mixture was stirred for 1 h at room temperature, and the precipitate was filtered and washed with water. A yellow powder was obtained. Yield: 80%, ^{1}H NMR (400 MHz, $CDCl_3$), δ: 8.1 (s, vinylic protons), 7.3 (d, 2H), 7.8-7.9 (m, 8H).

2.4.5 Synthesis of 3,6-Dibromo-N-(2-ethylhexyl)carbazole (M13)

To a solution of 3,6-dibromocarbazole (6.5 g, 20 mmol) dissolved in 50 mL of anhydrous DMF was added potassium carbonate (5.5 g, 40 mmol). The mixture was allowed to stir for 1 h, after which 2-ethylhexylbromide (5.8 g, 30 mmol) was added drop wise. The reaction was allowed to reflux for 2 days. It was cooled, the mixture was poured into water and extracted with chloroform three times and the combined organic layer was dried over anhydrous magnesium sulfate. The solvent and the unreacted 2-ethylhexylbromide were removed under reduced pressure and the residue was purified by column chromatography with hexane and ethyl acetate (v/v) to afford the compound as a waxy solid. Yield: 80%. M.P: 62-63 $^{\circ}$C. ^{1}H NMR (400 MHz, $CDCl_3$), δ: 8.17 (s, 2H), 7.60-7.52 (d, 2H), 7.30-7.23 (d, 2H), 4.15-4.09 (m, 2H), 2.01-1.97 (m, 1H), 1.35-1.25 (m, 8H), 0.96-0.85 (m, 6H).

2.4.6 Synthesis of benzo[c][1,2,5]oxadiazole

2.4.6.1 1,2-Bisdecyloxybenzene

Sodium hydroxide (8 g, 0.2 mol) was dissolved in methanol (200 mL) at 0°C for 30 min; catechol (10 g, 90.8 mmol) was added slowly. The solution turned to deep green and finally dark. At this time, 1-bromodecane (42.5 mL, 0.2 mmol) was added to the mixture drop wise. The mixture was refluxed in dry nitrogen atmosphere with stirring. After 8 h, the reaction mixture was cooled to room temperature and the solvent was evaporated under reduced pressure. The organic layer was separated using ethyl acetate, dried over anhydrous magnesium sulfate ($MgSO_4$) and concentrated. The compound obtained was triturated from methanol. Yield: 75 %. ^{1}H NMR

(400 MHz, $CDCl_3$), δ: 6.87 (m, 4H), 3.99~3.95 (t, 4H), 1.83~1.76 (m, 4H), 1.48~1.41 (m, 4H), 1.33~1.26 (m, 24H), 0.88~0.85 (t, 6H).

2.4.6.2 1,2-Dinitro-4,5-bis(decyloxy)benzene

65% HNO_3 (20 mL) was added drop wise to a two-necked round bottom flask containing 1,2-bis(decyloxy)benzene (10 g, 25 mmol), CH_2Cl_2 (140 mL), and AcOH (140 mL) and was cooled to 10°C . The reaction mixture was warmed to room temperature and stirred for 1 h. The mixture was cooled to 10°C and conc HNO_3 (50 mL) was added drop wise. The mixture was warmed to room temperature and stirred for 40 h before being poured into ice water. The CH_2Cl_2 layer was separated and the aqueous phase extracted with CH_2Cl_2. The organic phases were combined, washed sequentially with water, sat. $NaHCO_3$ (aq), and brine, and dried with $MgSO_4$. Concentration under vacuum gave a crude product that was recrystallized from EtOH. Yield: 95%. ^{1}H NMR (400 MHz, $CDCl_3$), δ: (s, 2H), 4.3 (t,4H), 1.9 (m, 4H), 1.4-1.6 (m, 28H), 1.3 (t, 6H).

2.4.6.3 5,6-Bis(decyloxy)benzo[c][1,2,5]oxadiazole

A mixture of 1,2- dinitro-4,5-bis (decyloxy) benzene (2.848 g, 6 mmol), NaN_3 (1.95g, 30 mmol), and n-Bu_4NBr (0.39 g, 1.2 mmol) was heated under reflux in toluene (10 mL) for 12 h. At this point, the starting material has been consumed (TLC); PPh_3 (1.9 g, 7.2mmol) was added and the mixture was heated under reflux for additional 24 h. The reaction mixture was cooled to room temperature and filtered through a short silica plug; the plug was rinsed with CH_2Cl_2. Evaporation of the solvents from the combined organic phases, under reduced pressure, afforded a crude solid that was recrystallized (EtOH) to yield an off-white solid Yield: 63%. ^{1}H NMR

(400 MHz, $CDCl_3$), δ: 7.2 (s, 2H), 4.3 (t, 4H), 1.9 (m, 4H), 1.3-1.4 (m, 28H), 1.1 (t, 6H).

2.4.6.4 4,7-Dibromo-5,6-bis(decyloxy)benzo[c][1,2,5]oxadiazole (M14)

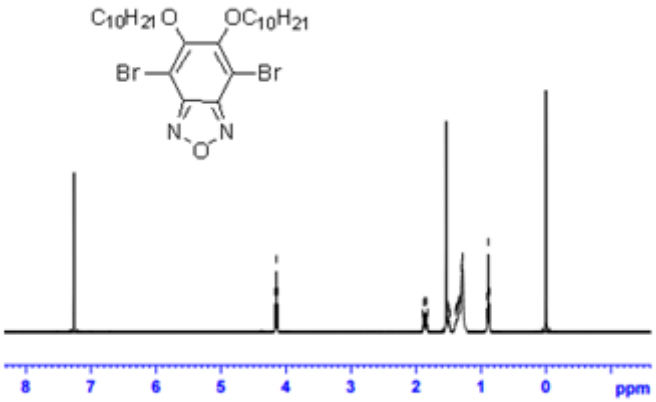

AcOH (10 mL) and Br_2 (2 mL, 25 mmol) were added sequentially to a solution of 5,6-bis (decyloxy) benzo[c][1,2,5] oxadiazole (2.5 g, 6 mmol) in CH_2Cl_2 (80 mL). The resulting mixture was stirred in the dark for 3 days at room temperature. The reaction mixture was poured into aqueous NaOH solution (10 g in 200 mL). The organic compounds were extracted with CH_2Cl_2; the combined organic extracts were washed with brine and concentrated under reduced pressure to afford a crude solid that was purified through column chromatography to yield a white solid. Yield: 79%. ^{1}H NMR (400 MHz, $CDCl_3$), δ: 4.2 (t, 4H), 1.8 (m, 4H), 1.2-1.3 (m, 28H), 0.9 (t, 6H).

2.5 Conclusion

A series of monomers were successfully synthesized. The strategies used for synthesizing the monomers were discussed in this chapter. All the compounds synthesized were spectroscopically characterized.

References

[1] N. Lior, Energy, 2008,33, 842.

[2] H. Hottel, Solar Energy, 1989, 43, 10

[3] V. Balzani, A. Credi, M. Venturi, Chem. Sus. Chem, 2008, 1, 26.

[4] D. Wöhrle, D.Meissner, Adv. Mater., 1991, 3, 129.

[5] N. S. Sariciftci, Mater. Today, 2004, 7, 40.

[6] J. Y. Kim, K. Lee, N. E. Coates, D. Moses, T.Q. Nguyen, M. Dante, A. J. Heeger, Science, 2007, 317, 222.

[7] H. H. Fong, V. A. Pozdin, A.Amassian, G. G.Malliaras, D.M .Smilgies, M. He, S. Gasper, F. Zhang, M. Sorensen, J. Am. Chem. Soc., 2008, 130, 13202.

[8] H. Hoppe, N. S. Sariciftci, J. Mater. Chem., 2006, 16, 45.

[9] D. M. de Leeuw, M. M. J .Simenon, A. R. Brown, R. E. F.Einerhard, Synth. Met, 1997, 87, 53.

[10] M. C. Scharber, D. Mühlbacher, M. Koppe, P. Denk, C.Waldauf, A. J. Heeger, C. J. Brabec,, Adv. Mater, 2006, 18, 789.

[11] J. Roncali, Chem. Rev., 1997, 97, 173.

[12] J. L. Bre´das, J. Chem. Phys., 1985, 82, 3808.

[13] K.Y. Jen, M. R. Maxfield, L. W. Shacklette, R. L. Elsenbaumer, J. Chem. Soc., Chem. Commun., 1987, 309.

[14] J. M. Raimundo, P. Blanchard, I. Rak, R. Hierle, L.Michaux, J. Roncali, Chem. Commun., 2000, 1597.

[15] H. A. Ho, H. Brisset, P. Fre` re, J. Roncali, J. Chem. Soc., Chem. Commun. 1995, 2309.

[16] H. A. Ho, H. Brisset, E. Elandaloussi, P. Fre` re, J. Roncali, Adv. Mater. 1996, 8, 990.

[17] H. Cha , H. N. Kim , T. K. An ,M. S. Kang , S. K. Kwon , Y. H. Kim,C. E. Park, ACS Appl. Mater. Interfaces, 2014 ,6, 15774.

[18] J. Roncali, R. Garreau, A. Yassar, P. Marque, F. Garnier, M. Lemaire, J. Phys. Chem., 1987, 91, 6706.

[19] R. D. McCullough, Adv. Mater., 1998, 10, 93.

[20] H. Sirringhaus, P. J. Brown, R. H. Friend, M. M. Nielsen, K. Bechgaard, B. M. W. Voss, A. J. H. Spiering, R. A. J. Janssen, E. W. Meijer, P. Hervig, D. M. de Leeuw, Nature, 1999, 401, 685.

[21] F. Wudl, M. Kobayashi, A. J. Heeger, J. Org. Chem., 1984, 49, 3382.

[22] M. Pomerantz, B. Gill, M. O. Harding, J. J. Tseng, W. J. Pomerantz, J. Chem. Soc., Chem. Commun., 1992, 1672.

[23] S. Y. Hong, D. S. Marynick, Macromolecules, 1992, 25, 4652.

[24] G. A. Sotzing, K. Lee, Macromolecules, 2002, 35, 7281.

[25] Y.Y. Liang, J. Am. Chem. Soc., 2009 , 131, 7792.

[26] J. M. Szarko, J. Guo, Y. Liang, B. Lee, B. S. Rolczynski, J. Strzalka, T. Xu, S. Loser, T. J. Marks, L. Yu, L. X. Chen, Adv. Mater., 2010 , 22, 5468.

[27] F. He, W. Wang, W. Chen, T. Xu, S. B. Darling, J .Strzalka, Y. Liu, L. Yu, J. Am. Chem..Soc., 2011, 3284.

[28] A. T. Yiu, P. M.Beaujuge, O. P. Lee, C. H. Woo, M. F. Toney, J. M. J. Frŕchet, J. Am.Chem. Soc., 2012, 134, 2180.

[29] (a) Y. P.Zou, A. Najari, P. Berrouard, S. Beaupre, B. R. Aich, Y. Tao, M. Leclerc, J. Am. Chem. Soc., 2010, 132, 5330

(b) E.G. Wang, Appl. Phys. Lett., 2008, 92 , 033307.

[30] G. A. Sotzing, J. R. Reynolds, J. Chem. Soc. Chem. Commun., 1995, 703.

[31] G. A. Sotzing, C. A. Thomas, J. R. Reynolds, Macromolecules, 1998, 31, 3750.

[32] V. Seshadri, G. A. Sotzing, Chem Mater, 2004, 16, 5644 ; (b) H. Padhy, D. Sahu, D. Patra, M. Krishnapola, J. Huang, C. Chu, K. Wei, H. Lin, J. Polym. Sci. A. Polym. Chem, 2011, 49, 3417.

[33] (a) K .Tajima, Y. Suzuki, K. Hashimoto, J. Phys. Chem C, 2008, 112, 8507

(b) T. Kietzke, H. Hörhold, D. Neher, Chem. Mater.,2005,176532

(c) N. Tore, E. A. Parlak, T. A. Tumay, P. Kavak, S. Sarioglan, S. Bozar, S. Gunes, C. Ulbricht, D. A. M. Egbe, J. Nanopart. Res., 2014, 16, 2298

[34] D. Fichou, Handbook of Oligo and Polythiophenes, Wiley-VCH, Weinheim, 1999.

[35] W.Ma, C. Yang, X .Gong, K. Lee, A. J. Heeger, Adv. Funct. Mater., 2005, 15, 1617.

[36] R. Miyakoshi, A. Yokoyama, T. Yokozawa, J. Am. Chem. Soc., 2005, 127, 17542.

[37] G. L. Schulz, X. Chen, S. Holdcroft, Appl. Phys. Lett., 2009, 94, 023302.

[38] C. E. Song, I. N. Kang, J. H. Kim, D. H. Hwang, J. C. Lee, T. Ahn, W. S. Shin, S. J. Moon, S. K. Lee, J. Polym. Sci. A. Polym. Chem., 2013, 51, 1512.

[39] N. Blouin, A. Michaud, D. Gendron, S. Wakim, E. Blair, R. Plesu, M. Belletête, G. Durocher, Y. Tao, M. Leclerc, J. Am. Chem. Soc., 2008, 130, 732.

[40] S. H. Park, A. Roy, S. Beaupre, S. Cho, N. Coates, J. S. Moon, D. Moses, M. Leclerc, K. Lee, A. J. Heeger, Nat. Photonics, 2009, 3, 297.

[41] R. P. Qin, W. W. Li, C. H. Li, C. Du, C. Veit, H. F. Schleiermacher,. M. Andersson, Z. S. Bo, Z. P. Liu, O. Inganas, U. Wuerfel,. F. L. Zhang, J. Am. Chem. Soc., 2009, 131, 14612.

[42] P. M. Beaujuge, W. Pisula, H. N. Tsao, S. Ellinger, K. Muüllen, J. R. Reynolds, J. Am. Chem. Soc., 2009, 131, 7514.

[43] H.Y. Chen, J. Hou, A.E. Hayden, H. Yang, K.N. Houk, Y. Yang, Adv. Mater., 2010, 22, 371.

[44] J.H. Hou, H.Y. Chen, S.Q. Zhang, G. Li, Y. Yang, J. Am. Chem. Soc., 2008, 130,16144..

[45] L. J. Huo, H. Y. Chen, J. H. Hou, T. L. Chen, Chem. Comm., 2009, 37, 5570.

[46] R. C. Coffin, J. Peet, J. Rogers , G. C. Bazan , Nat. Chem., 2009, 1,657.

[47] G. C. Welch, G. C. Bazan, J. Am. Chem. Soc., 2011, 133, 4632 .

[48] Z. B. Henson, G. C. Welch, T. Poll, G. C. Bazan, J. Am. Chem. Soc., 2012, 134, 3766.

[49] L. Ying, G. C. Bazan, J. Am. Chem. Soc., 2011, 133, 18538.

[50] H. Brisset, C. T. Gautier, A.Gorgues, M. Jubault, J.Roncali. J. Chem. Soc. Chem. Commun., 1994, 1305.

[51] Z. Feiz, R. S. Ashraf, Z. Huang, J. Smith, J. Kline, P. D. Angelo, T. D. Anthopoulos, J. R. Durrant, I. McCullocha, M. Heeney, Chem. Commun., 2012, 48, 2955.

[52] R. Zhao, X. Zhan, J. Yao, G. Sun, Q. Chen, Z. Xie, Y. Ma**,** Polym. Chem.**,** 2013**,** 4, 5382.

[53] N. Lin, G. W. Toh, Y. Feng, X. Y. Liu , H. Xu , J. Mater. Chem. B, 2014, 2, 2136.

[54] P. Sonar, J. Zhang, A. C. Grimsdale, K. Mullen, M. Surin, R. Lazzaroni, P. Leclerc, S. Tierney, M. Heeney, I. McCulloch, Macromolecules, 2004, 37, 709.

[55] X. Zhang, X. Ji, S. Jiang, L. Liu, B. L. Weeks, Z. Zhang, Green Chem., 2011, 13, 1891.

[56] M. Younus, A. D, Kohler, S .Cron, N Chawdary, M. R. A. Mandhary, M.S. Khan, J . Lewis, N. J. Long, R. H. Friend, P. R, Raithby, Angew. Chem., 1998, 37, 3036.

[57] (a) E. W. Fager,. J. Am. Chem. Soc., 1945, 67, 2217.

(b) K. Krishnamoorthy, A. V. Ambade, M. Kanungo, A. Q. Contractor, A. Kumar, J. Mater. Chem. 2001, 11, 2909.

[58] F. Banishoeib, A. Henckens, S. Fourier, G. Vanhooyland, M. Breselge, J. Manca, T.J. Cleij, L. Lutsen, D. Vanderzande, L. H. Nguyen, H. Neugebauer, N. S. Sariciftci, Thin Solid Films, 2008, 516, 3978.

[59] X. Wu, Y. Liu , D. Zhu , J. Mater. Chem., 2001, 11, 1327.

[60] B. Liu, W. Yu, Y. Lai, W. Huang, Chem. Mater., 2001**,** 13, 1984.

[61] J. M. Jiang, P. Yang, T. Hsieh, K. Wei, Macromolecules, 2011, 44, 9155.

Chapter 3

COMPUTATIONAL STUDIES OF MONOMERS AND POLYMERS

Contents

Design of conjugated polymers through band gap and energy level tuning has been playing a key role in developing new materials for efficient organic solar cells. Low band gap materials are suited for better harvesting of the solar spectrum. The control of this parameter is a research area of current interest. Computationally driven material design is an appropriate strategy to accelerate the search for conjugated polymeric materials with desirable properties. Herein we present an overview of quantum chemical tools used for the theoretical studies of the electronic and structural properties of polymers. On the basis of donor-acceptor strength of the monomers, polymers were designed. The electronic structure and band gap of these designed polymers were evaluated. Here the band structure of the polymers were evaluated by Density Functional Theory in the Periodic Boundary Condition Formalism. This method will provide valuable guidance for a judicious design of conjugated polymers with desirable device characteristics.

3.1 Introduction

Harvesting solar energy is considered as one of the most important technologies for the future sustainability of humans. Polymer solar cells (PSCs) have attracted tremendous interest and attention over the past two decades due to their potential advantage to be fabricated into large area, light-weight, ease of processability, low cost etc. Search for π-conjugated materials exhibiting high power conversion efficiency is the prime objective of ongoing OPV research. However, the current challenges for OPVs are still to improve photovoltaic efficiency as well as cost effectiveness, to compete with silicon-based solar cells.[1,2]

One well-established approach to obtain conjugated polymers with desired optoelectronic properties is based on the strategy of donor–acceptor polymers, which will tune the electronic structure of conjugated polymers. Polymers with a desired energy gap can be obtained by incorporating an electron donating and/or withdrawing unit into the polymer backbone. In order to maximize the overall performance of a solar cell, the design requires an achievable high V_{OC} or high J_{SC} in conjunction with a high PCE.[3,4]

The conventional approach of developing novel conjugated polymers is based on the chemical intuition of synthetic chemists, but is time consuming. Instead, the application of computational design combined with chemical intuition leads to a rational and more efficient approach. The use of computational chemistry tools to predict electronic properties offers significant advantages compared to the conventional approach: (1) it is more time and cost-efficient; and (2) it can reduce the number of steps and promising synthetic targets for experimental design.[5-8]

Computational modelling can provide information about the factors that affect photovoltaic device operation and properties that are crucial in material design as well as light absorption, electronic structures and so on. A detailed knowledge of structural fine-tuning in relation to energy level modulation is needed for judicious design of conjugated polymers. It also predicts how different functional groups modulate electronic properties in order to guide the organic synthesis.[9-17]The molecular orbital contribution of the respective donor and acceptor moieties in the repeating unit of the donor–acceptor polymer can be evaluated by Quantum chemical calculations.

Recently, S. M. Bouzzine has studied polythiophene and its derivatives containing different substituents in the 3 and 4 positions, such as electron-donating or electron-withdrawing groups (Fig. 3.1). All molecular geometries were optimized at DFT/B3LYP/6-31G (d,p) level of theory and investigated the stability and electrical properties. They found that the energy gap between the HOMO and LUMO levels is related to the π-conjugation in the PTh polymer backbone. The theoretical calculations show that the substituted forms are stable, have low band gap, and are in good agreement with the experimental observations.[18]

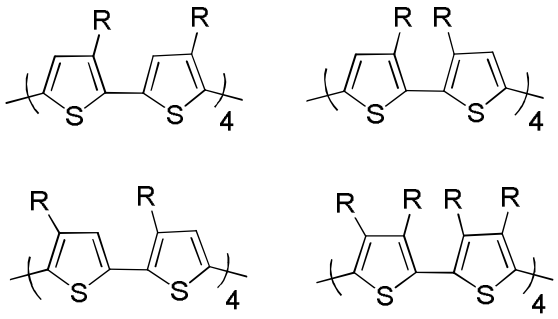

Fig. 3.1: Sketch of the structures used for the study

It is not an easy task to predict the electronic properties of a polymer, because, polymeric materials consist of large molecules with a wide range of molecular weights. Density functional theory (DFT)[19] is a quantum-mechanical method among the popular and versatile quantum chemical tools. It is used to investigate the electronic structure of polymers using functional of the electron density. The properties of conjugated polymers are typically estimated by extrapolation of properties of oligomers to infinite chain lengths. This generally accepted approximation used to estimate polymer band gap, fails for long oligomers, because convergence behaviour is observed for band gaps. Although the oligomer approach can be used to study the properties of conjugated polymers, periodic boundary condition (PBC) calculation is more computationally cost effective. In PBC calculation, polymer molecule of infinite chain length is optimized using translational symmetry. The oligomer calculations are only appropriate for molecular systems and are incapable of determining whether a polymer has a direct (or indirect) band gap, which is an essential property for describing optoelectronic and electron-transport efficiencies in these systems.[20]

In addition to this, PBC allows the calculation of band structure in the positive region of the first Brillouin zone (between k=0 and k=π/a). The starting unit cell geometries for the periodic boundary condition (PBC/DFT) calculations were taken from the central portion of the optimized oligomer and optimized inside a given lattice length on the constraints of periodic boundary condition by assuming that the unit cell is repeated identically an infinite number of times along the translation vector. Band structures in the positive region of the first Brillouin zone (between k=0 and k=π/a) were calculated along the k-vector of these one dimensional polymers with

30 k-points after the optimization using the B3LYP level of theory[21-23]. The lowest 4 unoccupied and highest 4 occupied bands in the positive region of the first Brillouin zone were plotted. Since the electronic properties of polymers depend on the constituent monomers, we have started with studying the properties of monomers. The study of the electronic structure of polymers consists of the following steps. The first step involves the optimisation of structure and geometry of the monomers followed by the evaluation of band gap of the monomers. On the basis of HOMO-LUMO energy levels of the monomers, various polymers were designed. These structures were geometrically optimized and the band gaps were calculated using suitable electronic structure package.

3.2 Theoretical calculations

Quantum chemical calculations were used to investigate the band structure and electronic properties of a series of monomers and on the basis of the data obtained; various polymers were designed and evaluated using Density Functional Theory (DFT) calculations. DFT calculations using the Gaussian 09[24, 25] suite of codes by employing HSE06 hybrid functional with full periodic boundary conditions (PBC) were used to obtain band gaps of the conjugated polymers. The basis sets used for the calculations were the split valence 6-31G (d) basis set for all the atoms. DFT/ PBC/HSE06/6-31G (d) is a very good method to reliably predict the band gap of conjugated polymers. Time-dependent DFT (TD-DFT) calculations were also performed to assess the excited-state vertical transition energies and oscillator strengths based on the optimized molecular geometries. Using TD-DFT, U. Salzner calculated electronic states of long oligomers and found that UV spectra of neutral and

oxidized or reduced species can be compared with in situ UV spectra recorded during doping. DFT calculations also established that there were no bound bipolarons in conjugated polymers and defect localization was not crucial for spectral changes observed during doping.[26] For computational simplification, the alkyl side chains on the donor unit were replaced with methyl groups, and the backbones were simplified to two repeating units. It is worth mentioning that, the present approach is able to provide a systematic evaluation of the intrinsic properties of the polymers, and computational studies show that the methods used in the present studies can be suitable for this purpose. Electronic structure, absorption and emission properties obtained from the studies suggest whether the designed polymers are good candidates for the intented applications.

3.3 Results and discussion

Conjugated polymers based on thiophene, quinoxaline, fluorene are among the best conjugated materials used in optoelectronic devices. One such example is EDOT based polymers. They show strong electron donor effect, the ether groups present in the ring confers high reactivity to the free α, α' positions. EDOT is used for the design of various classes of molecular π-conjugated systems with electronic and optical properties specifically tailored for applications in light-emitting devices, chromophores for nonlinear optics, photovoltaics etc.[27-30]

Here, quantum chemical investigation has been performed to find out the optical and electronic properties of a series of monomers based on fluorene, thiophene and quinoxaline. Various structural variations were introduced into the system to investigate their effects on the electronic

structure. We have focused on (i) incorporation of cyano substituents into the acceptor moiety and the effect of increasing conjugation (M10, M11, M12) and (ii) incorporation of conjugated fused rings (quinoxaline systems, M5, M6, M7 etc.). The effect of alkyl, alkoxy substituents on the electronic properties were also explored as in M2, M13 etc. Fig 3.2 gives the structure of the monomer moieties used for the computational studies. Through these structural modifications, we aim to provide guidance and chemical methodologies for the judicious design of conjugated polymers, especially to meet the particular requirements of different device architectures in optoelectronic applications.

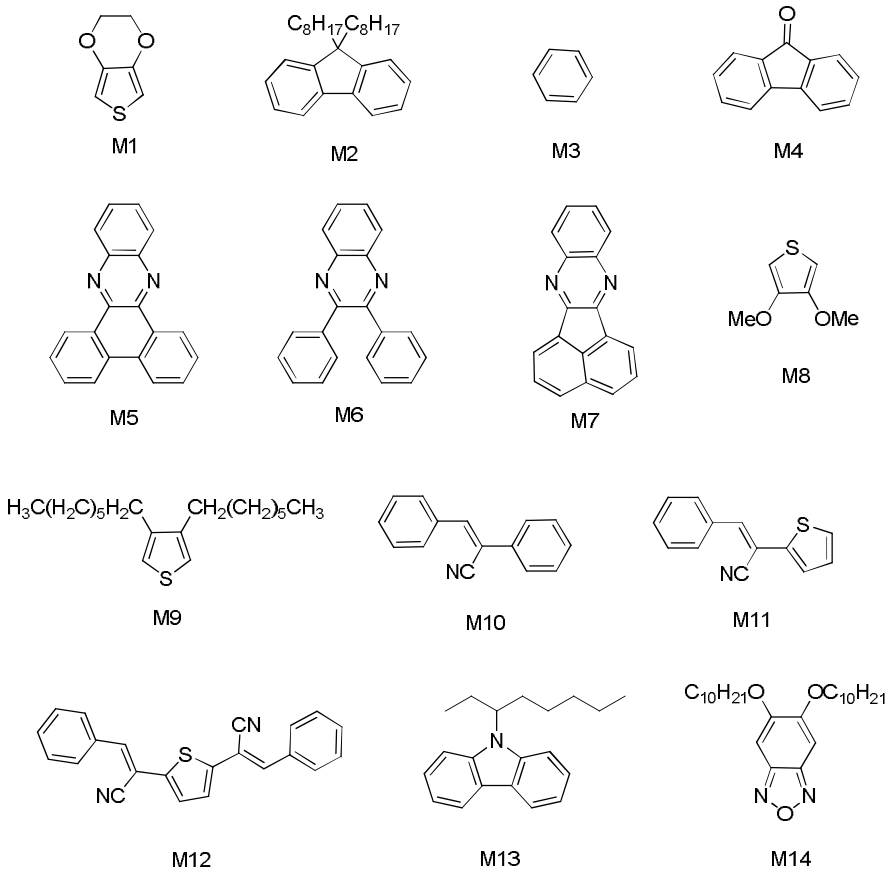

Fig. 3.2: Building units as donor/acceptor moieties

The structures of the above monomers were optimized by means of DFT method and examined the HOMO and LUMO levels of these monomers (Fig 3.3).

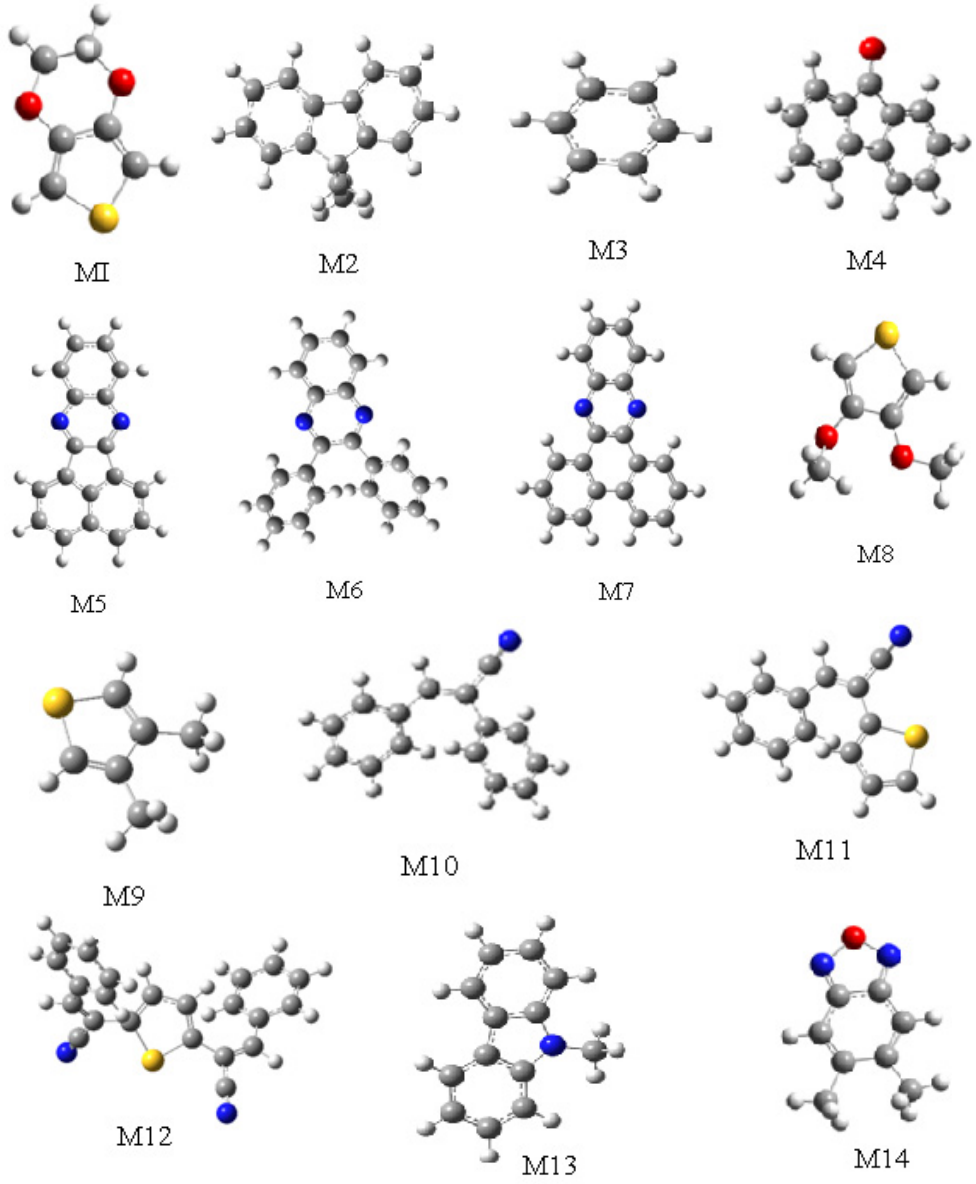

Fig. 3.3: Optimized geometries obtained by HSE06/6-31G of the monomers

3.3.1 Effects of electron withdrawing substituents in the monomer units

Effects of electron withdrawing groups like cyano group and carbonyl group were studied and found that the substitution helps to fine tune the energy levels of the polymer. This substitution will affect the HOMO and LUMO levels that is evident from fig 3.4 (M4, M10, M11, and M12). Introduction of such units brings about low band gap polymers. In most cases the introduction of such units will bring about structural irregularity. Increasing the number of electron withdrawing groups will further increase the acceptor strength of the desired polymers.

In addition, the incorporation of electron withdrawing imine nitrogen atoms will also increase the acceptor strength, as occurs for conjugated materials based on quinoxaline, benzoxadiazole etc (M5, M6, M7, M14 **)** which act as potential acceptor units in polymeric materials.

In Table 1, the band gap of three cyano substituted monomers are given as M10 (4.44 eV), M11 (4.33 eV), M12 (4.23 eV). Here the lowest band gap is shown by the one with two cyano substituents which shows that increasing the number of electron withdrawing cyano group results in lowering of band gap. But introduction of cyano groups results in lowering of polymer solubility. So during copolymerisation we have to consider the solubility factor also. That is, in the preparation of devices, the ability of the polymer to form a smooth film is of great importance. Film forming ability depends on the solubility of the polymer in different solvents which in turn helps in the spin coating of the polymer.

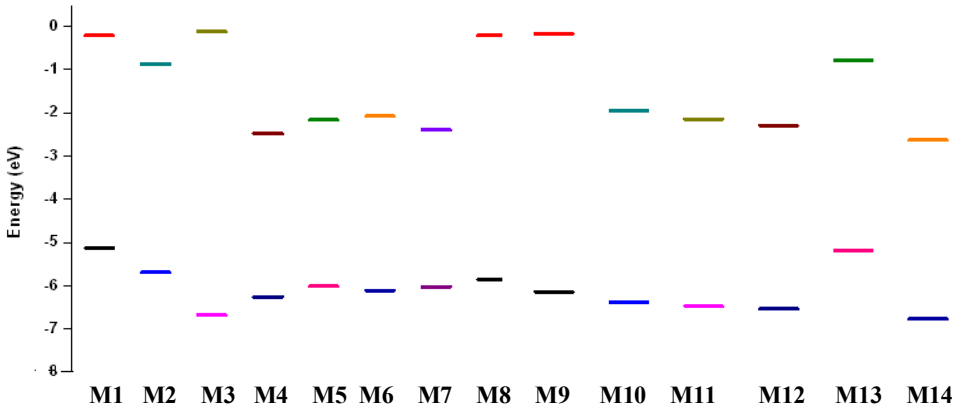

Fig.3.4: Sketch of DFT/ HSE06/6-31G calculated energy of the HOMO, LUMO levels of studied molecule

Table 2.1: Energy values of E_{HOMO} (eV), E_{LUMO} (eV), E_{gap} , $E_{activation}$ (eV), O.S, λ_{max}(nm) (eV) of the studied molecules obtained by HSE06/6-31G.

Molecules	E_{HOMO} (eV)	E_{LUMO} (eV)	E_{gap}(eV)	$E_{activation}$(eV)	O.S	λ_{max}(nm)
M1	-5.12	-0.21	5.51	5.43	0.16	228
M2	-5.69	-0.86	4.82	4.75	0.25	260
M3	-6.67	-0.11	6.55	5.69	0.00	217
M4	-6.25	-2.48	3.76	3.08	0.03	402
M5	-6.01	-2.16	3.84	3.08	0.03	362
M6	-6.10	-2.07	4.02	3.42	0.003	363
M7	-6.02	-2.39	3.63	3.41	0.004	385
M8	-5.85	-0.21	4.82	5.61	0.12	220
M9	-6.11	-0.13	5.97	5.99	0.12	206
M10	-6.35	-1.91	4.43	3.98	0.38	311
M11	-6.44	-2.11	4.33	3.66	0.33	338
M12	-6.51	-2.26	4.24	3.20	0.48	387
M13	-5.15	-0.75	4.40	4.12	0.03	300
M14	-6.73	-2.59	4.14	4.20	0.04	294

We have also computed the oscillator strength and activation energy of the designed polymers by employing the Time Dependent- Density Functional Theory (TD-DFT). It is possible to find the polymers with high absorption coefficient by this method, which is an important factor governing

the performance of the polymers. It is found that, the incorporation of imine nitrogen in quinoxaline monomers (where M7, a phenanthrene based quinoxaline shows the lower band gap value) results in even deeper energy levels than cyano substituted monomers (M10, M11, and M12). This demonstrates the strong electron withdrawing effect of imine nitrogen in an aromatic ring. The structural changes (i.e. by incorporating electron-withdrawing cyano, carbonyl or imine nitrogen) on the acceptor units will contribute to the LUMOs of the donor–acceptor polymers in the same way as to the LUMOs of the separated acceptor units. If we consider the case of thiophene based polymers containing acceptor units with electron withdrawing substituents having lone pairs like fluorene, there will be interaction of the lone pair on fluorene with π orbital of thiophene in the donor–acceptor polymer which in turn stabilizes the system that is not possible for the imine nitrogen atoms on the acceptor units.

The incorporation of conjugated fused heteroarenes like in carbazole is a useful approach that can result in rigid and coplanar polymer backbones, enhancing effective π-conjugation and facilitating intra- and intermolecular charge transport. In the present study, in fused systems, in order to improve the solubility, long alkyl substituents were attached which resulted in the loss of rigidity and coplanarity of the ring. As a result, conductivity decreases when compared to the unsubstituted ones. The extent of conjugation results in lowering the band gap of the monomer like M12, whose band gap is lower when compared to M10 and M11.

One can modulate the energy levels while keeping the HOMO–LUMO energy gaps almost unchanged through structural modifications. One can also tune the HOMO–LUMO energy gaps while maintaining an identical

HOMO level and LUMO level modulated by chemical methods. Reducing the energy band gap while keeping comparable HOMO level results in improvement of device performance.

The HOMO and LUMO levels of various monomers were calculated. The energy gap is evaluated as the difference between the HOMO and LUMO energies. The ground state energies and oscillator strengths were investigated using the TD/DFT calculations on the optimized geometries. Excitation to the S1 state corresponds almost exclusively to the promotion of an electron from the HOMO to the LUMO orbital. The absorption wavelengths arising from $S_0 \rightarrow S_1$ electronic transition increase progressively with the increase of conjugation length. It is reasonable to argue that HOMO→LUMO transition is predominant in $S_0 \rightarrow S_1$ electronic transition. The results show that there is a decrease of the LUMO and an increase of the HOMO level. Of the various monomer systems studied, it was found that the band gap of M7 acenaphthene based quinoxaline showed the lowest value.(3.63eV).From the energy level and band gap values of the various monomers studied, few polymers were designed and evaluated.

3.3.1.1 Quinoxaline based polymers

Here, few fluorene-quinoxaline copolymers were designed and studied after analysing the properties of the constituent monomers i.e., fluorene and quinoxaline. It is observed that the LUMO levels of quinoxaline units are lower showing higher acceptor strength. The LUMO levels of fluorene monomer is -0.86 eV where as in quinoxaline monomers it is -2.16 eV for M5, -2.07 eV for M6 and -2.39 eV for M7. The band gap calculated for the three polymers, P(FQ-A), P(FQ-B), P(FQ-P) are 2.57 eV, 2.6 eV, 2.43 eV respectively. Here, in

the polymers, HOMO is localized on the fluorene unit, while LUMO is strongly confined to the quinoxaline units which act as the acceptor. Energy levels of four monomers and three polymers are shown in fig 3.5.

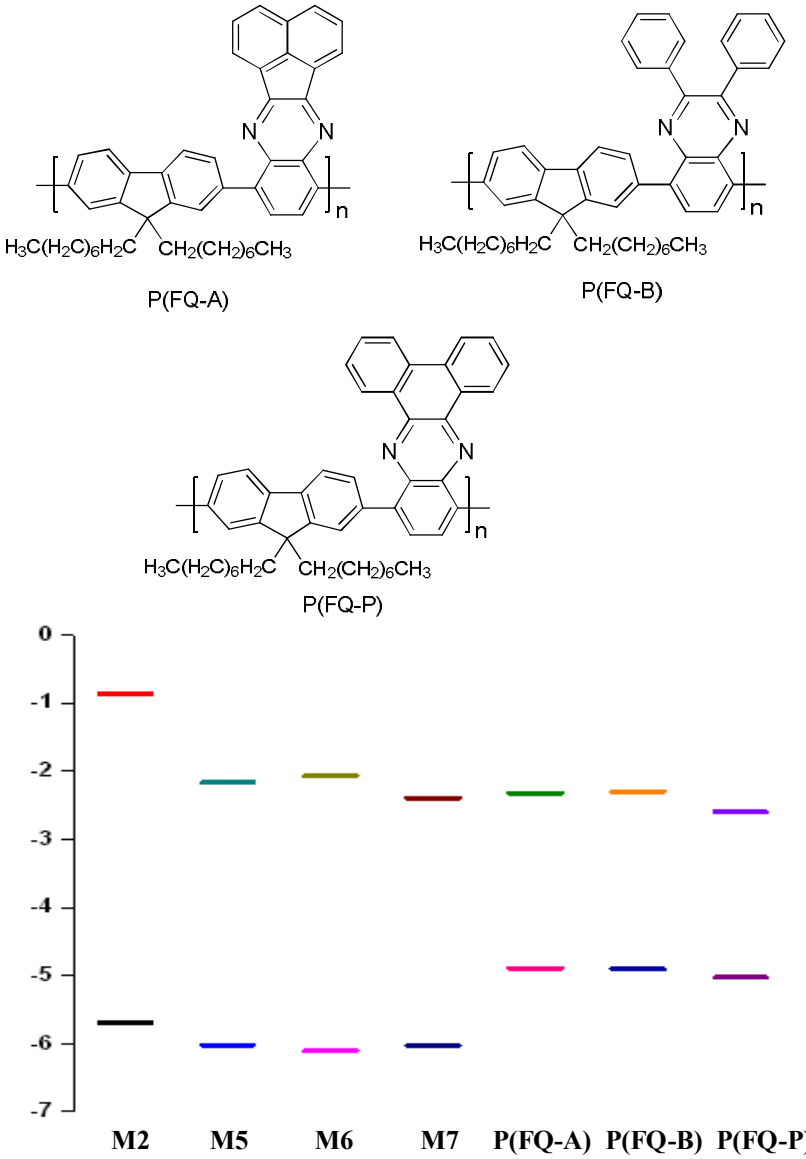

Fig.3.5: Energy levels of M2, M5, M6, M7 and the polymers P(FQ-A), P(FQ-B) and P(FQ-P)

The energy levels and band gap of the polymers were calculated by DFT/PBC/HSE06/6-31G method. The energy levels of the HOMO and LUMO were determined from the maximum point of the highest occupied molecular level and the minimum point of the lowest unoccupied molecular levels respectively. The energy gap (Egap) is evaluated as the difference between the HOMO and LUMO energies. Band gap of the polymers, P(FQ-A), P(FQ-B), P(FQ-P) are 2.57 eV, 2.6 eV, 2.43 eV respectively. Here among the three polymers P(FQ-P) shows lower band gap. Band structures of the three polymers are shown in fig 3.7. The ground state energies and oscillator strengths were also investigated using the TD/DFT calculations on the optimized geometries (Table 2). The optimized repeating unit for the periodic boundary calculation is given in fig 3.6. Horizontal lines represent the translational vector which is equal to the one dimensional cell size.

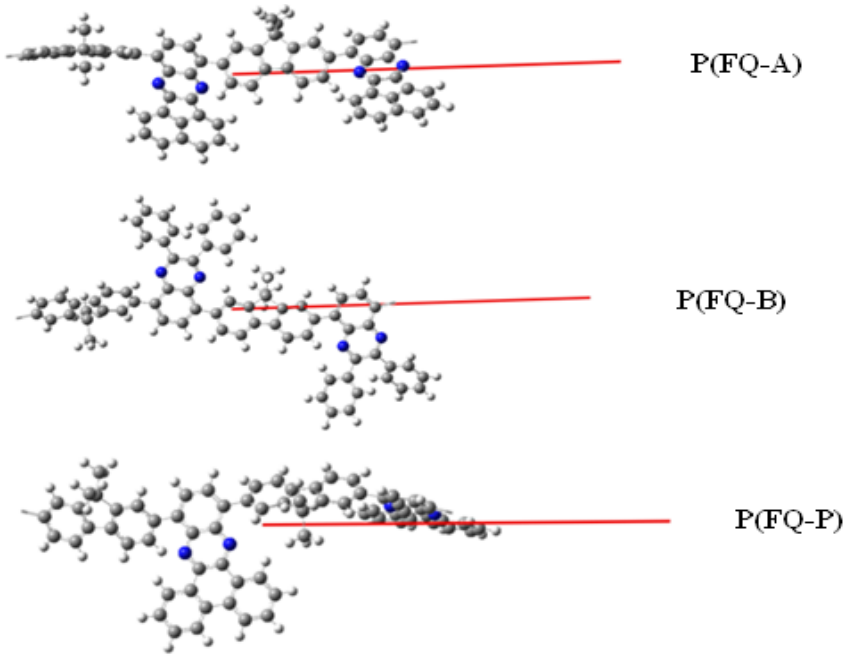

Fig.3.6: Unit cell of the Polymers for PBC/HSE06/6-31G calculation. Red line represents the translational vector

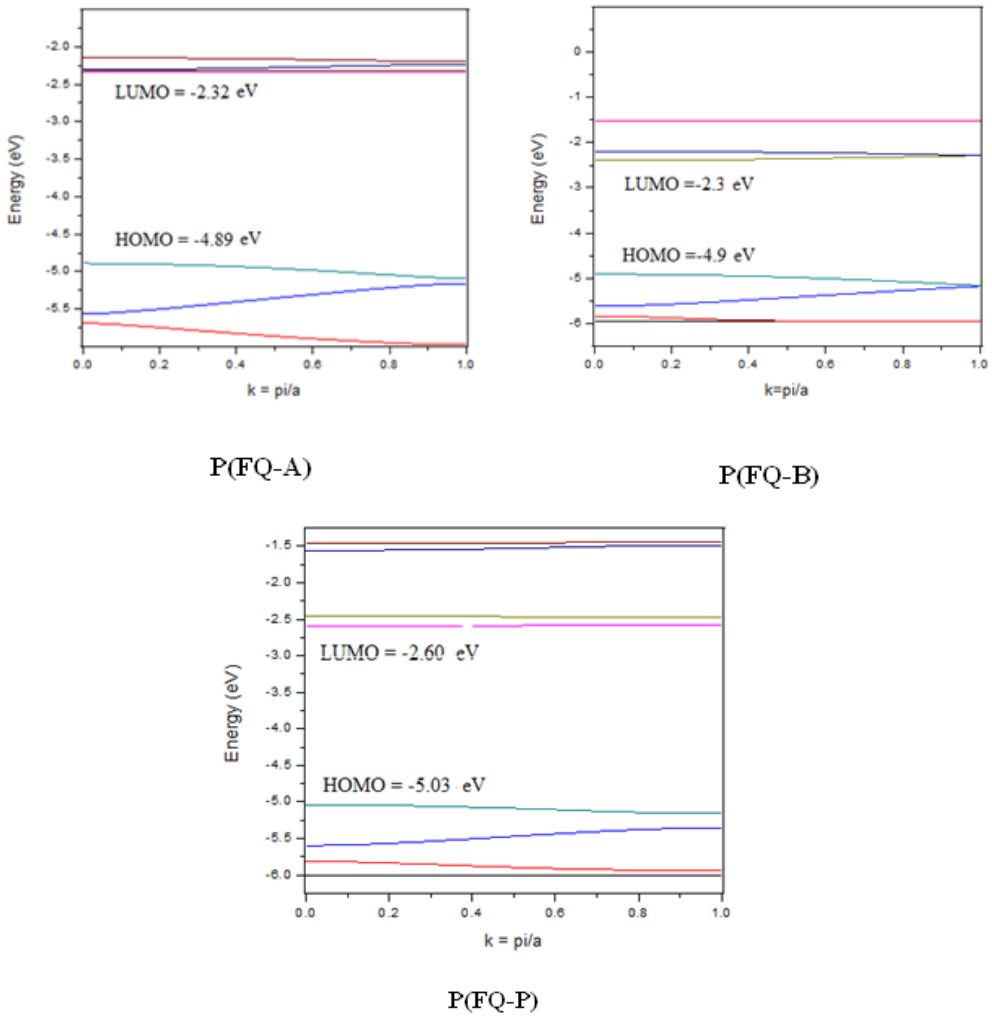

Fig. 3.7: Band structure of P(FQ-A), P(FQ-B) and P(FQ-P)

Table 3.2: Band structure data of P(FQ-A), P(FQ-B) and P(FQ-P)

Polymer	E_{HOMO} (eV)	E_{LUMO} (eV)	E_{gap}(eV)	$E_{activation}$ (eV)	O.S
P(FQ-A)	-4.89	-2.32	2.57	1.76	0.22
P(FQ-B)	-4.9	-2.3	2.6	1.97	0.07
P(FQ-P)	-5.03	-2.6	2.43	2.14	0.53

3.3.1.2 Fluorene-thiophene copolymers

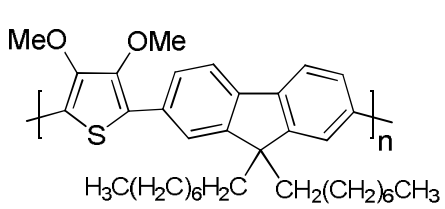

P(FMT)

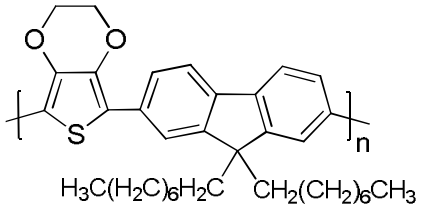

P(EF)

Two fluorene-thiophene copolymers were designed and the electronic structure of the polymers were studied. DFT method using Gaussian 09 software package was used for the electronic structure studies. The studies were carried out using HSE06 method that incorporates a portion of exact exchange functional from Hartree–Fock theory with exchange and correlation from other sources (*ab initio* or empirical). Energy levels obtained are summarised in figure 3.8.The LUMO levels of the monomers EDOT (M1), dioctylfluorene (M2), dimethoxythiophene (M8) are -0.21 eV,-0.86 eV , -0.21 eV respectively. Monomer with lower LUMO energy level has the higher acceptor strength. From the figure, it is evident that after copolymerisation HOMO levels of the polymers were elevated while the LUMO levels were lowered. Here, the band gap of P(EF) is lower than P(FMT)**.**The low band gap is due to the charge transfer between the donor and acceptor which improves the π electron delocalisation and thus decreases the bond length alteration.

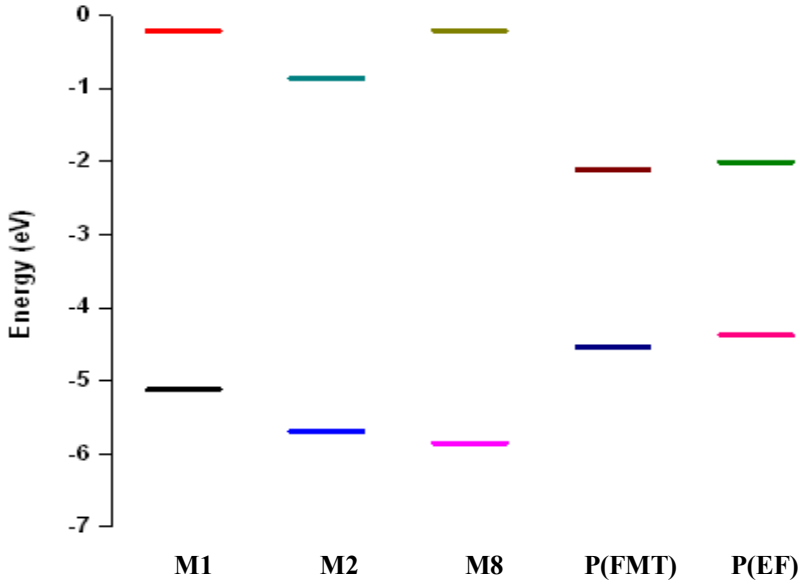

Fig.3.8: Energy levels of M1, M2, M8 and the polymers P(FMT) and P(EF)

The band structure data of the polymers are given in the Table 3.3 and band structure is shown in fig 3.10. The band gap calculated for the two polymers, P(FMT) and P(EF) are 2.42 eV and 2.36 eV respectively. The optimized repeating unit for the periodic boundary calculation is given in fig.3.9.

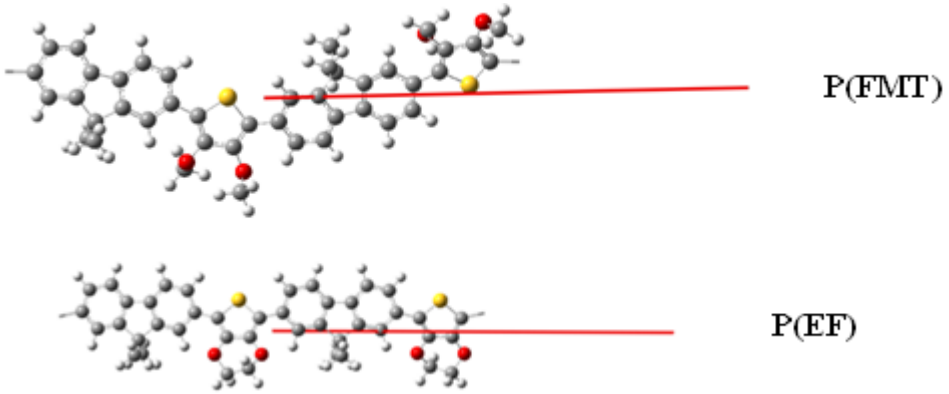

Fig.3.9: Unit cell of the polymers P(FMT) and P(EF) for PBC/HSE06/6-31G calculation. Red line represents the translational vector

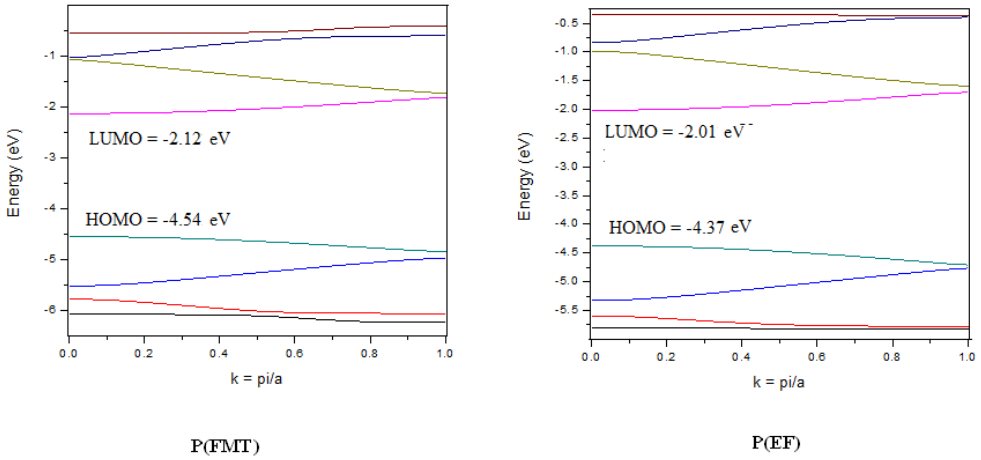

Fig. 3.10: Band structure of P(FMT) and P(EF)

Table 3.3: Band structure data of P(FMT) and P(EF)

Polymer	E_{HOMO} (eV)	E_{LUMO} (eV)	E_{gap}(eV)	$E_{activation}$ (eV)	O.S
P(FMT)	-4.54	-2.12	2.42	2.83	0.02
P(EF)	-4.37	-2.01	2.36	3.04	2.54

3.3.1.3 EDOT based polymers

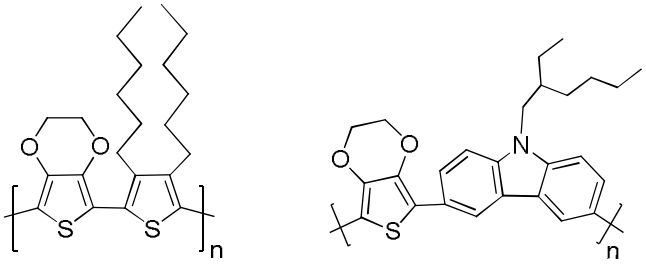

A major advantage of the EDOT building block lies in a unique combination of strong electron donor properties and self-structuring effects related to intramolecular non-covalent interactions between oxygen and

sulphur. This has an influence on the structure and electronic properties of pi-conjugated polymers incorporating EDOT units. One demerit of EDOT based polymers is the low solubility which can be overcome by the incorporation of alkyl groups. The theoretical data of two EDOT based polymers P (EHT) and P(EC) are discussed. From the LUMO levels of the monomers, EDOT, hexyl thiophene and carbazole (fig 3.11) it is clear that in the polymers EDOT acts as the donor where as hexyl thiophene and carbazole act as the acceptors and charge transfer takes place from donor to the acceptor units.

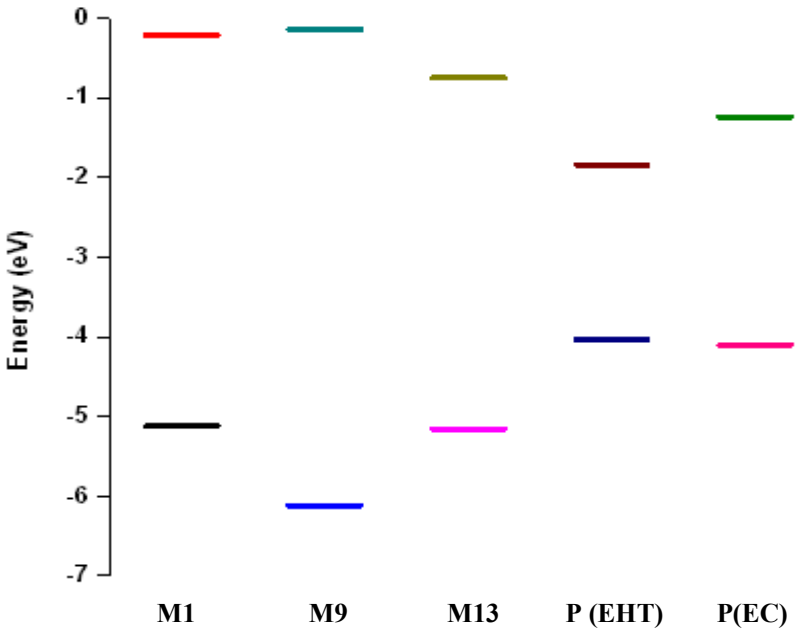

Fig.11: Energy levels of M1, M9, M13 and the polymers P (EHT) and P(EC)

The optimised unit cell for PBC calculation is shown in fig 3.12. Here the band gap of the two polymers was calculated as 2.2 eV and 2.86 eV respectively. The band structure data of the polymers are summarized in

Table 3.4. It is evident that after coupling, HOMO levels of the polymers were elevated while the LUMO levels were lowered giving low band gap polymers. The band structure of the two polymers are given in fig 3.13.

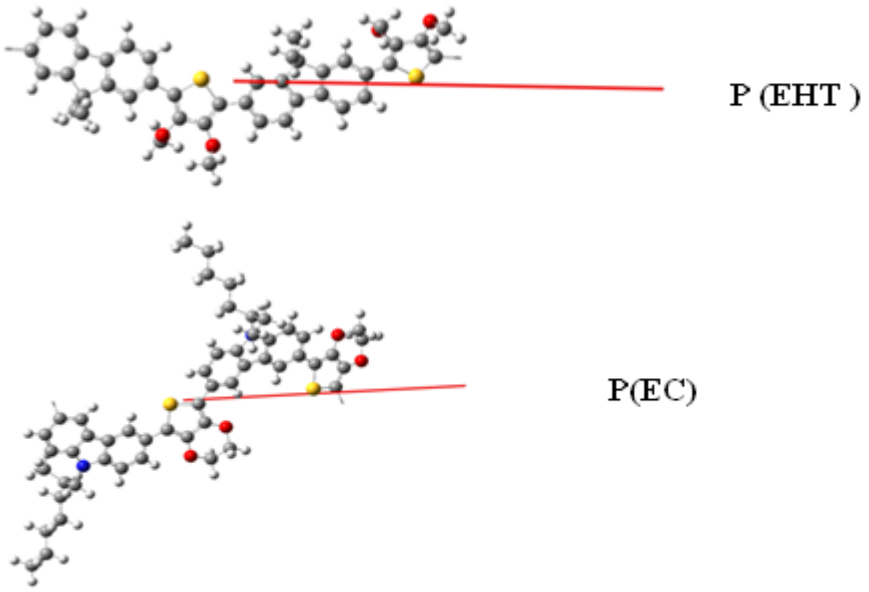

Fig.3.12: Unit cell of the polymers P(EHT) and P(EC) for PBC/HSE06/6-31G calculation. Red line represents the translational vector

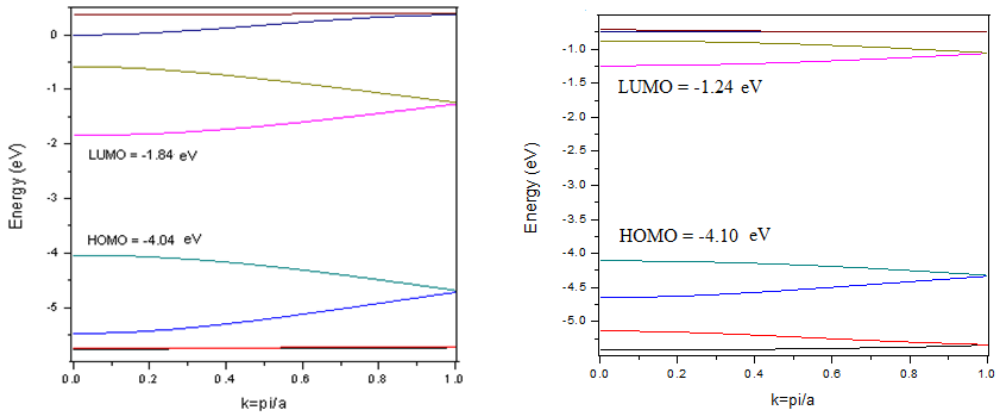

P (EHT) P(EC)

Fig.3.13: Band structure of P (EHT)and P(EC)

Table 3.4: Band structure data of (EHT) and P(EC)

Polymer	E_{HOMO}(eV)	E_{LUMO} (eV)	E_{gap}(eV)	$E_{activation}$(eV)	O.S
P(EHT)	-4.04	-1.84	2.2	3.75	1.22
P(EC)	-4.10	-1.24	2.86	3.48	0.97

3.3.1.4 Cyanovinylene based polymers

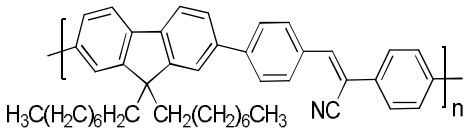

P(CN1)

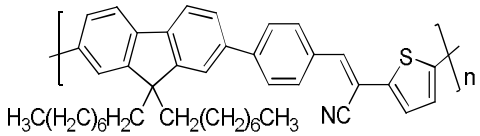

P(CN2)

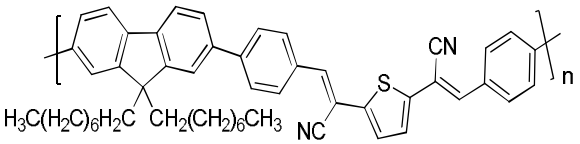

P(CN3)

There were many reports on the utilization of variable band gap conjugated polymers based on cyanovinylene groups for optoelectronic, redox applications including organic photovoltaics, colour tunable light emitting diodes, and electrochromics. The design of three cyanovinylene based polymers and the effect of structural modification on the electronic properties of the polymers is reported. From fig 3.4 it is clear that LUMO level of the three cyano substituted monomers decreases in the order of M10 > M11 > M12. Monomer M12 which contains two cyano groups has the low lying LUMO level which is expected to be the most effective acceptor among the group. Here in these polymers, charge transfer takes place from

fluorene to the cyanovinylene acceptor units. One drawback usually noticed in the cyano substituted polymers is their low solubility. But here, the dioctyl group present in the polymer chain is expected to increase the solubility of the polymer.

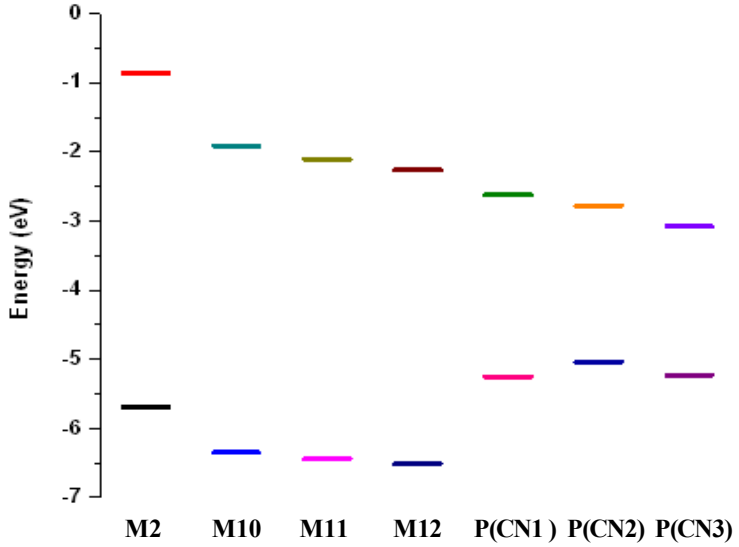

Fig.3.14: Energy levels of M2, M10, M11, M12 and the polymers P (CN1), P(CN2) and P(CN3)

Band structure of the polymers are shown in the fig 3.16.The band gap calculated for the three polymers, P(CN1), P(CN2) and P(CN3) are 2.62 eV, 2.25 eV, 2.15eV respectively and is summarized in table 3.5. As expected from the studies on the monomers, P(CN3) has the lowest band gap among the three polymers. The optimized repeating unit for the periodic boundary calculation is given in fig 3.15. Horizontal lines represent the translational vector which is equal to the one dimensional cell size.

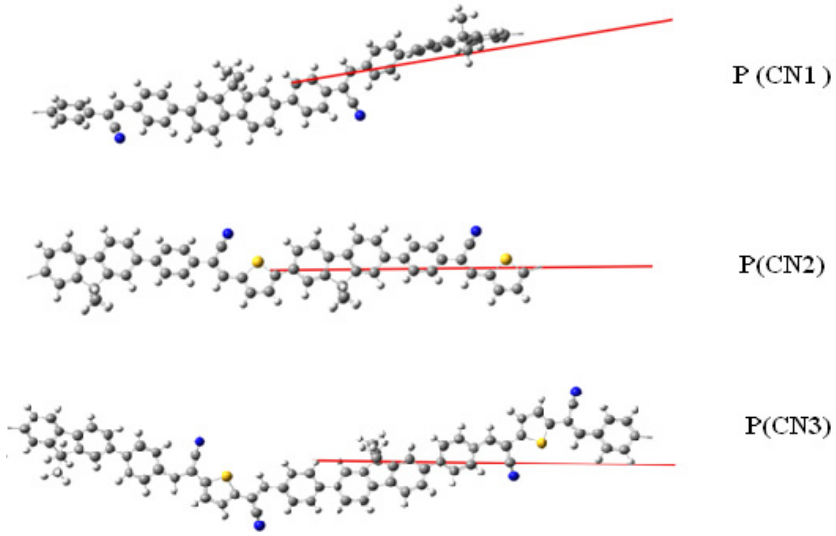

Fig.3.15: Unit cell of the polymers P(CN1), P(CN2) and P(CN3) for PBC/HSE06/6-31G calculation. Red line represents the translational vector

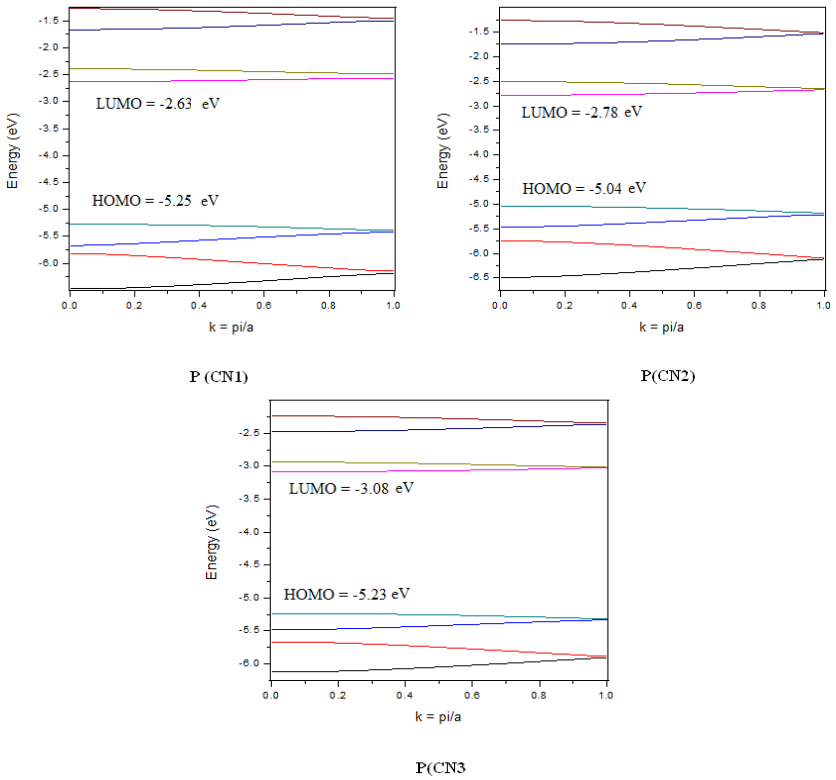

Fig. 3.16: Band structure of P (CN1), P(CN2) and P(CN3).

Table 3.5: Band structure data of P (CN1), P(CN2) and P(CN3)

Polymer	E_{HOMO} (eV)	E_{LUMO} (eV)	E_{gap}(eV)	$E_{activation}$ (eV)	O.S
P (CN1)	-5.25	-2.63	2.62	3.18	0.02
P (CN2)	-5.04	-2.78	2.25	2.83	1.33
P (CN3)	-5.23	-3.08	2.15	2.81	0.81

3.3.1.5 Polymers containing phenylene comonomer units

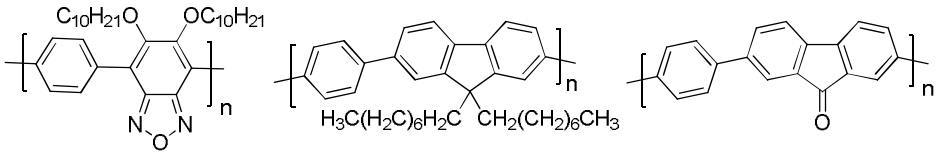

P(PDO) **P(POF)** **P(PF)**

Three copolymers containing phenylene comonomer units were designed and studied using PBC/HSE06/6-31G method. The electronic properties of the monomers and polymers are given in the fig 3.17.

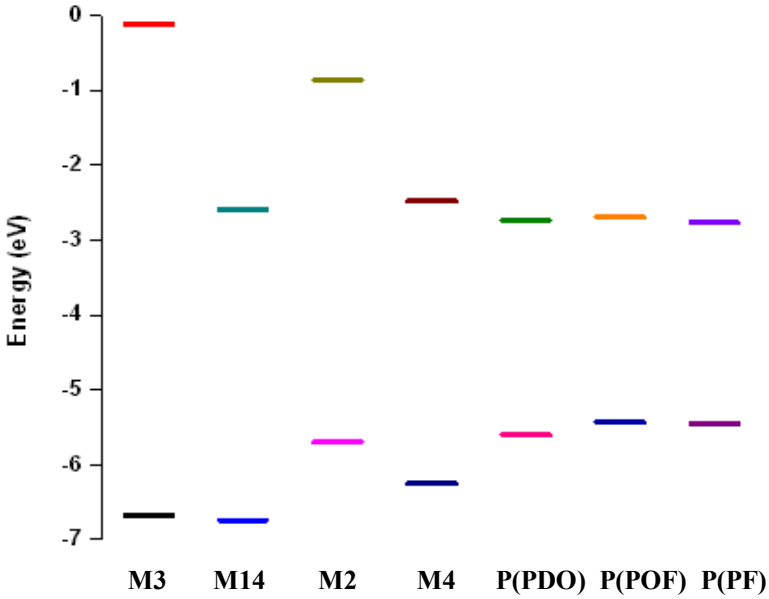

Fig.3.17: Energy levels of M3, M14, M2, M4 and the polymers P(PDO), P(POF) and P(PF)

The LUMO levels of the three acceptors are given as -2.59 eV,-0.86 eV and -2.48 eV respectively. The lowest LUMO value is shown by M14 (decylbenzoxadiazole). Here in the three polymers, charge transfer is from donor phenylene to the benzoxadiazole, fluorene and fluorenone units.

Band gaps of the three polymers, P(PDO), P(POF) and P(PF) are 2.86 eV, 2.73 eV, 2.68 eV respectively and the optimized repeating unit for the periodic boundary calculation is given in fig 3.18. Lowest band gap is obtained for P(PF) when compared with the other polymers. Band structure of polymers are shown in fig 3.19. Band structure data are presented in Table 3.6.

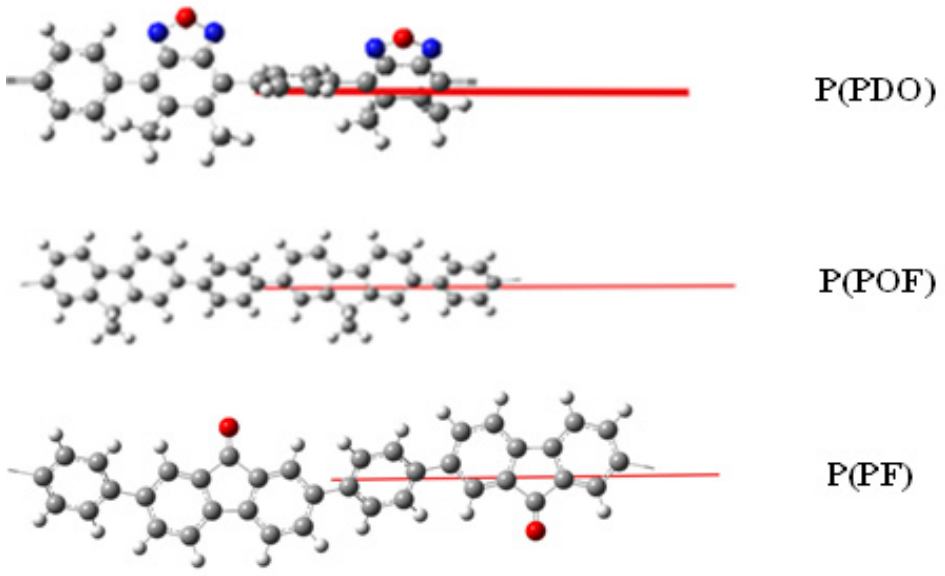

Fig. 3.18: Unit cell of the polymers P(PDO), P(POF) and P(PF) for PBC/ HSE06/6-31G calculation. Red line represents the translational vector

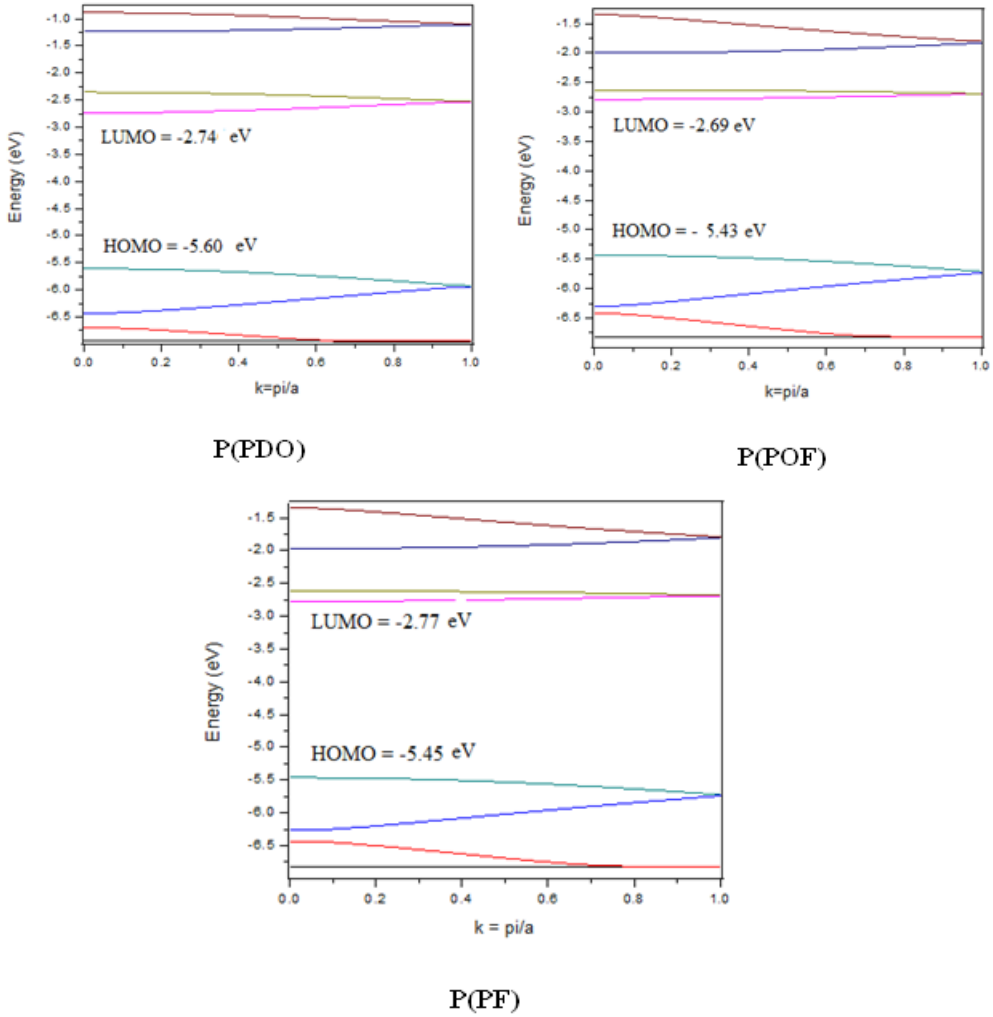

Fig. 3.19: Band structure of P(PDO), P(POF) and P(PF)

Table 3.6: Band structure data of P(PDO), P(POF) and P(PF)

Polymer	E_{HOMO} (eV)	E_{LUMO} (eV)	E_{gap}(eV)	$E_{activation}$ (eV)	O.S
P(PDO)	-5.60	-2.74	2.86	3.35	0.30
P(POF)	-5.43	-2.69	2.73	4.08	0.0002
P(PF)	-5.45	-2.77	2.68	2.76	0.08

3.4 Conclusion

Thirteen polymers were designed and their electronic structures were calculated using PBC/HSE06/6-31G method. Of the thirteen polymers designed P(CN3) showed the lowest bandgap of 2.15 eV. It was found that the HOMO and the LUMO energy levels of the monomers are very important factors to determine whether effective charge transfer will take place between donor and acceptor. The reduction of band gap is a function of the acceptor strength. Studies implied that different structural variations, especially the effect of the substituents on the ring play key roles on the electronic properties (HOMO and LUMO) of the polymers. Time-dependent DFT (TD-DFT) calculations were performed to assess the excited-state vertical transition energies and oscillator strengths based on the optimized molecular geometries.

References

[1] G. Li, R. Zhu, Y. Yang, Nat. Photonics, 2012, 6, 153.

[2] C. J. Brabec, Sol. Energy Mater. Sol. Cells, 2004, 83, 273.

[3] E. E. Havinga, W. T. Hoeve, H. Wynberg, Polym. Bull., 1992, 29, 119.

[4] W. Zhuang, A. Lundin, M. R. Andersson, J. Mater. Chem. A, 2014, 2, 2202.

[5] X. W. Zhou, J. A. Zimmerman, B. M. Wong, J. J. Hoyt, J. Mater. Res., 2008, *23*, 704.

[6] B. M. Wong, D. Lacina, I. M. B. Nielsen, J. Graetz, M. D. Allendorf,. J. Phys. Chem. C 2011,115, 7778.

[7] D. K. Ward, X. W. Zhou,B. M. Wong, F. P. Doty, J. A. Zimmerman,. J. Chem. Phys., 2011, 134,244703.

[8] B. M. Wong, F. Léonard,Q. Li, G. T. Wang, Nano Lett., 2011, 11, 3074.

[9] B. M. Wong, A. H. Steeves, R. W. Field, J. Phys. Chem. B, 2006, 110, 18912.

[10] H. A. Bechtel, A. H. Steeves,B. M. Wong,R. W. Field, Angew. Chem. Int. Ed,. 2008, 47, 2969.

[11] B. M. Wong, Phys. Chem. Chem. Phys., 2008, 10, 5599.

[12] B. M. Wong, J. Comput. Chem., 2009, 30, 51.

[13] K. R. Dey, B. M. Wong, M. A. Hossain,.Tetrahedron Lett., 2010, 51, 1329.

[14] M. A. Hossain, M. A. Saeed, F. R. Fronczek,B. M. Wong, K. R. Dey, J. S. Mendy, D. Gibson, Cryst. Growth Des,.2010, 10, 1478.

[15] M. A. Saeed, B. M. Wong,F. R. Fronczek, R. Venkatraman, M. A. Hossain, Cryst. Growth Des., 2010, 10, 1486.

[16] M. Işiklan, M. A. Saeed, A. Pramanik,B. M. Wong, F. R. Fronczek, M. A. Hossain, Cryst. Growth Des., 2011, 11, 959.

[17] (a) B. M. Wong, J. G. Cordaro, J. Chem. Phys., 2008, 129, 214703

(b) B. M. Wong, M. Piacenza, F. D. Sala, Phys. Chem. Chem. Phys.,2009, 11, 4498.

[18] S. M. Bouzzine,G. S. Morán, M. Hamidi, M. Bouachrine, A. G. Pacheco, D. G. Mitnik, Journal of Chemistry, 2015, 2015, Article ID 296386, 1.

[19] R. G. Parr, W. Yang, Density-Functional Theory of Atoms and Molecules, Oxford University Press, New York, 1989.

[20] S. S. Zade, N. Zamoshchik , M. Bendikov, Acc. Chem. Res., 2010, 44, 14.

[21] A. D. Becke, J. Chem. Phys., 1993, 98, 5648.

[22] Lee, W. Yang, R. G. Parr, Phys. Rev. B., 1994, 37, 785.

[23] P. J. Stephens, F. J. Devlin, C. F. Chabalowski, M. J. Frisch, J. Phys. Chem., 1994, 98, 11623.

[24] (a) W. J. Hehre, D. R, J. A. Pople, J. Chem. Phys., 1972, 56, 2257

(b) P. C. Harihara, J. A. Pople, Theor. Chim. Acta, 1973, 28, 213.

[25] M. J. Frisch, G. W. Trucks, H. B. Schlegel, G. E. Scuseria, M. A. Robb, J. R. Cheeseman, G.Scalmani, V. Barone, B. Mennucci, G. A. Petersson, H. Nakatsuji, M. Caricato, X. Li, H. P.Hratchian et al,Gaussian 09 Revision B.01, Gaussian, Inc.,Wallingford, CT, 2010.

[26] U. Salzner, WIREs Comput Mol Sci, 2014, 4, 601.

[27] (a) F. Jonas, L. Shrader, Synth. Met., 1991, 831, 41

(b) G. Heywang, F. Jonas, Adv. Mater., 1992, 4, 116.

[28] M. Dietrich, J. Heinze, G. Heywang, F. Jonas, J. Electroanal. Chem., 1994, 369, 87.

[29] L. Groenendaal, F. Jonas, D. Freitag, H. Pielartzik, J. R. Reynolds, Adv. Mater., 2000, 12, 481.

[30] L. Groenendaal, G. Zotti, P.-H. Aubert, S. M. Waybright and J. R. Reynolds, Adv. Mater., 2003, 15, 855

Chapter 4

SYNTHESIS OF POLYMERS AND THEIR CHARACTERISATION

Contents

This chapter discusses about the synthesis of designed polymers by means of Suzuki and Direct arylation polymerisation reactions. The synthesised polymers were characterised by UV-Vis, ^{1}H NMR, PL Spectroscopic techniques, TG/DTG and Cyclic Voltammetry techniques. Detailed synthetic procedures and characterisation data are presented in this chapter. The frontier orbital energy levels and band gap were experimentally determined using cyclic Voltammetric studies and optical measurement. The theoretically calculated values are in good agreement with the experimental results.

4.1 Introduction

Conducting polymers represent new advanced materials that play a key role in the development of new devices and structures offering combination of various properties required for advanced applications. When key structural requirements are met, conjugated polymers exhibit properties such as solution processability, low band gap, high conductivity, large charge transporting capabilities, and broad optical absorption. As a result, conjugated polymers can be utilized for the fabrication of organic electronic and photonic devices. Zero band gap and intrinsic conductivity have been a major goal for the band gap control of π-conjugated polymers. Although materials with optimal band gap values can be synthesised using known synthetic tools, the difficulty lies in the need to incorporate optimal light-harvesting properties, a rather-low HOMO level and a high hole mobility. Different strategies are used for band-gap control, but roughly divided into two main routes. The first approach involves the planarization, rigidification and quinoidization of the conjugated system which results in a reduction of BLA (Bond Length Alteration). This method leads to a large increase in the photoluminescence efficiency, decrease the reorganization energy and thus to improve the charge mobility. A major drawback of this approach is that, it requires long and complex synthetic work. The second route lies in the association of donor and acceptor units leading to the possibility of intramolecular charge-transfer. This can lead to very low band gaps and is now the most preferred one for the synthesis of polymers for optoelectronic applications.[1-6]

The D-A approach still poses several fundamental problems related to the effects of the mode of connection and relative strengths of the D and A

units in the π-conjugated system. These structural parameters control the width of the band gap as well as the electronic distribution in the conjugated system and hence the charge-transport properties of the material.

π-conjugated systems designed as active materials for electronic and photonic devices must combine processability and high environmental and photochemical stability. These materials will have to be produced by means of cost-effective, simple and straightforward synthetic procedures taking into account of environmental constraints: atom economy, minimal use of organic solvents and toxic metal catalysts, and use of renewable starting materials.

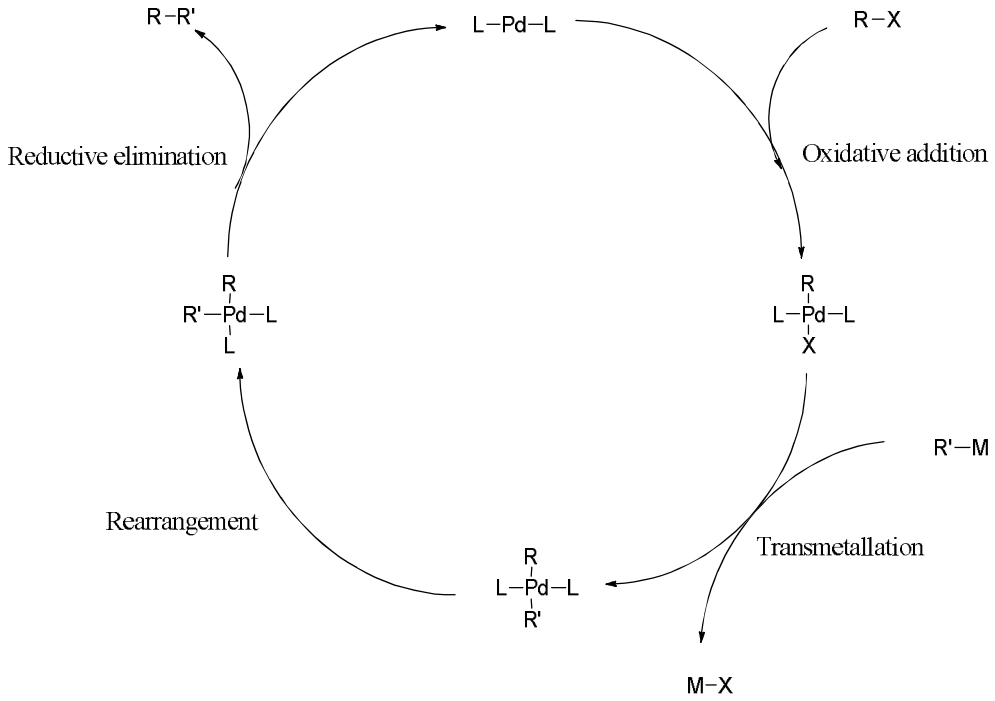

Fig. 4.1: Catalytic cycle for Pd catalysed reaction

Although these complex problems represent major challenges for the chemistry of functional π-conjugated systems, their solutions will determine,

the future applications of π -conjugated systems in electronic and photonic devices.[7(a)] Here we discuss the synthesis of donor-acceptor conjugated polymers by means of Pd catalysed cross- coupling reactions. Most palladium catalysed reactions are believed to follow a similar catalytic cycle and is shown in figure 4.1.[7(b)]

4.1.1 Pd catalysed polymerisations

In the present work, either Suzuki or Direct arylation polycondensation has been employed to synthesize the conjugated donor-acceptor polymers. Both the Suzuki and Direct arylation are palladium catalysed intermolecular cross-coupling reactions. Suzuki polymerisation, a common cross-coupling reaction involves several advantages that, it is highly tolerant to different functional groups, and boron containing by-products are easily removed by a simple alkali work-up. Although the most commonly used method for the formation of aryl-aryl bonds, the Suzuki reaction is just as effective for the synthesis of highly substituted products.[7(c)]

D. Muenmart et al reported a range of stable emulsions of spherical and rod-like conjugated polymer nanoparticles (CPN) via Suzuki−Miyaura cross-coupling reactions of 9,9-dioctylfluorene-2,7-diboronic acid bis (1,3-propanediol) ester with a number of different dibromoarene monomers in xylene, stabilized in water by the nonionic surfactant, Triton X-102. High molar mass poly (9,9-dioctylfluorene) (PF8), poly (9,9-dioctylfluorene-alt-benzothiadiazole) (PF8BT), poly (9,9-dioctylfluorene-alt-4-sec-butyl phenyl diphenylamine) (PF8TAA) and poly (9,9-dioctylfluorene-alt-bithiophene) (PF8T2) emulsions were obtained[8] (Scheme 1).

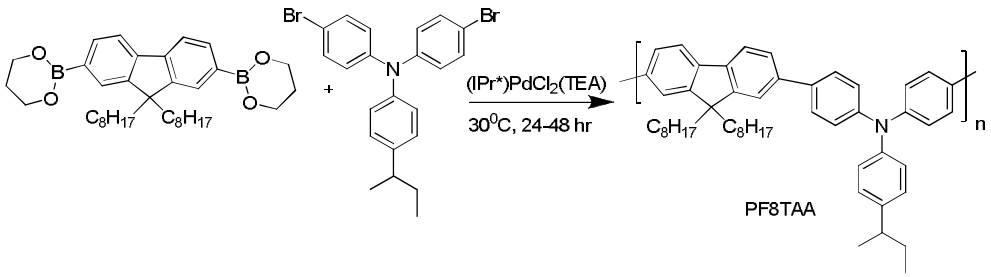

Scheme 1: Synthesis of polymer by Suzuki–Miyaura cross-coupling

E Lim reported a series of carbazole-benzothiadiazole-triazole based copolymers, poly [(N-9′-heptadecanyl-2,7-carbazole)-co-(5,5-(4′,7′-di-2-thienyl-2′,1′,3′-benzothiadiazole))-co-((4-(4-butylphenyl)-3,5-diphenyl-4H-1,2,4] triazole))] (PCz3TBTz) by Suzuki coupling polymerization[9] (Scheme 2).

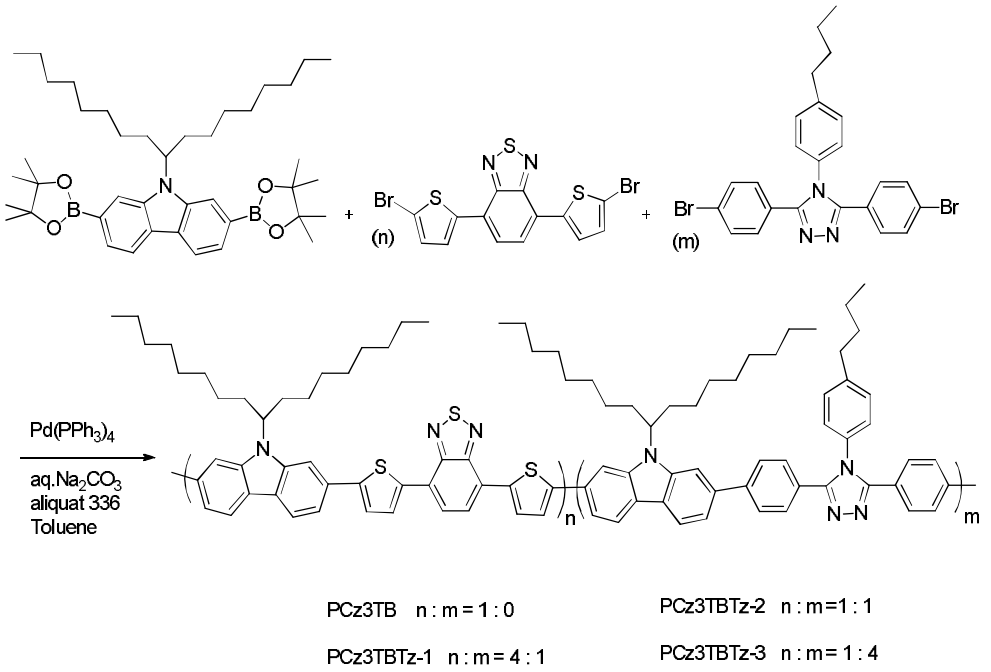

Scheme 2: Synthesis of carbazole-benzothiadiazole-triazole based copolymers

Direct (hetero) arylation is an advantageous tool for the synthesis of regioregular polymers as well as alternating copolymers. This methodology has several advantages (1) it reduces the number of steps (2) utilizes monomers with long-term stability that can be easily manipulated (3) produces only acid as a byproduct (4) can give rise to polymeric material with higher molecular weights than those obtained by other methods. High functional group tolerance has been displayed. This method enables more effective preparation of highly efficient known polymers and provide entry into novel and promising materials.[10]According to some recent reports, materials prepared by this method has been successfully incorporated into organic electronic devices such as OTFTs,[11] OLEDs [12] and BHJ-SCs.[13,14]

X. Wang et al reported the synthesis of thiophene-flanked benzothiadiazole derivatives (DTBTs**)** *via* direct arylation coupling. DTBTs were further polymerized with fluorene dibromide *via* direct arylation polycondensation to give well-defined alternating copolymers[15] (Scheme 3).

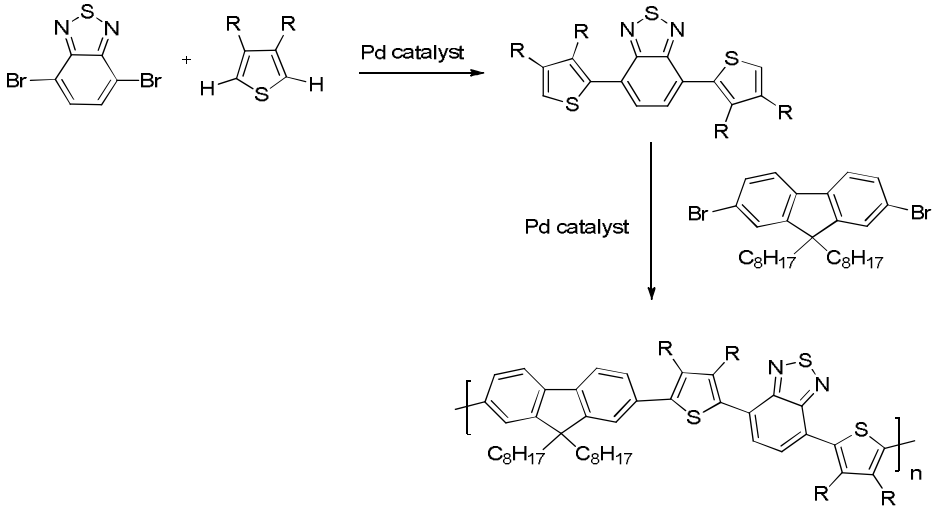

Scheme 3: Synthesis of fluorene- thiophene copolymers

Recently, T. Kanbara and co-authors have focused on the Ru-catalyzed direct arylation of pyrrole derivatives bearing a directing group. This resulted in cross-coupling reaction at the α-position of the pyrrole monomer without protecting the β-position. In particular, they successfully proved the directed site-selective polycondensation of 1-(2-pyrimidinyl) pyrrole with 2,7-dibromo-9,9-dioctylfluorene with the 2-pyrimidinyl substituent as directing group[16] (Scheme 4).

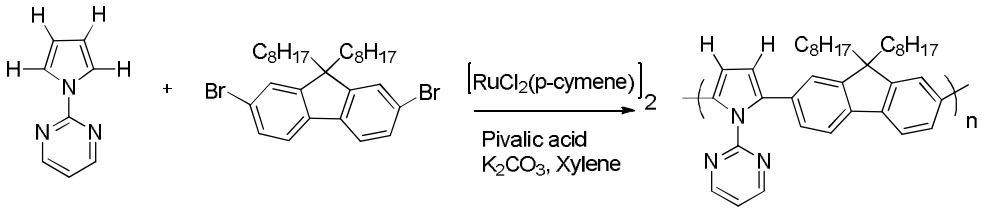

Scheme 4: Synthesis of polymer consisting of pyrrole and fluorine units

4.2 Polymer Synthesis

4.2.1 Synthesis of fluorene-quinoxaline polymers

The three theoretically designed fluorene-quinoxaline polymers were synthesised by Suzuki cross-coupling reaction using $Pd(PPh_3)_4$ as the catalyst. The dibromoquinoxaline derivatives was reacted with the dioxaborolane derivative of fluorene in the presence of the catalyst, $Pd(PPh_3)_4$ to form the corresponding polymers. The crude polymers were purified by precipitating from methanol followed by soxhlet extraction using methanol and hexane. The polymers were soluble in common organic solvents such as chloroform, chlorobenzene and THF. The synthetic route towards the Fluorene -Quinoxaline polymer is depicted in Scheme 5.

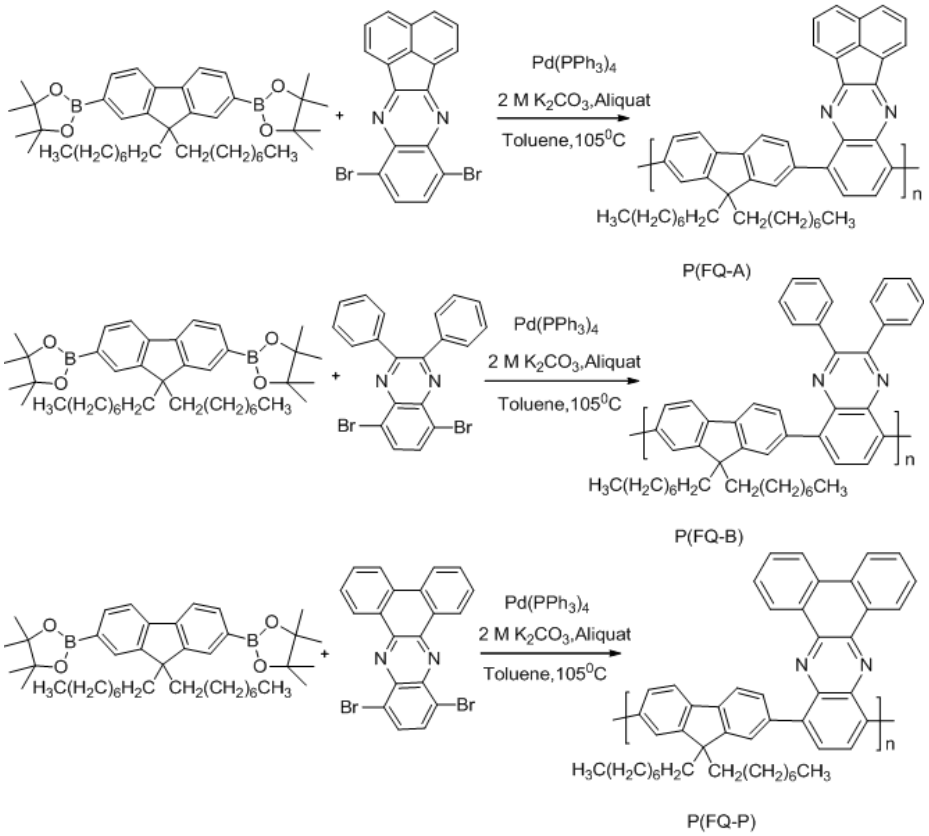

Scheme 5: Synthesis of P(FQ-A), P(FQ-B) and P(FQ-P)

The three polymers were characterized using ^{1}H NMR, UV-Visible spectroscopy, GPC, Cyclic voltammetry, TGA etc. The molecular weights of the polymers were obtained from gel permeation chromatography in THF referring to polystyrene standards. Among the three polymers, P(FQ-A) showed high molecular weight. The copolymer exhibited number average molecular weight (M_n) of 12228 and weight average molecular weight (M_w) of 18384 with polydispersity index (PDI) of 1.50.Table 1 summarizes the molecular weight and polydispersity index (PDI) of the copolymers. M_p is the peak molecular weight. Here M_p is the mode of molecular weight

distribution. It is the molecular weight of the highest peak. The polymers P(FQ-A), P(FQ-B) and P(FQ-P) show peak molecular weight of 14270,14683 and 10575 respectively.

Table 4.1: Results of the polymerisation reaction

Polymer	M_n	M_w	M_p	PDI
P(FQ-A)	12228	18384	14270	1.50
P(FQ-B)	11753	16240	14683	1.38
P(FQ-C)	8332	11195	10575	1.34

The ^{1}H NMR spectra of the polymers (a) P(FQ-A), (b) P(FQ-B) and (c) P(FQ-P) are shown in figure 4.2. The ^{1}H NMR spectrum of P(FQ-A) showed multiplets at δ 0.85-2.1 due to aliphatic protons. It also showed multiplets at δ 7.5-8.5 due to aromatic protons present in the copolymer. Likewise, P(FQ-B) and P(FQ-P) also showed multiplets in the aliphatic and aromatic region.

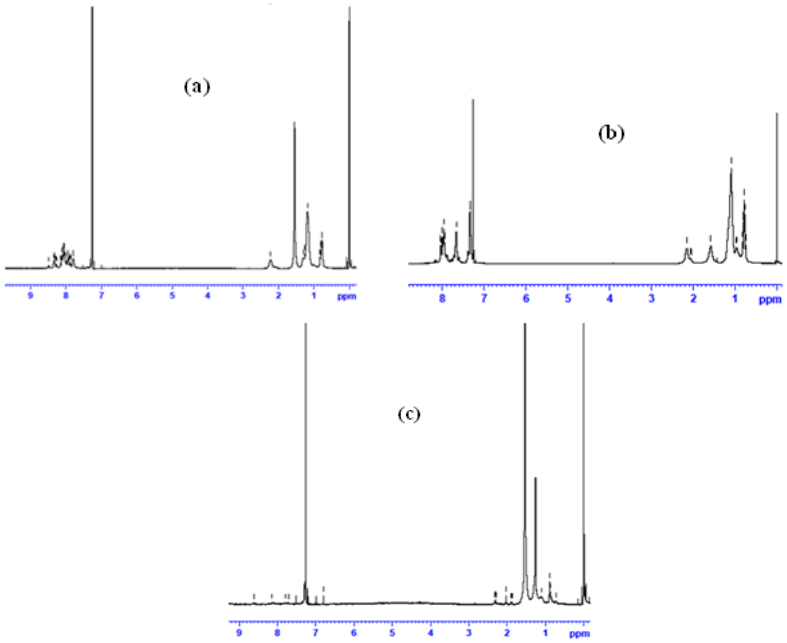

Fig.4.2: ^{1}H NMR spectrum of a) (FQ-A), (b) P(FQ-B) and (c) P(FQ-P)

4.2.1.1 Optical and photoluminescence properties

Figure 4.3 shows the absorption spectra of the polymers. The optical properties of the polymers, P(FQ-A) and P(FQ-B were investigated in chloroform and P(FQ-P) with the help of UV-Vis-DRS method. The polymers, P(FQ-A), P(FQ-B and P(FQ-P) showed absorption maximum around 321 nm, 310 nm and 330 nm respectively. In the absorption spectrum, the band with absorption maximum below 350 nm is due to π- π transition of the backbone and the peak at longest wave length (400 nm- 700 nm) is due to the intermolecular charge transfer (ICT) band. The absorption onset of P(FQ-A), P(FQ-B) and P(FQ-P) occurs at 473 nm, 471 nm, and 505 nm respectively. The optical band gap calculated was found to be 2.62 eV, 2.63 eV and 2.32 eV respectively. From quantum chemical calculations, band gaps obtained were 2.57 eV, 2.60 eV and 2.43 eV respectively. The band gaps calculated from optical methods are in good agreement with the theoretical values.

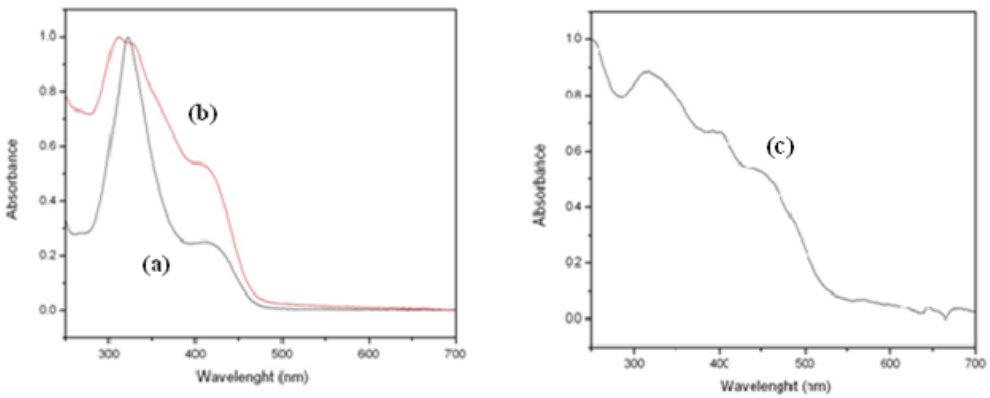

Fig 4.3: UV-Vis spectra of the polymer: (a) P(FQ-A) and (b) P(FQ-B) in 2mg/10mL chloroform and UV-Vis-DRS of (c) P(FQ-P)

Fig 4.4 shows the emission spectra of P(FQ-A),P(FQ-B) and P(FQ-P) in chloroform. The maximum emission shown by the three polymers are at 516 nm, 520 nm and 557 nm respectively. As expected, the emission spectrum of the polymer P(FQ-P) was redshifted when compared to the other two polymers.

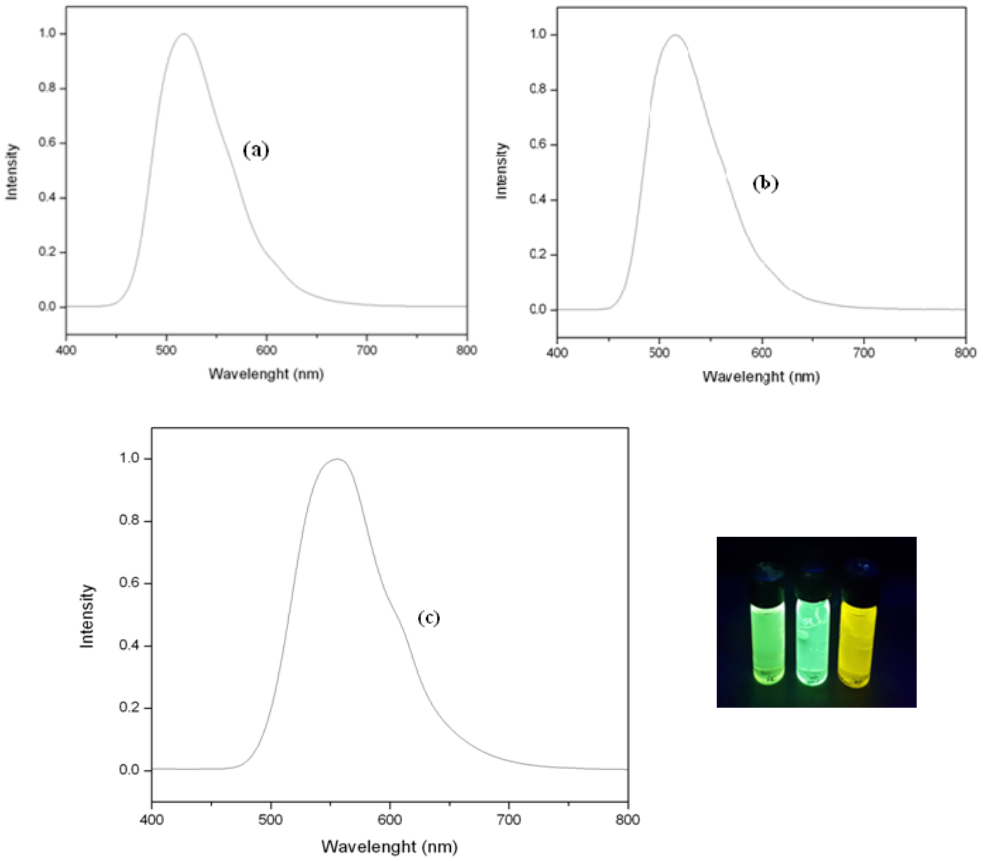

Fig. 4.4: PL Spectra of the polymers: (a) P(FQ-A), (b) P(FQ-B) and (c) P(FQ-P) in 2mg/10mL chloroform (Excitation wavelength 365 nm)

4.2.1.2 Thermal properties

The thermal characteristics of the polymers were investigated by TG-DTG studies. From the TG traces, it is clear that the first two polymers follow single degradation pattern while the third shows step wise degradation.The moisture content present in the polymer was lost below 100°C. In P(FQ-A), DTG traces showed onset of degradation around 380°C and degradation at temperature 450°C, around 18 % weight loss as the onset loss point. In P(FQ-B), the onset of degradation is around 400°C and the degradation temperature is at 450°C. Here only 5 % weight loss took place at the onset loss point. P (FQ-B) is more stable compared to P (FQ-A). Among the three polymers, P(FQ-P) is the least stable one where degradation starts around 300°C. TG-DTG traces of the polymers are shown in the figure 4.5.

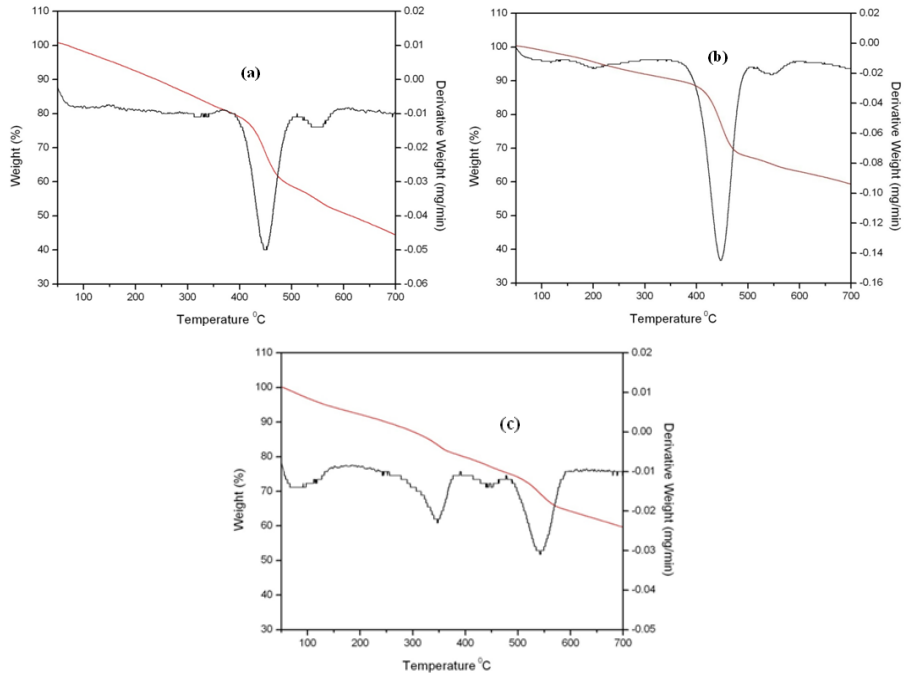

Fig.4.5: TG, DTG traces of the polymers: (a) P(FQ-A), (b) P(FQ-B) and (c)P(FQ-P)

4.2.1.3 Electrochemical studies

Cyclic voltammetric studies were carried out to determine the HOMO, LUMO levels and band gap of the polymers. CV studies were performed in a solution of Bu_4NPF_6 (0.1 M) in dry acetonitrile at 100 mV/s under nitrogen atmosphere. The set up consists of a Ag/Ag+ reference electrode, a platinum button electrode (0.08 cm^2) coated with thin copolymer as the working electrode, and a platinum wire as the counter electrode. From the onset of oxidation, the HOMO levels of P(FQ-A), P(FQ-B) and P(FQ-P) were calculated to be -5.74 eV, -5.50 eV and -5.48 eV respectively by using the equation, HOMO = -(4.4 + Eox^{onset}). The LUMO energy levels (from the onset of reduction potentials) of P(FQ-A) , P(FQ-B) and P(FQ-P) were calculated to be -2.77 eV, -1.73 eV and -1.078 eV respectively. The HOMO and LUMO energies were lowered on copolymerisation which indicated the enhanced electron accepting / transporting properties in conjugated polymers. Eventhough some deviations are there, the results are in good agreement with the values obtained from optical and theoretical methods. This is because, the predicted band gaps are for the isolated gas phase chains and also, the solid state effects such as polarisation effects and intermolecular packing forces are neglected.[17,18] Band gap calculated by means of theoretical, electrochemical and optical methods are depicted in Table 2.

Table 4.2: Band gaps calculated by means of theoretical, electrochemical and optical methods

Polymer	Eg (theoretical) eV	Eg (Electrochemical) eV	Eg (Optical) eV
P(FQ-A)	2.57	2.9	2.62
P(FQ-B)	2.60	2.66	2.63
P(FQ-P)	2.43	2.2	2.32

4.2.2 Synthesis of fluorene-thiophene copolymer

Fluorene-thiophene copolymers were synthesised through the direct arylation polymerisation method. The synthesis of the polymers is shown in Scheme 6. Thiophene based monomers containing active hydrogen atoms were coupled with dibromo derivative of fluorene in the presence of Pd catalyst and phase transfer catalyst to form the corresponding polymers. The resulting polymers were purified by precipitating from methanol followed by soxhlet extraction using methanol and hexane. The polymers are soluble in common organic solvents such as chloroform, chlorobenzene and THF.

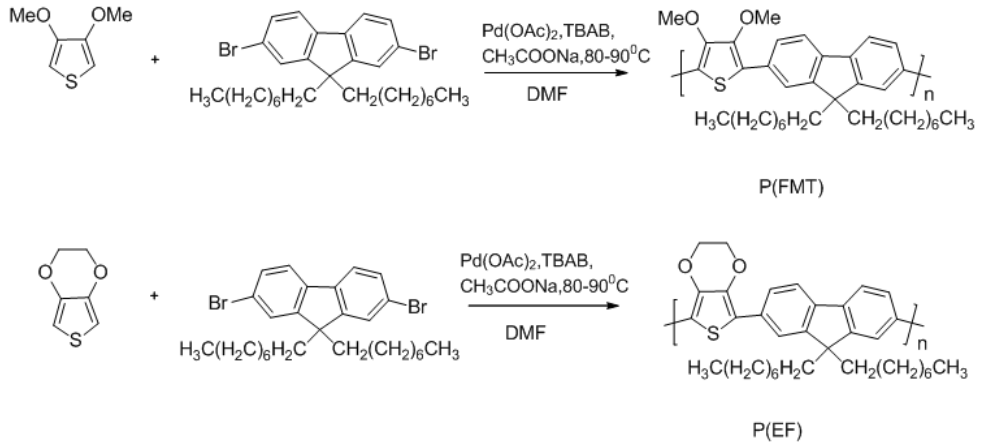

Scheme 6: Synthesis of P(FMT) and P(EF)

The polymers were characterized using ^{1}H NMR, UV-Visible spectroscopy, GPC, Cyclic voltammetry, TGA etc. The molecular weights of the polymers were obtained from gel permeation chromatography in THF referring to polystyrene standards. P(FMT) shows number average molecular weight (M_n) of 14801 and weight average molecular weight (M_w) of 33144 with polydispersity index (PDI) of 2.24. The peak molecular

weight (M_p) of the polymer is 24136. P(EF) shows number average molecular weight (M_n) of 10873 and weight average molecular weight (M_w) of 18270 with polydispersity index (PDI) of 1.68. The peak molecular weight (M_p) of the polymer is 12158. GPC results were given in the table 4.3.

Table 4.3: Results of the polymerisation reaction of (a) P(FMT) and (b) P(EF)

Polymer	M_n	M_w	M_p	PDI
P(FMT)	14801	33144	24136	2.24
P(EF)	10873	18270	12158	1.68

The ^{1}H NMR spectra of the polymers P(FMT) and P(EF) are shown in figure 4.6. The two polymers showed multiplets in the aliphatic and aromatic regions. In addition to that for P(FMT), it showed a singlet at δ 4.0 due to methoxy hydrogens. In the case of P(EF) an extra multiplet at δ 4.0 due to -CH_2-O- was observed.

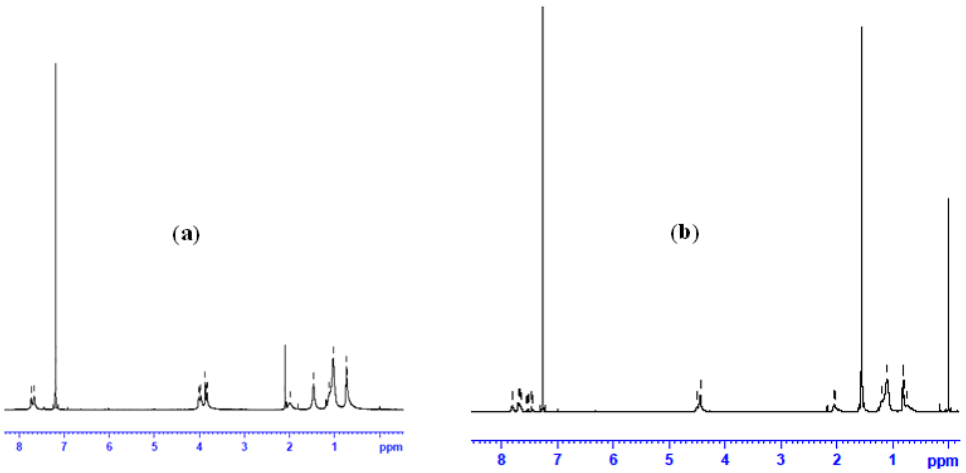

Fig.4.6: ^{1}H NMR spectra of the polymers :(a) P(FMT) and (b) P(EF)

4.2.2.1 Optical and photoluminescence properties

Figure 4.7 shows the absorption spectra of the polymers. The optical properties of the polymers, P(FMT) and P(EF) were investigated in chloroform. P(FMT) and P(EF) showed absorption maximum around 476 nm and 450 nm respectively which are due to the intramolecular charge transfer (ICT) band. The absorption onset of P(FMT) and P(EF) occurs at 588 nm and 540 nm respectively. The optical band gap calculated was found to be 2.11 eV and 2.63 eV respectively. The band gaps calculated from optical methods are in good agreement with the theoretical values. From quantum chemical calculations, band gap obtained are 2.42 eV and 2.36eV respectively.

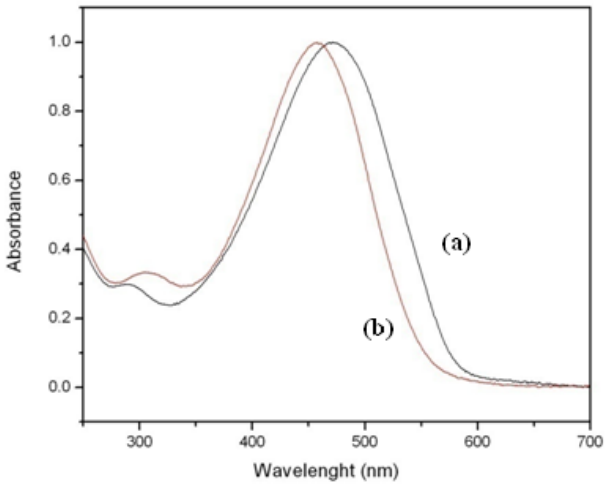

Fig.4.7: UV-Vis Spectra of the polymers: (a) P(FMT) and (b) P(EF) in chloroform (2mg/10mL)

Fig 4.8 shows the emission spectra of P(FMT) and P(EF) in chloroform. The maximum emission shown by the polymers are 554 nm and 548 nm respectively.

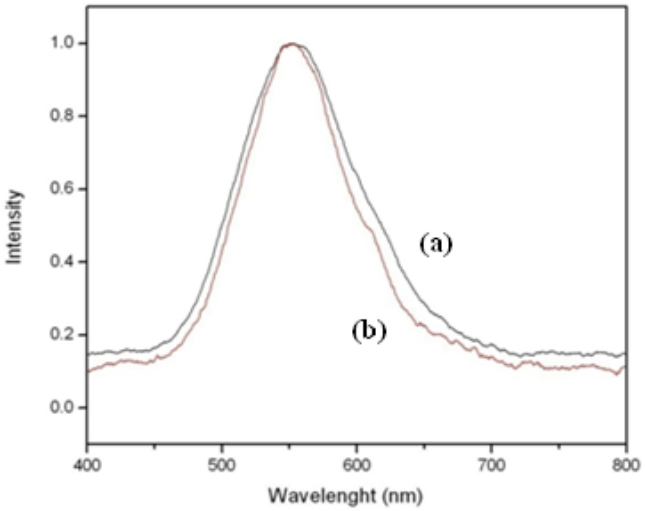

Fig.4.8: PL spectra of the polymers: (a) P(FMT) and (b) P(EF) in 2mg/10mL chloroform solution (Excitation wavelength 365 nm)

4.2.2.2 Thermogravimetric studies

The thermal characteristics of the polymers were investigated by TG-DTG studies. From figure 4.9 it is clear that the P(FMT) follow multiple degradation pattern while P(EF) shows single degradation pattern. In P(FMT), DTG traces showed that the major onset of degradation was around 300°C and degradation temperature was around 400°C, losing around 25 % weight at the onset loss point. In P(EF), the onset of degradation is around 350°Cand the degradation temperature is at 430°C. Here only 5% weight loss took place at the onset loss point. As shown by the TG-DTG curve, it is clear that the polymer P(EF) shows good thermal stability. The polyfluorene backbone becomes more rigid on the incorporation of EDOT units.[19] This is due to the fact that EDOT units encourage stronger interchain Vander Waals bonding.

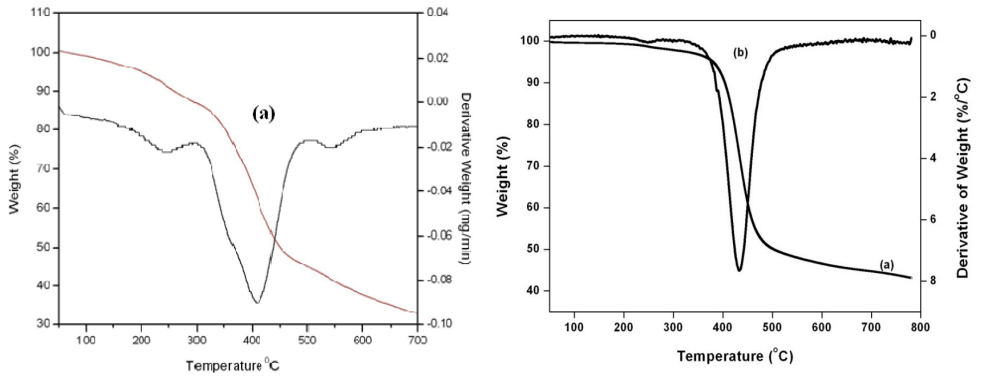

Fig.4.9: TG and DTG traces of the polymers: (a) P(FMT) and (b) P(EF)

4.2.2.3 Electrochemical studies

Cyclic voltammetric studies were carried out to determine the HOMO, LUMO levels and band gap of the polymers. From the onset of oxidation, the HOMO levels of P(FMT) and P(EF) were calculated to be 5.91 eV and -5.19 eV respectively by using the equation, HOMO = -(4.4 + Eox^{onset}). The LUMO energy levels (from the onset of reduction potentials) of P(FMT) were calculated to be -3.71 eV and for P(EF) LUMO level (-2.9 eV) was estimated using optical band gap. In conclusion, the incorporation of the donor units effectively increases the HOMO level and reduces the LUMO level of the polymers. Band gap calculated by means of theoretical, electrochemical and optical methods are depicted in Table 4.4.

Table 4.4: Band gap calculated by means of theoretical, electrochemical and optical methods

Polymer	Eg (theoretical) eV	Eg (Electrochemical) eV	Eg (Optical) eV
P(FMT)	2.42	2.2	2.11
P(EF)	2.36	2.63	2.63

4.2.3 Synthesis of EDOT based polymers

Usually EDOT based polymers are synthesised by electropolymerisation technique.[20] Here we have synthesised two EDOT based polymers, P(EHT) and P(EC) by means of direct arylation polymerisation and is shown in Scheme 7. EDOT based monomers were coupled with dibromo derivative of thiophene and carbazole in the presence of Pd catalyst and phase transfer catalyst to form the corresponding polymers. The polymers were purified by precipitating from methanol followed by soxhlet extraction using methanol and hexane. The polymers are soluble in common organic solvents such as chloroform, chlorobenzene and THF.

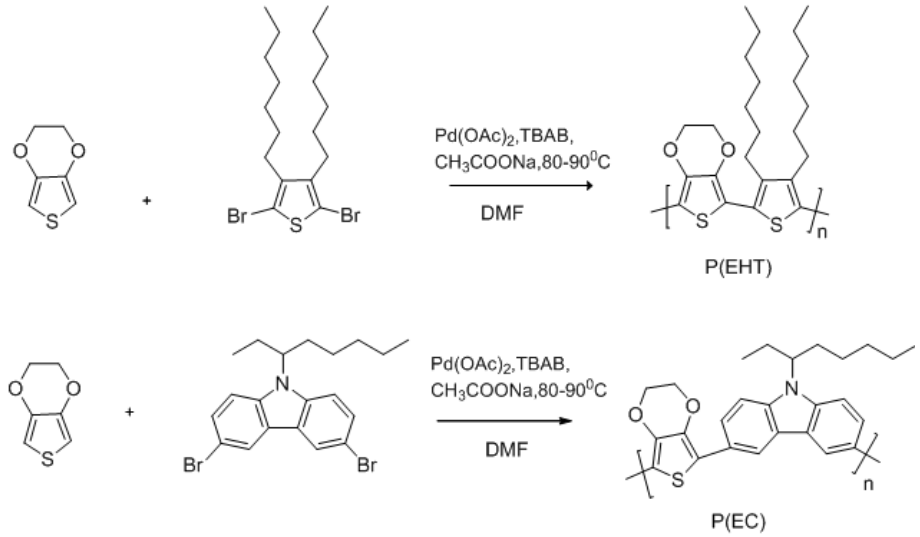

Scheme 7: Synthesis of P(EHT) and P(EC)

The polymers were characterized using ^{1}H NMR, UV-Visible spectroscopy, GPC, Cyclic voltammetry, TGA etc. The molecular weights of the polymers were obtained from gel permeation chromatography in THF referring to polystyrene standards. P(EHT) shows number average molecular

weight (M_n) of 12592 and weight average molecular weight (M_w) of 20248 with polydispersity index (PDI) of 1.61. The peak molecular weight (M_p) of the polymer is 12805. P(EC) shows number average molecular weight (M_n) of 2328 and weight average molecular weight (M_w) of 3021 with polydispersity index (PDI) of 1.30.The peak molecular weight (M_p) of the polymer is 2306. GPC results are presented in Table 4 5.

Table 4.5: Results of the Polymerisation of (a) P(EHT) and (b) P(EC)

Polymer	M_n	M_w	M_P	PDI
P(EHT)	12592	20248	12805	1.61
P(EC)	2328	3021	2306	1.30

The ^{1}H NMR spectra of the polymers P(EHT) and P(EC) are shown in figure 4.10**.** The ^{1}H NMR spectrum of P(EHT) showed multiplets at δ 0.9-8.5 due to aliphatic protons. It also showed a multiplet at δ4.0 due to -CH_2-O- in EDOT unit. In the case of P(EC), it showed both aliphatic and aromatic protons.

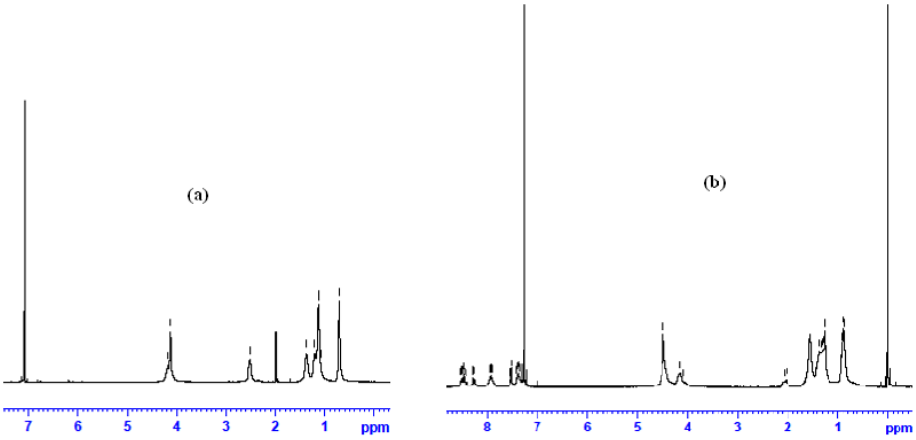

Fig. 4.10: ^{1}H NMR of the polymers: (a) P (EHT) and (b) P(EC)

4.2.3.1 Optical and photoluminescence properties

Figure 4.11 shows the absorption spectra of the polymers. The optical properties of the polymers, P (EHT) and P(EC) were investigated in chloroform. The polymers, P (EHT) and P(EC) showed absorption maximum around 440 nm and 382 nm respectively. The absorption onset of P (EHT) and P(EC) occurs at 583 nm and 571 nm respectively. The optical band gap calculated was found to be 2.12 eV and 2.16 eV respectively. The band gaps calculated from optical methods are in good agreement with the theoretical values. From quantum chemical calculations, band gap obtained are 2.2 eV and 2.86 eV respectively.

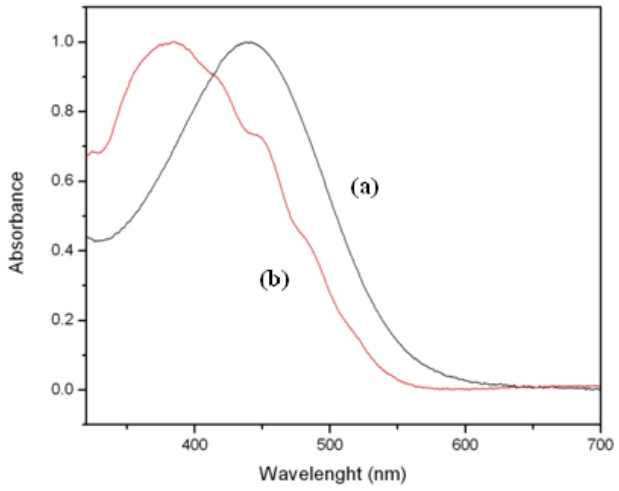

Fig.4.11: UV-Vis spectra of the polymers: (a) P (EHT) and (b) P(EC) in 2mg/10mL chloroform

Fig 4.12 shows the emission spectra of P (EHT) and P(EC) in chloroform. The maximum emission shown by the polymers are at 568 nm and 546 nm respectively. The emission and absorption spectrum of P (EHT) is red shifted than that of P(EC).

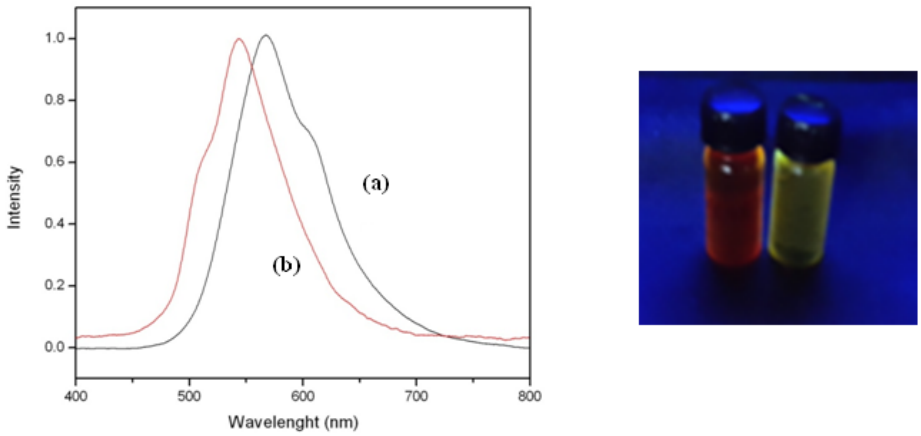

Fig.4.12: PL Spectra of the polymers :(a) P (EHT) and (b) P(EC) in 2mg/10 mL chloroform solution(Excitation wavelength 365 nm)

4.2.3.2 Thermal properties

The thermal characteristics of the polymers were investigated by TG-DTG studies. In P(EHT), DTG traces showed onset of degradation around 300 °C and degradation temperature at 400°C, losing around 5 % weight at the onset loss point. P(EC) shows multiple degradation pattern, the onset of degradation is around 200°C. Here, about 15% weight loss took place at the onset loss point. From the plot it is clear that P(EHT) is thermally more stable compared to P (EC).TG-DTG traces of the polymers are shown in the fig 4.13.

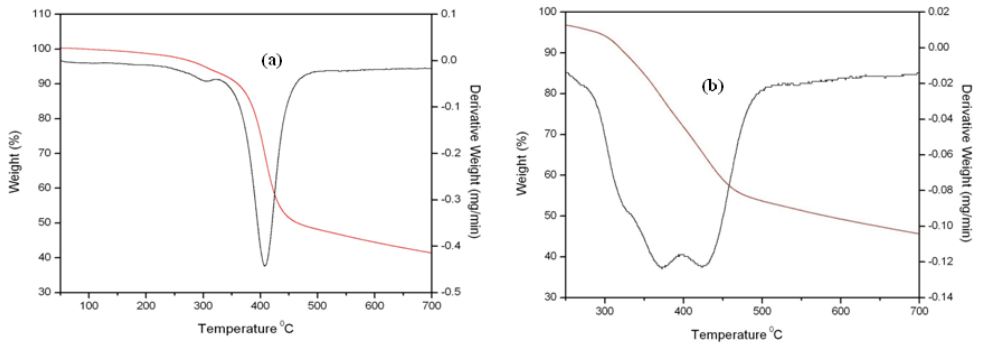

Fig.4.13: TG and DTG traces of the polymers: (a) P (EHT) and (b) P(EC)

4.2.3.4 Electrochemical studies

From the Cyclic voltammetric studies carried out, the HOMO levels (the onset of oxidation) of P(EHT) and P(EC) were calculated to be -5.76 eV and -5.58 eV respectively by using the equation, HOMO = - (4.4 + Eox^{onset}). The LUMO energy levels (from the onset of reduction potentials) of P(EHT) and P(EC) were calculated to be -3.24 eV and -3.33 eV. The band gaps calculated for P(EHT) and P(EC) are 2.5 eV and 2.25 eV respectively. In conclusion, after copolymerisation HOMO levels were elevated and LUMO levels of the polymers were lowered. Band gap calculated by means of theoretical, electrochemical and optical methods are depicted in Table 4.6.

Table 4.6: Band gap calculated by means of theoretical, electrochemical and optical methods

Polymer	Eg (theoretical) eV	Eg (Electrochemical) eV	Eg (Optical) eV
P(EHT)	2.2	2.5	2.12
P(EC)	2.86	2.25	2.16

4.2.4 Synthesis of cyanovinylene based polymers

The three theoretically designed cyanovinylene based polymers (P(CN1), P(CN2) and P(CN3))were synthesised by Suzuki cross-coupling reaction using $Pd(PPh_3)_4$ as the catalyst. The dibromocyanovinylene derivatives were reacted with the dioxaborolane derivative of fluorene in the presence of the catalyst $Pd(PPh_3)_4$ to form the corresponding polymers. The crude polymers were purified by precipitating from methanol followed by soxhlet extraction using methanol and hexane. The polymers P(CN1) and P(CN2) are soluble in common organic solvents such as chloroform, chlorobenzene and

THF while P(CN3) is only sparingly soluble in these solvents. The synthetic route towards the copolymers is depicted in Scheme 8.

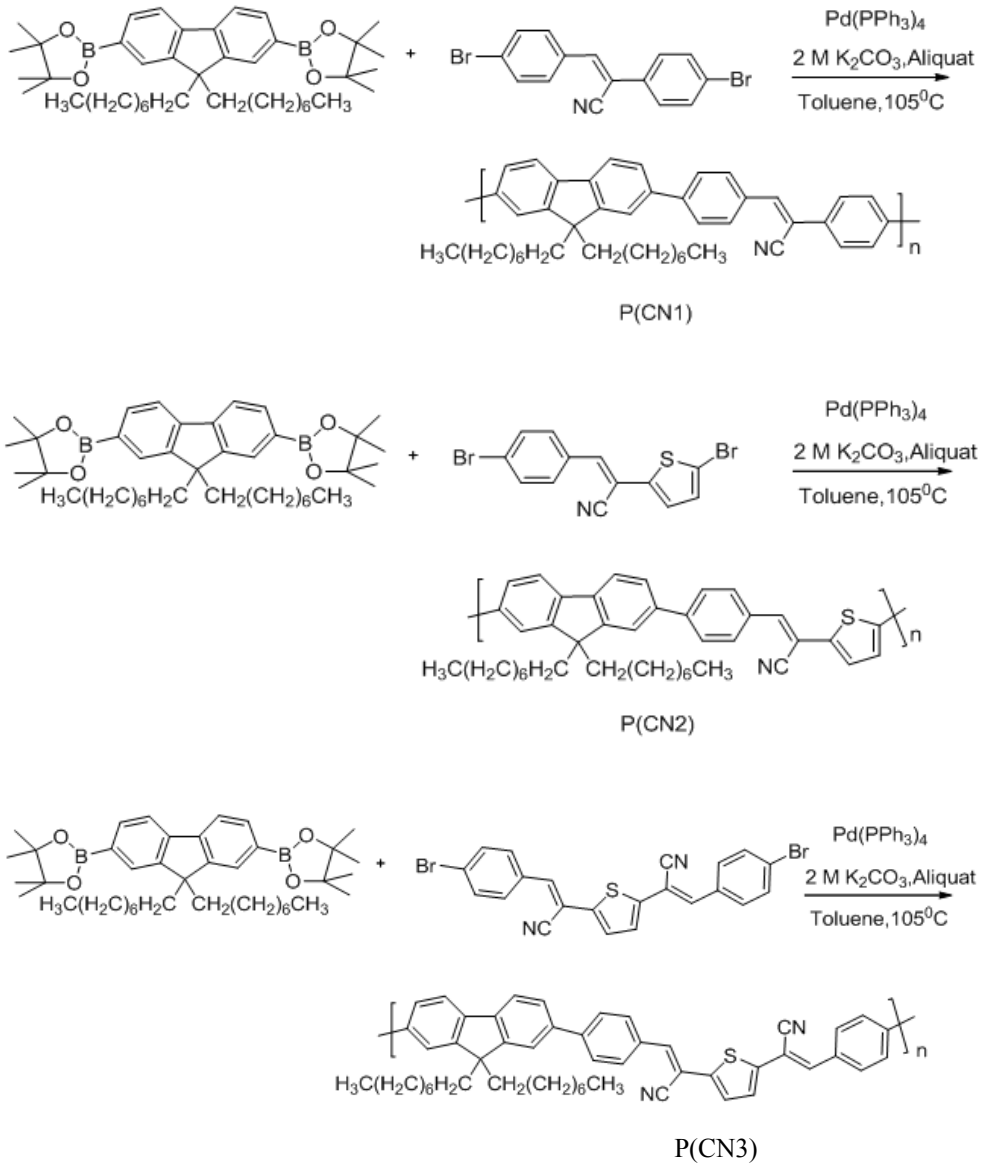

Scheme 8: Synthesis of P(CN1), P(CN2) and P(CN3)

The three polymers were characterized using ^{1}H NMR, UV-Visible spectroscopy, GPC, Cyclic voltammetry, TGA etc. The molecular weights of the polymers were obtained from gel permeation chromatography in THF referring to polystyrene standards. Among the three polymers, P(CN3) showed high molecular weight. The copolymer exhibited number average molecular weight (M_n) of 14398 and weight average molecular weight (M_w) of 16379 with polydispersity index (PDI) of 1.14. Table 4 7 summarizes the molecular weight and polydispersity index (PDI) of the copolymers.

Table 4.7: Results of the polymerisation reaction

Polymer	M_n	M_w	Mp	PDI
P(CN1)	7803	12820	8975	1.64
P(CN2)	7321	11061	7835	1.51
P(CN3)	14398	16379	11845	1.14

The ^{1}H NMR spectra of the polymers P(CN1) and P(CN2) are shown in figure 4.14. Here, the two polymers showed peaks in the aliphatic and aromatic regions. Peaks in the δ 7.0- 8.0 are due to protons of the fluorene, thiophene and phenyl rings and one hydrogen substituted to vinyl group. Because of the poor solubility we could not obtained the ^{1}H NMR spectrum of the polymer P(CN3).

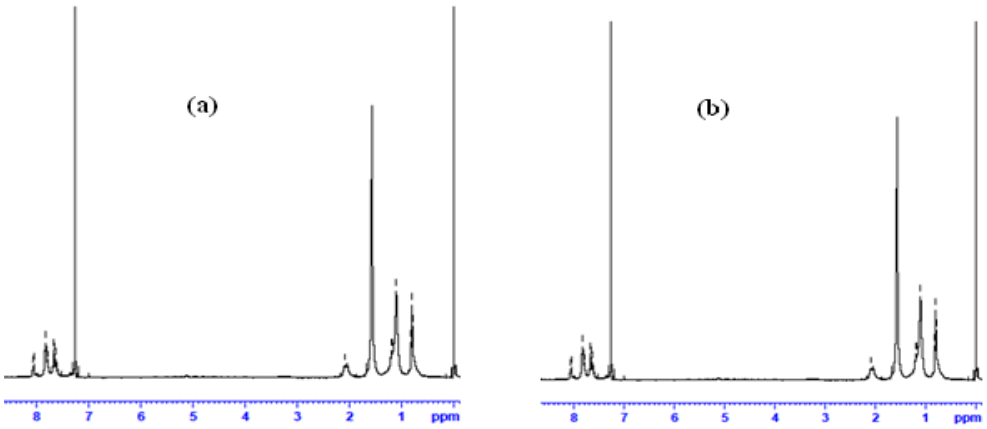

Fig.4.14: ^{1}HNMR of the polymers: a - P (CN1) and b) P(CN2)

4.2.4.1 Optical and photoluminescence properties

Figure 4.15 shows the absorption spectra of the polymers. The optical properties of the polymers, P(CN1) and P(CN2) were investigated in chloroform and P(CN3) with the help of UV-Vis-DRS method. The polymers, P(CN1), P(CN2) and P(CN3) showed absorption maximum around 393 nm, 431 nm and 375 nm respectively. The absorption onset of P(CN1), P(CN2) and P(CN3) occurs at 456 nm, 543 nm, and 575 nm respectively. The optical band gap calculated was found to be 2.71 eV, 2.28 eV and 1.97 eV respectively. The band gaps calculated from optical methods are in good agreement with the theoretical values. From Quantum chemical calculations, band gap obtained are 2.62 eV, 2.25eV and 2.15 eV respectively.

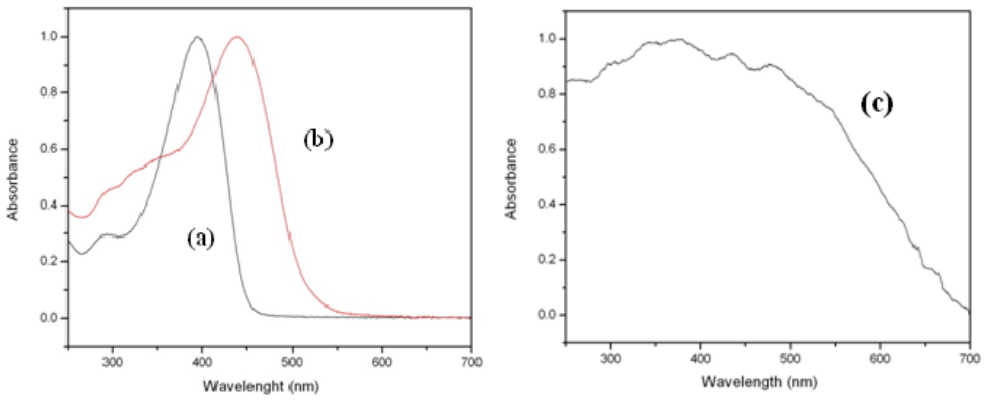

Fig.4.15 : UV-Vis Spectra of the polymer : (a) P(CN1) and (b) P(CN2) in 2mg/10mL chloroform solution (c) UV-Vis-DRS spectra of P(CN3)

Figure 4.16 shows the emission spectra of P(CN1) and P(CN2) in chloroform. The maximum emission shown by the two polymers are 494 nm and 547 nm respectively. Here the emission spectrum of the polymer P(CN2) is red shifted when compared to the other polymer due to extensive conjugation present in the polymer.

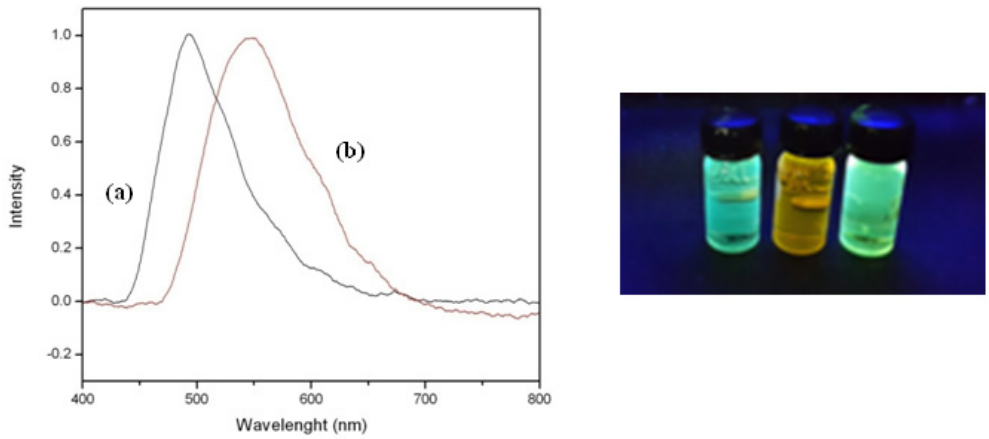

Fig 4.16: PL Spectra of the polymer: (a) P(CN1) and (b) P(CN2) in 2mg/10mL chloroform solution (Excitation wavelength 365 nm)

4.2.4.2 Thermal properties of polymers

From thermogravimetric studies, it is clear that the first two polymers, P(CN1) and P(CN2) follow single degradation pattern and shows degradation temperature around 430°C, while the third shows step wise degradation. In P(CN3), degradation starts around 200°C. In the first two polymers around 15% weight loss took place at the onset loss point. TG-DTG traces of the polymers are shown in figure 4.17.

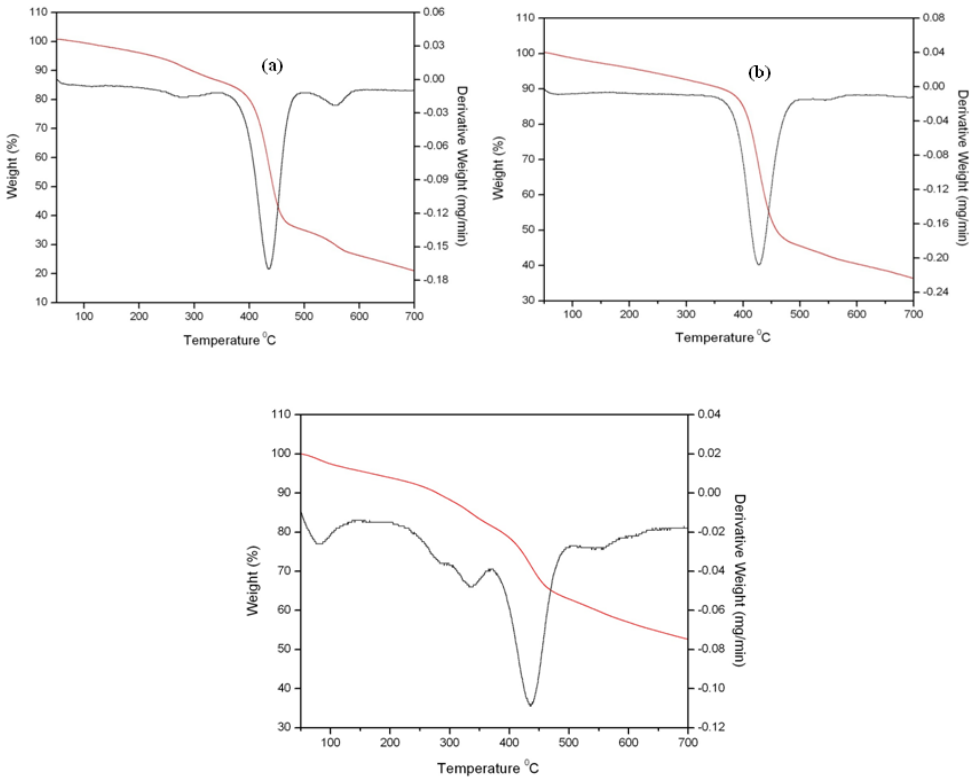

Fig 4.17: TG and DTG traces of the polymers: P(CN1), P(CN2) and P(CN3)

4.2.4.3 Electrochemical studies

From the cyclic voltammetric studies carried out, the HOMO levels (the onset of oxidation) of P(CN2) and P(CN3) were calculated to be -5.9 eV and -5.76 eV respectively by using the equation, HOMO = - (4.4 + Eox^{onset}). The LUMO energy levels (from the onset of reduction potentials) of P(CN2) and P(CN3) were calculated to be -3.21 eV and -3.6 eV. The band gap calculated for P(CN1), P(CN2) and P(CN3) are 2.71 eV, 2.70 eV and 2.0 eV respectively. Band gap calculated by means of theoretical, electrochemical and optical methods are depicted in the Table 4.8.

Table 4.8: Band gap calculated by means of theoretical, electrochemical and optical methods

Polymer	Eg (theoretical) eV	Eg (Electrochemical) eV	Eg (Optical) eV
P(CN1)	2.62	2.71	2.71
P(CN2)	2.25	2.70	2.28
P(CN3)	2.15	2.0	1.97

4.2.5 Synthesis of phenylene based polymers

Phenylene based polymers, P(PDO), P(POF) and P(PF) were synthesised by Suzuki cross-coupling reaction using $Pd(PPh_3)_4$ as the catalyst. The dibromo derivatives of benzoxadiazole, fluorene and fluorenone were reacted with the benzene 1,4-diboronic acid in the presence of the catalyst $Pd(PPh_3)_4$ to form the corresponding polymers. The crude polymers were purified by precipitating from methanol followed by soxhlet extraction using methanol and hexane. The polymer P(PDO), P(POF) and P(PF) are only sparingly soluble in common organic solvents such as chloroform, chlorobenzene and THF. The synthetic route towards the copolymers is depicted in Scheme 9.

The polymers were characterized using ^{1}H NMR, UV-Visible spectroscopy, GPC, Cyclic voltammetry, TGA etc. Among the polymers, P(PDO) shows high molecular weight. It shows number average molecular weight of 11359 and weight average molecular weight (M_w) of 12603 with polydispersity index (PDI) of 1.11. The molecular weight data of the polymers are summarized in Table 4.9.

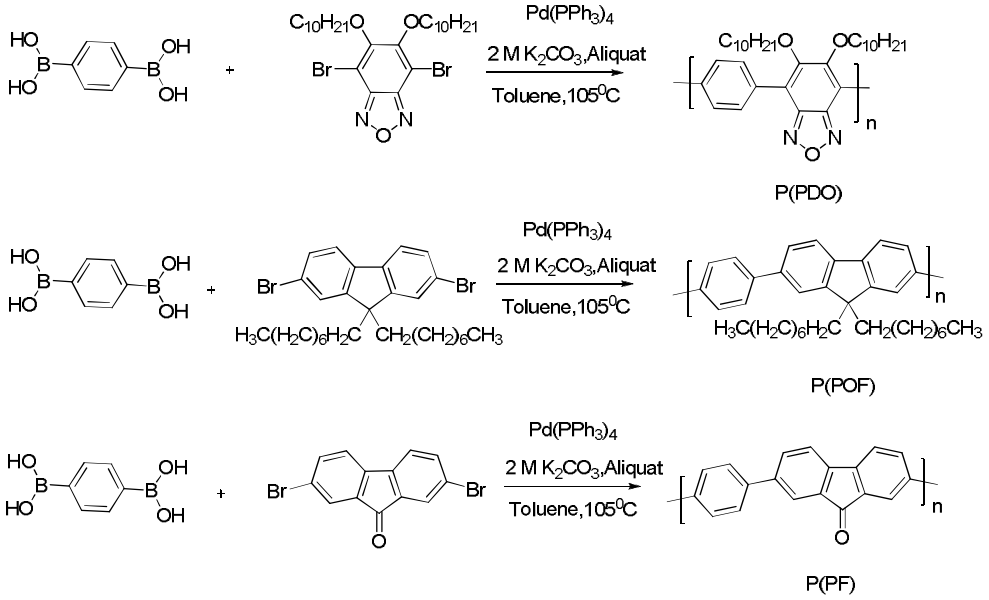

Scheme 9: Synthesis of P(PDO), P(POF) and P(PF)

Table 4.9: Results of the polymerisation reaction

Polymer	M_n	M_w	M_p	PDI
P(PDO)	11359	12603	12419	1.11
P(POF)	2645	2804	2754	1.06
P(PF)	5666	8144	8992	1.44

The ^{1}H NMR spectra of the polymers P(PDO), P(POF) and P(PF) are shown in figure 4.18. P(PDO) showed multiplets at δ 0.8 -2 due to aliphatic protons. It showed multiplets at δ4.0 due to -CH_2-O-. It also showed multiplets in the aromatic region. In the case of P(POF), it showed multiplets in both aliphatic and aromatic regions whereas, in P(PF), it showed multiplets only in the aromatic region.

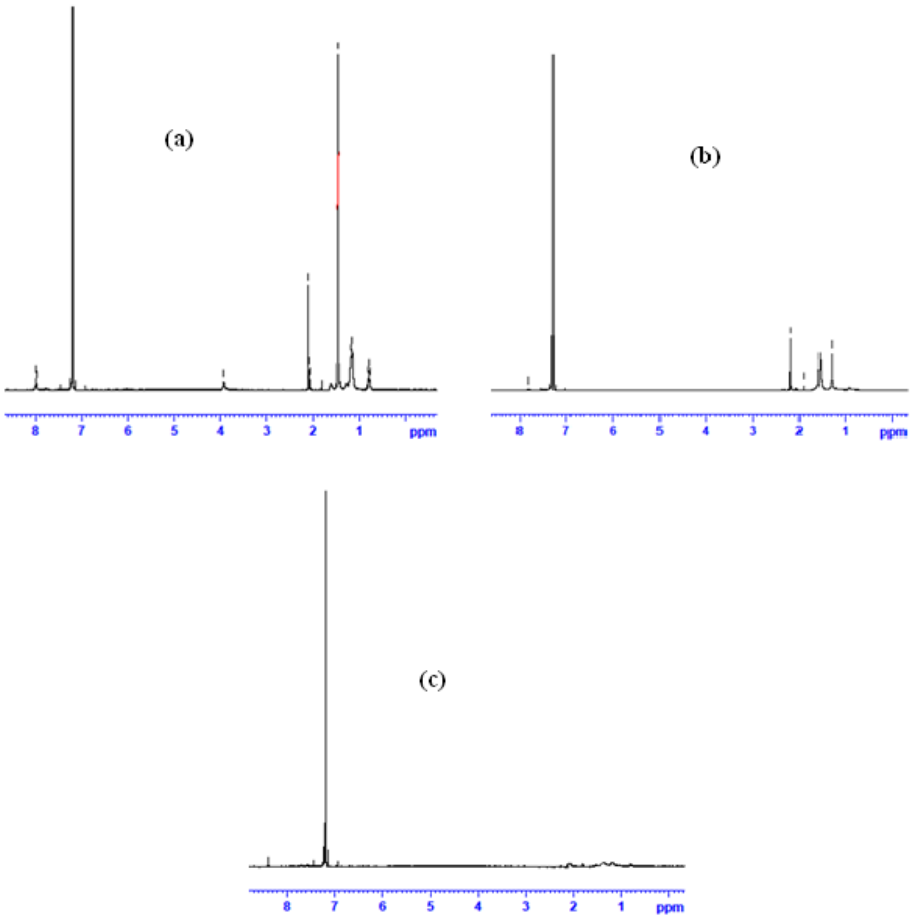

Fig 4.18: ^{1}H NMR of the polymers: a) P(PDO), b) P(POF) and c) P(PF)

4.2.5.2 Optical and photoluminescence properties

Figure 4.19 shows the absorption spectra of the polymers. The optical properties of the polymers, P(PDO) and P(PF) were investigated by UV-Vis-DRS. P(PDO) and P(PF) showed absorption maximum around 360 nm and 380 nm respectively. The absorption onset of P(PDO) and P(PF) occur at 462 nm and 581 nm respectively. The optical band gap calculated was found to be 2.68 eV and 2.0 eV respectively. The band gaps calculated from optical methods are in agreement with the theoretical values. From quantum chemical calculations band gap obtained are 2.86 eV and 2.68 eV respectively.

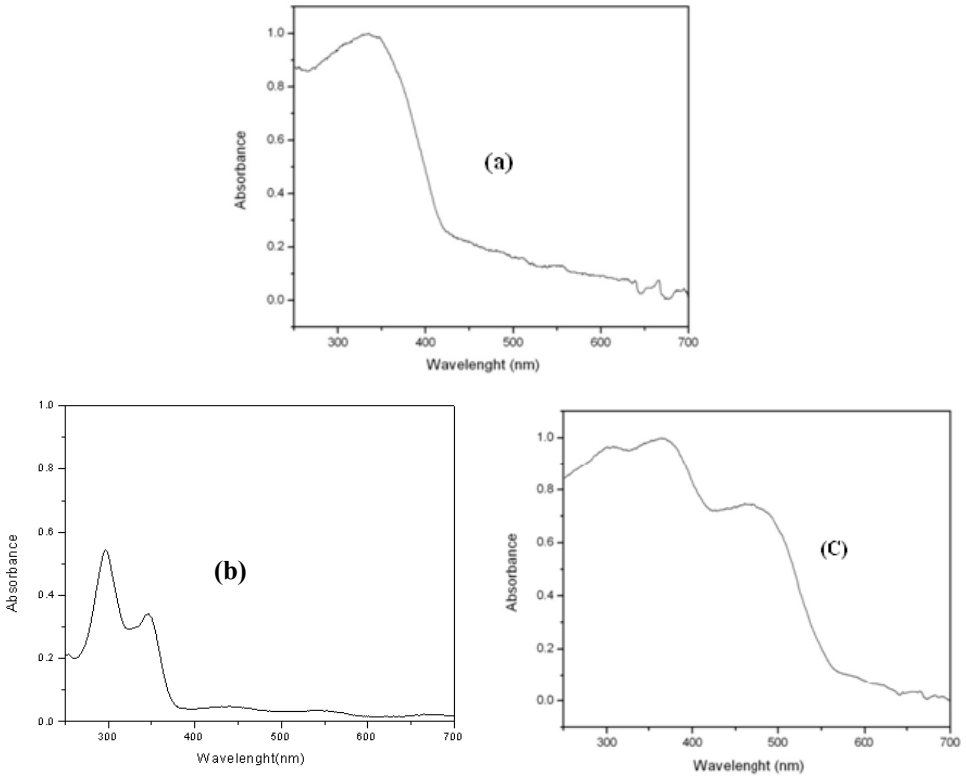

Fig 4.19: UV-Vis-DRS of the polymers: (a) P(PDO), (b) P(POF) and (c) P(PF))

Figure 4.20 shows the emission spectra of P(PDO) and P(PF) in chloroform. The maximum emission shown by the two polymers are at 496 nm and 541 nm respectively. Here the emission spectrum of the polymer P(PF) is red shifted when compared to the other polymer due to strong electron withdrawing carbonyl group in the polymer.

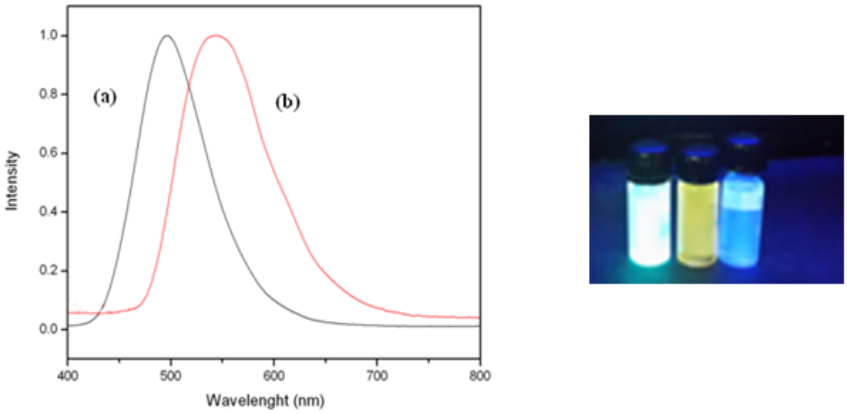

Fig 4.20: PL spectrum of the polymers: (a) P(PDO) and (b) P(PF) in 2mg/10mL chloroform solution (Excitation wavelength 365 nm)

4.2.5.3 Thermal and electrochemical studies

The thermal characteristics of the polymers were investigated by TG-DTG studies and are shown in figure 4.21.The polymers showed multiple degradation peaks. In the polymers, P(PDO), P(POF) and P(PF) degradation starts around 200°C. Cyclic voltammetric studies were carried out to determine the HOMO, LUMO levels and band gap of the polymers. From CV studies, the band gap value calculated for the polymers, P(PDO), P(POF) and P(PF) are 2.68 eV, 2.8 eV, and 2.2 eV respectively. Band gap calculated by means of theoretical, electrochemical and optical methods are depicted in Table 4.10.

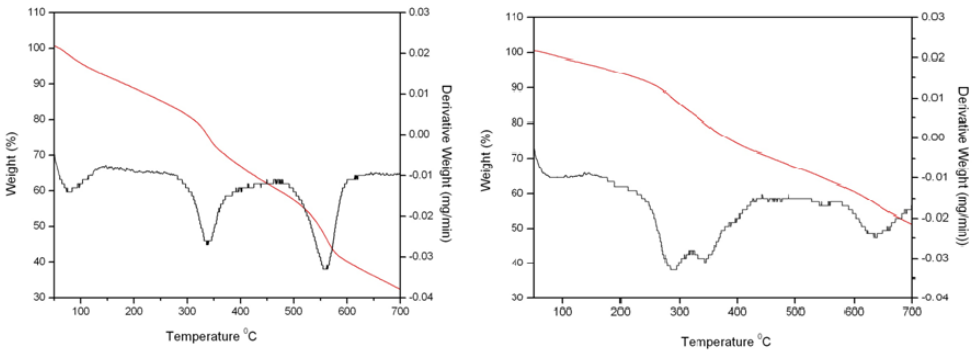

Fig.4.21: TG and DTG traces of the polymers:P(PDO) and P(PF)

Table 4.10: Band gap calculated by means of theoretical, electrochemical and optical methods

Polymer	Eg (theoretical) eV	Eg (Electrochemical) eV	Eg (Optical) eV
P(PDO)	2.86	2.68	2.68
P(POF)	2.73	2.8	3.2
P(PF)	2.68	2.2	2.0

4.3 Experimental part

4.3.1 Synthesis of fluorene-quinoxaline polymers

Synthesis of P(FQ-A)

Under nitrogen atmosphere, 5,8-dibromoacenaphthyl quinoxaline (0.25 g, 0.60 mmol), 2,7-bis(4,4,5,5-tetramethyl-1,3,2-dioxaborolan-2-yl)-9,9-dioctylfluorene (0.39 g, 0.60 mmol) were mixed together with 10 mol% of $Pd(PPh_3)_4$ and aliquat 336 in 20 mL of toluene. Degassed solution (15 min) of 2.0 M potassium carbonate (10 mL) and toluene (20 mL) were added to the reaction mixture. The mixture was stirred vigorously at 80-90°C for 72 h under nitrogen atmosphere. The resulting solution was added drop wise into methanol with stirring to precipitate

the polymer. The solid was collected by filtration and washed with methanol and water. The product was washed continuously with methanol and acetone for 2 days in a Soxhlet extractor to remove the oligomers and catalyst residues. The product was dried under reduced pressure.

Yield	:	40 %
UV-Vis ($CHCl_3$) λmax	:	321 nm
^{1}H NMR (400 MHz, $CDCl_3$)	:	δ 0.8 (6 H, m), 1.3 (4H, m), 1.6 (20 H, s), 2.1 (4 H, m) , 7.5-8.5 (12 H, m)

Synthesis of P(FQ-B)

Under nitrogen atmosphere, 5,8-dibromo-2,3-diphenyl quinoxaline (0.16 g, 0.36 mmol), 2,7-bis(4,4,5,5-tetramethyl-1,3,2-dioxaborolan-2-yl)-9,9-dioctylfluorene (0.24 g, 0.36 mmol) were mixed together with 10 mol% of $Pd(PPh_3)_4$ and aliquat 336 in 20 mL of toluene. Degassed (15 min) aqueous solution of 2.0 M potassium carbonate (10 mL) and toluene (20 mL) were added to the flask. The mixture was stirred vigorously at 80-90°C for 72 h under nitrogen atmosphere. The resulting solution was added drop wise into methanol with stirring to precipitate the polymer. The solid was collected by filtration and washed with methanol and water. The product was washed continuously with methanol and acetone for 2 days in a Soxhlet extractor to remove the oligomers and catalyst residues. The product was dried under reduced pressure.

Yield	:	45 %
UV-Vis ($CHCl_3$) λmax	:	310 nm
^{1}H NMR (400 MHz, $CDCl_3$)	:	δ 0.9 (6 H, m), 1.2 (20H, s), 1.6 (4 H, m), 2.3 (4 H, m) , 7 - 8 (18 H, m)

Synthesis of P(FQ-P)

Under nitrogen atmosphere, 10,13-dibromodibenzo[a,c]phenazine (0.27 g, 0.61 mmol), 2,7-bis (4,4,5,5-tetramethyl-1,3,2-dioxaborolan-2-yl)-9,9-dioctylfluorene (0.40 g, 0.61 mmol) were mixed together with 10 mol % of $Pd(PPh_3)_4$ and aliquat 336 in 20 mL of toluene. Degassed (15 min) aqueous solution of 2.0 M potassium carbonate (10 mL) and toluene (20 mL) were added to the flask. The mixture was stirred vigorously at 80-90°C for 72 h under nitrogen atmosphere. The resulting solution was added drop wise into methanol with stirring to precipitate the polymer. The solid was collected by filtration and washed with methanol and water. The product was washed continuously with methanol and acetone for 2 days in a Soxhlet extractor to remove the oligomers and catalyst residues. The product was dried under reduced pressure.

Yield	:	35 %
UV-Vis ($CHCl_3$) λmax	:	330 nm
^{1}H NMR (400 MHz, $CDCl_3$)	:	δ 0.9 (6 H, m), 1.2 (4H, m), 1.6 (20 H, s), 2.1 (4 H, m), 6.8 – 8.5 (16 H, m)

4.3.2 Synthesis of fluorene-thiophene copolymer

Synthesis of P(FMT)

To a stirred solution of 3,4-dimethoxythiophene (0.05 g, 0.36 mmol) in DMF (10 mL) was added tetrabutylammonium bromide (0.11 g, 0.36 mmol) and sodium acetate (0.12 g, 1.46 mmol) and stirred at room temperature for 15 min followed by the addition of 2,7-dibromo-9,9-dioctyl-9H-fluorene (0.20 g, 0.36 mmol) and palladium acetate (10 mol%). The reaction mixture was stirred at 90°C for 48 h. The mixture was cooled

and poured in to cold methanol. The precipitate was filtered and purified by soxhlet extraction using methanol and hexane as solvent. The polymer was dissolved in minimum amount of chloroform and precipitated by adding methanol. The precipitate was filtered and dried under vacuum for 24 h.

Yield	:	40 %
UV-Vis ($CHCl_3$) λmax	:	476 nm
^{1}H NMR (400 MHz, $CDCl_3$)	:	δ 0.8 (6 H, m), 1.2 (20H, s), 1.6 (4 H, m), 2.1 (4 H, m), 4(6H, s),7.8 (5 H, m)

Synthesis of P(EF)

EDOT(0.26 g, 1.8 mmol), tetrabutylammonium bromide (0.60 g, 1.8 mmol) and sodium acetate (0.61 g, 7.5 mmol) in DMF (10 mL) were stirred at room temperature for 30 min followed by the addition of 2,7-dibromo-9,9-dioctyl-9H-fluorene (1.03 g, 1.8 mmol) and palladium acetate (10 mol%). The reaction mixture was stirred at 90°C for 48 h. The reaction mixture was cooled and poured in to cold methanol. The precipitate was filtered. The polymer was purified by Soxhlet extraction using methanol and hexane as solvent. The polymer was dissolved in minimum amount of chloroform and precipitated by adding methanol. The precipitate was filtered and dried under vacuum for 24 h.

Yield	:	55 %
UV-Vis ($CHCl_3$) λmax	:	450 nm
^{1}H NMR (400 MHz, $CDCl_3$)	:	δ 0.8 (6 H, m), 1.2 (4H, m), 1.7 (20 H, s), 2 (4 H, m) , 4 (4H, m) , 7-8 (6H, m)

4.3.3 Synthesis of thiophene and carbazole based polymers

Synthesis of P(EHT)

EDOT (0.05 g, 0.36 mmol), tetrabutylammonium bromide (0.117 g, 0.36 mmol), sodium acetate (0.12 g, 1.4 mmol) in DMF (10 mL) were stirred at room temperature for 15 min followed by the addition of 3,4-dihexyl-2,5-dibromothiophene (0.15 g, 0.36 mmol) and palladium acetate (10 mol%). The reaction mixture was stirred at 90°C for 48 h. The reaction mixture was cooled and poured in to cold methanol. The precipitate was filtered. The polymer was purified by soxhlet extraction using methanol and hexane as solvent. The polymer was dissolved in minimum amount of chloroform and precipitated by adding methanol. The precipitate was filtered and dried under vacuum for 24 h.

Yield	:	50 %
UV-Vis ($CHCl_3$) λmax	:	440 nm
^{1}H NMR (400 MHz, $CDCl_3$)	:	δ 0.9 (6 H, m), 1.2 (16 H,m), 1.4 (4 H, m), 2.5 (4 H, m) , 4 (4H,m)

Synthesis of P(EC)

EDOT(0.27 g, 1.89 mmol), tetrabutylammonium bromide (0.55 g, 1.89 mmol) and sodium acetate (0.66 g, 8 mmol) in DMF (10 mL) were stirred at room temperature for 15 min followed by the addition of 3,6-dibromo-N-(2-ethylhexyl) carbazole (0.83 g, 1.89 mmol) and palladium acetate (10 mol%). The reaction mixture was stirred at 90°C for 48 h. The reaction mixture was cooled and poured in to cold methanol. The precipitate was filtered. The polymer was purified by soxhlet extraction using methanol and hexane as solvent. The polymer was dissolved in minimum amount of

chloroform and precipitated by adding methanol. The precipitate was filtered and dried under vacuum for 24 h.

Yield	:	55 %
UV-Vis ($CHCl_3$) λmax	:	382 nm
^{1}H NMR (400 MHz, $CDCl_3$)	:	δ 0.9(6 H, m), 1.3(6H,m), 1.5 (2 H, m), 2.1 (2 H, m) , 4 (1H, m), 4.5 (4H,m), 7- 8.5 (6 H, m)

4.3.4. Synthesis of cyanovinyline based polymers

Synthesis of P(CN1)

Under nitrogen atmosphere, (E)-2,3-bis (4-bromophenyl) acrylonitrile (0.15 g, 0.41 mmol), 2,7-bis (4,4,5,5-tetramethyl-1,3,2-dioxaborolan-2-yl)-9,9-dioctylfluorene (0.23 g, 0.41 mmol) were mixed together with 10 mol % of $Pd(PPh_3)_4$ and aliquat 336 in 20 mL of toluene. Degassed (15 min) aqueous solution of 2.0 M potassium carbonate (10 mL) and toluene (20 mL) were added to the flask. The mixture was stirred vigorously at 80-90°C for 72 h under nitrogen atmosphere. The resulting solution was added drop wise into methanol with stirring to precipitate the polymer. The solid was collected by filtration and washed with methanol and water. The product was washed continuously with methanol and hexane for 2 days in a Soxhlet extractor to remove the oligomers and catalyst residues. The product was dried under reduced pressure.

Yield	:	35%
UV/Vis ($CHCl_3$) λmax	:	393 nm
^{1}H NMR (400 MHz, $CDCl_3$)	:	δ 0.8 (6 H, m), 1.2 (4H, m), 1.8 (20 H, s), 2.1 (4 H, m), 7- 8.3 (14H (Aromatic), 1H (vinyl), m)

Synthesis of P(CN2)

Under nitrogen atmosphere, (Z)-3-(4-bromophenyl)-2-(5-bromothiophen-2-yl) acrylonitrile (0.15 g, 0.4 mmol), 2,7-bis(4,4,5,5-tetramethyl-1,3,2-dioxaborolan-2-yl)-9,9-dioctylfluorene (0.22 g, 0.4 mmol) were mixed together with 10 mol% of $Pd(PPh_3)_4$ and aliquat 336 in 20 mL of toluene. Degassed (15 min) aqueous solution of 2.0 M potassium carbonate (10 mL) and toluene (20 mL) were added to the flask. The mixture was stirred vigorously at 80-90°C for 72 h under nitrogen atmosphere. The resulting solution was added drop wise into methanol with stirring to precipitate the polymer. The solid was collected by filtration and washed with methanol and water. The product was washed continuously with methanol and acetone for 2 days in a Soxhlet extractor to remove the oligomers and catalyst residues. The product was dried under reduced pressure.

Yield	:	40%
UV/Vis ($CHCl_3$) λmax	:	431 nm
^{1}H NMR (400 MHz, $CDCl_3$)	:	δ 0.9 (6 H, m), 1.2 (4H, m), 1.7 (20 H, s), 2.1 (4 H, m), 7- 8.5 (12 H (Aromatic), 1H (vinyl), m)

Synthesis of P(CN3)

Under nitrogen atmosphere, (2E,2'E)-2,2'-(thiophene-2,5-diyl)-bis-(3-(4-bromophenyl)acrylonitrile) (0.32 g, 0.65mmol), 2,7-bis(4,4,5,5-tetramethyl-1,3, 2-dioxaborolan-2-yl)-9,9-dioctylfluorene (0.36 g, 0.65 mmol) were mixed together with 10 mol% of $Pd(PPh_3)_4$ and aliquat 336 in 20 mL of toluene.

Degassed (15 min) aqueous solution of 2.0 M potassium carbonate (10 mL) and toluene (20 mL) were added to the flask. The mixture was stirred vigorously at 80-90°C for 72 h under nitrogen atmosphere. The resulting solution was added drop wise into methanol with stirring to precipitate the polymer. The solid was collected by filtration and washed with methanol and water. The product was washed continuously with methanol and acetone for 2 days in a Soxhlet extractor to remove the oligomers and catalyst residues. The product was dried under reduced pressure.

Yield : 50 %

UV/Vis ($CHCl_3$) λmax : 385 nm

4.3.5. Synthesis of Phenylene based polymers

Synthesis of P(POD)

Under nitrogen atmosphere, 4,7-dibromo-5,6-bis(decyloxy)benzo[c] [1,2,5]oxadiazole (0.32 g, 0.54mmol), benzene 1,4-diboronic acid (0.08 g, 0.54 mmol) were mixed together with 10 mol% of $Pd(PPh_3)_4$ and aliquat 336 in 20 mL of toluene. Degassed (15 min) aqueous solution of 2.0 M potassium carbonate (10 mL) and toluene (20 mL) were added to the flask. The mixture was stirred vigorously at 80-90°C for 72 h under nitrogen atmosphere. The resulting solution was added drop wise into stirring methanol to precipitate the polymer. The solid was collected by filtration and washed with methanol and water. The product was washed continuously with methanol and hexane for 2 days in a Soxhlet extractor

to remove the oligomers and catalyst residues. The product was dried under reduced pressure

Yield	:	55 %
UV/Vis ($CHCl_3$) λmax	:	404 nm
1H NMR (400 MHz, $CDCl_3$)	:	δ 0.8 (6 H, m), 1.2 (4H, m), 1.6 (24 H, s), 2 (4 H, m), 4 (4H,m),8 (4H, m)

Synthesis of P(POF)

Under nitrogen atmosphere, 2,7-dibromo-9,9-dioctyl-9H-fluorene (0.4 g, 0.72 mmol), benzene 1,4-diboronic acid (0.12 g, 0.72 mmol) were mixed together with 10 mol% of $Pd(PPh_3)_4$ and aliquat 336 in in 20 mL of toluene. Degassed (15 min) aqueous solution of 2.0 M potassium carbonate (10 mL) and toluene (20 mL) were added to the flask. The mixture was stirred vigorously at 80-90°C for 72 h under nitrogen atmosphere. The resulting solution was added drop wise into methanol with stirring to precipitate the polymer. The solid was collected by filtration and washed with methanol and water. The product was washed continuously with methanol and acetone for 2 days in a Soxhlet extractor to remove the oligomers and catalyst residues. The product was dried under reduced pressure

Yield	:	40 %
UV/Vis ($CHCl_3$) λmax	:	350 nm
^{1}H NMR (400 MHz, $CDCl_3$)	:	δ 0.9 (6 H, m), 1.2 (20 H, s), 1.6 (4 H, m), 2.2 (4 H, m), 7.2- 8 (10H, m)

Synthesis of P(PF)

Under nitrogen atmosphere 2,7-dibromofluorenone (0.5 g, 1.4 mmol), benzene 1,4-diboronic acid (0.24 g, 1.4 mmol) were mixed together with 10 mol% of $Pd(PPh_3)_4$ and aliquat 336 in 20 mL of toluene. Degassed (15 min) aqueous solution of 2.0 M potassium carbonate (10 mL) and toluene (20 mL) were added to the flask. The mixture was stirred vigorously at 80-90°C for 72 h under nitrogen atmosphere. The resulting solution was added drop wise into methanol with stirring to precipitate the polymer. The solid was collected by filtration and washed with methanol and water. The product was washed continuously with methanol and acetone for 2 days in a Soxhlet extractor to remove the oligomers and catalyst residues. The product was dried under reduced pressure

Yield	:	50 %
UV/Vis ($CHCl_3$) λmax	:	296 nm
^{1}H NMR (400 MHz, $CDCl_3$)	:	δ 7 – 8. (1 H, m),

4.4 Conclusion

Thirteen theoretically designed polymers were synthesised by means of Suzuki and Direct arylation reactions. All the polymers were characterized using ^{1}H NMR, UV-Visible spectroscopy, GPC, Cyclic voltammetry, TGA etc. HOMO level, LUMO level and band gap values for all the polymers were calculated by Optical and Electrochemical methods. It was found that experimental results were in good agreement with the theoretical results.

References

[1] J. M. Raimundo, P. Blanchard, H. Brisset, S. Akoudad, J. Roncali, Chem. Commun. 2000, 11, 939.

[2] J. Roncali, P. Fre` re, P. Blanchard, R. de Bettignies, M. Turbiez, S. Roquet, P. Leriche, Y. Nicolas, Thin Solid Films, 2006, 567, 511.

[3] A. Dhanabalan, J. K. J. van Duren, P. A. van Hal, J. L. J. Van Dongen, R. A. J. Janssen, Adv. Funct. Mater. 2001, 11, 255.

[4] C. J. Brabec, C. Winder, N. S. Sariciftci, J. C. Hummelen, A. Dhanabalan, P. A. van Hal, R. A. J. Janssen, Adv. Funct. Mater. 2002, 12, 709.

[5] L. M. Campos, A. Tontcheva, S. Gu¨nes, G. Sonmez, H. Neugebauer, N. S. Sariciftci, F. Wudl, Chem. Mater. 2005, 17, 4031

[6] (a) F. Zhang, E. Perzon, X. Wang, W. Mammo, M. R. Andersson, O. Ingana¨s, Adv. Funct. Mater. 2005, 15, 745

(b) Y. Xia, J. Luo, X. Deng, X. Li, D. Li, X. Zhu, W. Yang, Y. Cao, Macromol. Chem. Phys. 2006, 207, 511.

[7] (a)J. Roncali, Macromol. Rapid Commun. 2007, 28, 1761

(b) N. T. S. Phan, M. Van Der Sluys, C. W. Jones, Adv. Synth.Catal., 2006, 348, 609

(c) M. Baumann, I. R. Baxendale, Beilstein. J. Org. Chem., 2013, 9, 2265

[8] D. Muenmart , A. B. Foster , A. Harvey , M. Chen , O. Navarro , V. Promarak, M. C. McCairn , J. M. Behrendt , M. L. Turner, Macromolecules, 2014, 47, 6531.

[9] E. Lim, Int. J. Photoenergy, 2013, 1, 1.

[10] L. G. Mercier, M. Leclerc, Acc. Chem. Res., 2013, 46, 1597.

[11] F .Grenier, P. Berrouard, J. R. Pouliot, H. R. Tseng, A. J. Heeger, M. Leclerc, Polym. Chem., 2013, 4, 1836.

[12] W. Lu, J. Kuwabara, T. Iijima, H. Higashimura, H. Hayashi, T. Kanbara, Macromolecules, 2012, 45, 4128.

[13] J. Jo, A. Pron, P. Berrouard, W. L. Leong, J. D. Yuen, J. S. Moon, M . Leclerc, A. J. Heeger Adv. Energy Mater., 2012, 2, 1397.

[14] D. H . Wang, A. Pron, M. Leclerc, A. J. Heeger, Adv. Funct. Mater., 2013, 23, 1297.

[15] X. Wang, K. Wang, M. Wang, Polym. Chem.**,** 2015, 6, 1846.

[16] W. Lu, J. Kuwabara, T. Kanbara, Macromol. Rapid Commun., 2013, 34, 1151.

[17] P. Puschnig, C. A. Draxl, G. Heimel, E. Zojer, R. Resel, G. Leising, M. Kriechbaum, W. Graupner, Synth. Met., 2001, 116, 327.

[18] V. J. Eaton, D. Steele, J. Chem. Soc., Faraday Trans., 1973, 2, 1601.

[19] W. C. Wu, C. L. Liu, W. C. Chen, Polymer, 2006, 47, 527.

[20] M. Sendur, A. Balan, D. Baran, B. Karabay, L. Toppare, Organic Electronics, 2010, 11, 1877.

Chapter 5

PHOTOVOLTAIC AND NLO APPLICATIONS OF THE CONJUGATED POLYMERS

Contents

Conducting polymers have found a wide range of applications in the field of electronics and photonics, exploiting the unique physical, chemical and electrical properties of the polymers. Inherent electrical conductivity is the most notable property of conducting polymers, which is closely connected to the charge transfer rate and electrochemical redox efficiency. Most conducting polymers act as semiconductors, eventhough, several studies on metallic conducting polymers have been reported. In this chapter, the photovoltaic and nonlinear optical applications of conducting polymers are discussed. We have explored the photoactivity of the polymers by fabricating a heterojunction with a device structure of ITO/In_2S_3/polymer/ Ag. Further improvement in the power conversion efficiency can be achieved by optimizing the device parameters. The nonlinear absorption coefficient (β), nonlinear refractive index (n_2), the real and imaginary parts of $\chi^{(3)}$ (Re $\chi^{(3)}$ and Im $\chi^{(3)}$) and the third order nonlinear susceptibility $\chi^{(3)}$ of the polymers were also evaluated.

5.1 Introduction

In this `polymer age', tremendous advancement has been made in the field of optoelectronics by new designs and new concepts in materials science. The replacement of traditional inorganic semiconductors by organic molecules, polymeric or even biological materials has been termed as `molecular electronics'. Molecular electronic materials can offer viable alternatives to the traditional inorganic materials in many applications because of their abundance, diversity, ease of production, fabrication and potential high performance/ low cost.[1-10] Now-a-days, various polymeric materials have replaced the conventional materials such as metals and alloys in number of applications, like, aerospace, light engineering machinery, household goods, electronics etc, thus bringing about cost-effectiveness, reduction in size and weight. This has been possible because of the various mechanical and electrical properties which can be tailored into the polymers by a number of synthetic and processing techniques. Molecular engineering helps to control the electronic/optical properties of a resulting device by altering/modifying the polymer structure before fabricating the actual device. However, there still remains some fields where polymers have to enter in which metals still have an upper hand. Nevertheless, this situation may not last long since rapid advances are taking place in the field of conducting polymers. Literature suggests that they are promising in chemical and bio-sensors, field-effect transistors, light emitting devices, solar cells, super capacitors, actuators and separation membranes etc.[11-20]

The present chapter is concerned with the photovoltaic and third order nonlinear optical properties of the synthesised conjugated polymers.

5.1.1 Photovoltaics

As a solution to present-day energy crisis, solar energy has received much attention as an alternative source of energy due to its natural abundance and non-polluting nature. Amongst the various methods, photovoltaics has gained much popularity owing to its potential ability to provide cheap electricity. So far, only the traditional inorganic semiconductors (viz. CdS, Cu_2S, Si, GaAs etc.) have been mainly used in fabricating photovoltaic solar cells. After the emergence of conducting polymers, as a new class of semiconducting materials, it has generated considerable interest in the fabrication of polymer based solar cells.[20-26]

In the present chapter, we have explored the photovoltaic property of a bilayer heterojunction. In a bilayer OPV cell, sunlight is absorbed in the photoactive layers composed of donor and acceptor semiconducting polymeric materials to generate photocurrent. The donor material (D) donates electrons and mainly transports holes and the acceptor material (A) withdraws electrons and mainly transports electrons. Due to the concentration gradient, the excitons diffuse to the donor/acceptor interface (Exciton Diffusion) and separate into free holes (positive charge carriers) and electrons (negative charge carriers) (Charge Separation). A photovoltaic device is generated when the holes and electrons move to the corresponding electrodes by following either donor or acceptor phase (Charge Extraction). Fig 5.1 represents the fundamental architecture of bilayer heterojunction.

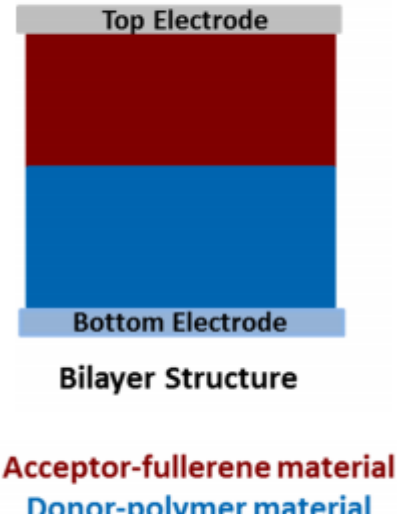

Fig. 5.1: Fundamental architecture of photoactive layer: bilayer heterojunction

In this thesis, the photovoltaic property of a bilayer heterojunction ITO/In_2S_3/polymer/Ag has been evaluated. In polymer solar cells, the front electrode is a transparent conducting oxide, such as indium-tin oxide (ITO), for hole collection. For the efficient operation of the device, the back electrode must be a low work function metal, which facilitates the collection of electrons.[27] However, these metals are reactive and get easily oxidized in air. The corrosion is normally addressed by capping the reactive metal with a less reactive metal and by encapsulating the device to protect it from environmental effects during operation. On the other hand, the devices can be made more stable by inverting the device geometry such that the holes and electrons generated in the active layer in the direction opposite to that in a normal device.[28] In this reversed geometry, a hole blocking layer, usually, an inorganic n-type semiconductor is inserted between the ITO and the active layer so that only electrons are collected by the ITO, where as the

back electrode becomes the hole collecting positive electrode, which can be made from a high work function metal that is more stable in air. Here, we have used indium sulfide (In_2S_3) as the electron selective layer. In_2S_3, an n type compound semiconductor with high electron affinity, wide band gap and excellent photosensitivity, should function as efficient electron acceptor/hole blocking layer in polymer photovoltaics. Its potential as buffer layer material in inorganic solar cells has already been demonstrated.[29]

5.1.2 Nonlinear optics

The unusual optical properties of conducting polymers like large nonlinear optical response, low switching energy, rapid switching times make them useful in the field of optoelectronics, which is aimed at replacing metal compounds that operate using electricity. Many approaches have been exploited to engineer the nonlinear optical response in conjugated polymers including the extension of conjugation length and the increase in planarity of the conjugated backbone.[30-33] It was found that magnitude of the third-order nonlinearity increases as the conjugation length increases and also incorporation of donors and acceptors into conjugated molecules could induce a charge redistribution upon photoexcitation resulting in exceptionally large third-order nonlinearities.[34-36]

Third order nonlinear optical properties provide the means to control light with light, to alter the frequency of the colour of light and to amplify one source of light with another.[32] Because of their large optical nonlinearities and good mechanical, chemical, thermal and optical stability, polymer materials are among the leading practical materials for device applications.[37] A number of techniques have been proposed to obtain information about the

dispersion, the sign and the contributions of both the real and imaginary parts of the nonlinear optical response. Five experimental techniques are currently widely used to characterize the third order nonlinear optical coefficient $\chi^{(3)}$ of materials ; a) The degenerate four wave mixing technique (DFWM), which gives the magnitude and response of $\chi^{(3)}$ b) Optical Kerr effect (OKE), which is normally sensitive to the real part of $\chi^{(3)}$, but can be modified to determine the imaginary part c) the Z-scan technique, which gives the size and sign of the nonlinearity and also allows time resolution d) third harmonic generation, which probes the electronic component of the nonlinearity and e) the electric field induced second harmonic generation technique (EFISH) which is used to measure the nonlinear response in liquids.[38]

5.1.2.1 Z-scan technique

The third order NLO properties of the polymers were investigated using z-scan technique.[39] The Z-scan technique was developed to simultaneously measure the magnitude of both the nonlinear refraction (NLR) and nonlinear absorption (NLA). The sign of the nonlinear refractive index (n_2) can also be obtained at the same time.

In nonlinear optics, z-scan measurement is used to measure the nonlinear refractive index n_2 and the nonlinear absorption coefficient via the "closed" and "open" methods respectively. In closed z-scan setup, an aperture is placed to prevent some of the light from reaching the detector. A lens focuses the laser to a certain point, and after this point, the beam naturally defocuses. After a further distance, an aperture is placed with a detector behind it. The aperture causes only the central region of the cone of

light to reach the detector. In open z-scan, the aperture is removed or enlarged to allow all the light to reach the detector. This is used in order to measure the nonlinear absorption coefficient. For materials with negative n_2, the profile of the z scan transmittance curve consists of a peak followed by a valley. For positive n_2 materials, the profile is reversed with a valley-peak sequence. The preceeding description asssumes that the sample is purely refractive and nonlinear absorption is not present. In cases in which the material has a significant nonlinear absorptive coefficient, the z scan profile is distorted, multiphoton absorption suppresses the peak and accentuates the valley, and saturation produces the opposite response.[40]

5.1.2.2 Optical limiting

An optical limiter is a device designed to keep the power, irradiance, energy or fluence transmitted by an optical system below some specified maximum value regardless of the magnitude of the input, i.e., maintaining a high transmittance at low input powers. The most important application of this device is the protection of sensitive optical sensors and components from laser damage. There are many other potential applications for these devices, including laser power regulation, stabilization or restoration of signal levels in optical data transmission or logic systems.[41-43]

Optical limiting effect results from intensity dependent optical nonlinear processes viz (a) nonlinear absorption (NLA) (b) nonlinear refraction (NLR) (c) nonlinear scattering (NLS), (d) photorefraction (PR) and (e) optically induced phase transitions. The minimum criteria identified for a material to act as an effective optical limiter are a) having a high linear transmittance b) a low limiting threshold c) a fast response time (e.g.

picoseconds or faster) c) a broad band response (e.g. the entire visible spectrum). d) low optical scattering.

Various approaches have been developed towards better optical limiting based on, e.g., electro-optical, magneto-optical, and all-optical mechanisms. The all-optical limiters rely on materials that exhibit one or more of the nonlinear optical mechanisms: two-photon absorption (TPA), excited state absorption (ESA), free carrier absorption, thermal defocusing and scattering, photorefraction, nonlinear refraction, induced scattering. Coupling two or more of these mechanisms has also achieved enhancement in optical limiting, like self-defocusing in conjunction with TPA, TPA in one molecule with ESA in another molecule.[44]

5.2 Results and discussion

5.2.1 Photovoltaic device fabrication

Photovoltaic activity of all the synthesised conjugated polymers were evaluated, in which one polymer was found to be promising. Heterojunction photovoltaic device was fabricated using the polymer (P(FMT) (poly-dimethoxythiophene–alt-dioctyl fluorene) as the active layer and the compound semiconductor In_2S_3 as the electron collecting layer. In_2S_3 is an n-type semiconductor having high electron affinity and is a potentially good acceptor material like CdS and TiO_2 for polymer solar cells. Indium sulfide (In_2S_3) thin films were deposited on ITO coated glass substrates by spraying aqueous solutions of indium chloride ($InCl_3$), and thiourea ($CS(NH_2)_2$), keeping the substrate at 350ºC with a spray rate of 4 ml/min. The thickness of the film was 200 nm. Heterojunctions were prepared by spin coating a solution of polymer in chlorobenzene, on top of the In_2S_3 layer. The layer

thickness was approximately 100 nm as obtained from Stylus profilometer measurements. Silver electrodes were vacuum deposited (at a pressure of ~6×10^{-6} Torr) on top of the polymer layer and served as the end contact. The schematic diagram is shown in figure 5.2. Dark and illuminated J-V characteristics of the cell were measured using a Keithley Source Measure Unit (SMU, K236) and Metric's Interactive Characterization Software (ICS). The cell was illuminated using a tungsten halogen lamp, with an intensity of 50mW/cm^2, on the substrate surface. An infrared filter, along with a water jacket, was used to ensure that there was no heating of the cell during the measurement.

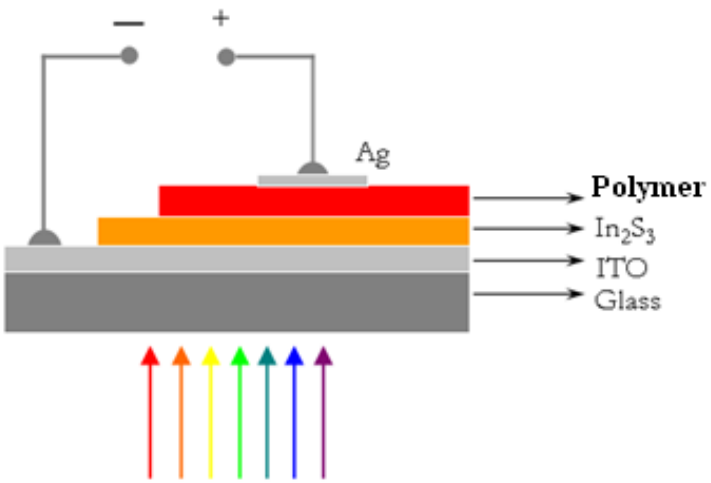

Fig. 5.2: Schematic diagram of In_2S_3/Polymer heterojunction

Figure 5.3 shows the current density-voltage (J-V) characteristics of the heterojunction of the polymer P(FMT) under illumination and in the dark. As could be seen, the device clearly exhibits rectifying behaviour in the dark which may be due to the barrier formed at the In_2S_3/ polymer

interface. Under white light illumination, the device of P(FMT) exhibits a short circuit current density (Jsc) of 0.69 mA/cm^2 and open circuit voltage (Voc) of 463 mV. The fill factor (FF) and efficiency for P(FMT) were calculated to be 30 and 0.09% respectively.

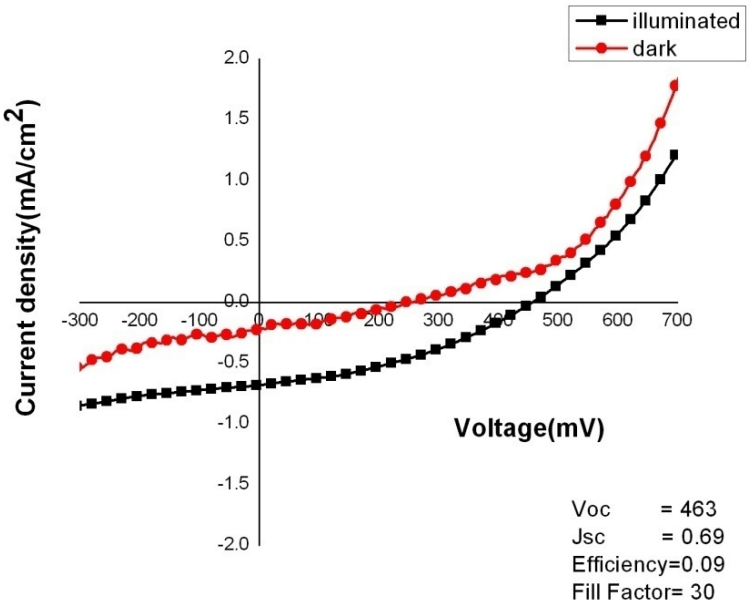

Fig. 5.3: J-V characteristics of ITO/In_2S_3/polymer/Ag heterojunction of P(FMT)

5.2.2 Open and Closed Scan Measurements

By employing the z-scan technique developed by Sheik Bahae et al, the third-order nonlinear susceptibility χ (3) of synthesized copolymers in chloroform was evaluated.[45] NLO measurements were performed by single by single beam z scan technique with nanosecond laser performed with a Q-switched Nd: YAG laser system (Spectra Physics LAB – 1760) with pulse width of 7 ns at 10 Hz repetition rate and 532 nm wavelength. In the

experiment, a Gaussian laser beam was focused to a narrow waist (42.56 μm). The sample was mounted on the translation stage and the transmitted intensity through the sample was measured, with and without the presence of an aperture at far field in front of the photodetector. As the sample moves through the beam focus (z = 0), self-focusing or self-defocusing modifies the wavefront phase, thereby modifying the detected beam intensity. The Rayleigh length, $Z_0 = \pi\omega_0^2/\lambda$, was calculated to be a higher value greater than the thickness of the sample cuvette (1mm), an essential requirement for z-scan experiments. The system was calibrated using CS_2 as the standard. The transmitted beam energy, reference beam energy and their ratios were measured simultaneously by an energy ratiometer having two identical pyroelectric detector heads. The effects of fluctuations of laser beam was eliminated by dividing the transmitted power by the power obtained at the reference detector. Optical power limiting measurements were also carried out to investigate the power limiting behaviour of the samples.[46]

To investigate the optical limiting property of the polymers, the nonlinear transmission was measured as a function of input fluence. Optical limiting property of a material is mainly due to absorptive nonlinearity, which corresponds to the imaginary part of third-order susceptibility, i.e., it could be due to TPA, free carrier absorption, RSA, self-focusing, self-defocusing or induced scattering. In conjugated polymeric materials, electrons can move in the molecular orbitals, which results from the linear superposition of the carbon p_z atomic orbitals. This leads to high optical nonlinearity, which increases with conjugation length. On the other hand, nonlinearity is the result of an optimum combination of various factors such as

π-delocalization length, donor– acceptor groups, dimensionality, conformation, and orientation for a given molecular structure. The results indicate that these polymers can be used for optical power limiting at high laser fluences.[47-50]

Here, the third order NLO properties of all the polymers were investigated using z-scan technique.[51] The open aperture (OA) z-scan trace of all the synthesized polymers were carried out. The nonlinear absorption coefficient, β was obtained by fitting the experimental scan plot of the OA measurement to equation (1): [51]

$$T(z) = \frac{C}{q_o\sqrt{\pi}}\int_{-\infty}^{\infty} \ln(1 + q_o e^{-t2})dt \quad \text{.....(5.1)}$$

where, $q_{o(z,r,t)} = \beta I_o(t)\ L_{eff}$ and $L_{eff} = {(1 - e^{-\alpha l})}/{\alpha}$ the effective thickness with linear absorption coefficient, α and 'I_0' is the irradiance at focus. The imaginary part of the third order susceptibility is given by the equation (2): [51]

$$I_m = \frac{n_o^2\ C^2\beta}{240\pi^2\omega} \quad \text{.....(5.2)}$$

where, n_o is the linear refractive index of the polymer solution, 'c' is the velocity of light in vacuum, 'ω' is the angular frequency of radiation used. Closed aperture z-scan technique was carried out to determine the sign and magnitude of nonlinear refraction (NLR) property of the polymers. The NLR z-scan curve after excluding nonlinear absorption effects was obtained from the ratio of closed aperture normalized z-scan data to the

corresponding normalized open aperture data. The normalized transmittance, T(z) for NLR is given by the equation, [51]

$$T_z = 1 - \frac{4x\Delta\emptyset_o}{(x^2+9)(x^2+1)} \quad \text{.....(5.3)}$$

where T(z) is the normalized transmittance for the pure refractive nonlinearity at different z, Φ_0 , is on- axis nonlinear phase shift and x is given by z/z_0 . The nonlinear refractive index (n_2), the real parts of $\chi^{(3)}$ (Re $\chi^{(3)}$) and third order nonlinear susceptibility ($\chi^{(3)}$) are calculated by the following equations. [51]

$$n_2(esu) = \frac{en_o}{40\pi}\gamma \quad \text{.....(5.4)}$$

$$Re\ \chi^3 = \frac{n_o\, n_2}{3\pi}\ (esu) \quad \text{.....(5.5)}$$

$$\chi^{(3)} = Re\ \chi^{(3)} + iI_m X^{(3)} \quad \text{.....(5.6)}$$

where, 'γ' is the molecular cubic hyperpolarizability of the polymer which can be estimated through the equations $\gamma = \frac{\Delta n_o}{I_o}$ and $\Phi\Delta n_o = \frac{\Delta\Phi_o}{kL_{eff}}$ where, 'k' is the wave vector.

a) Fluorene-Quinoxaline polymers

The open –aperture (OA) z-scan trace of the three polymers P(FQ-A), P(FQ-B) and P(FQ-P) in $CHCl_3$ is shown in figure 5.4.

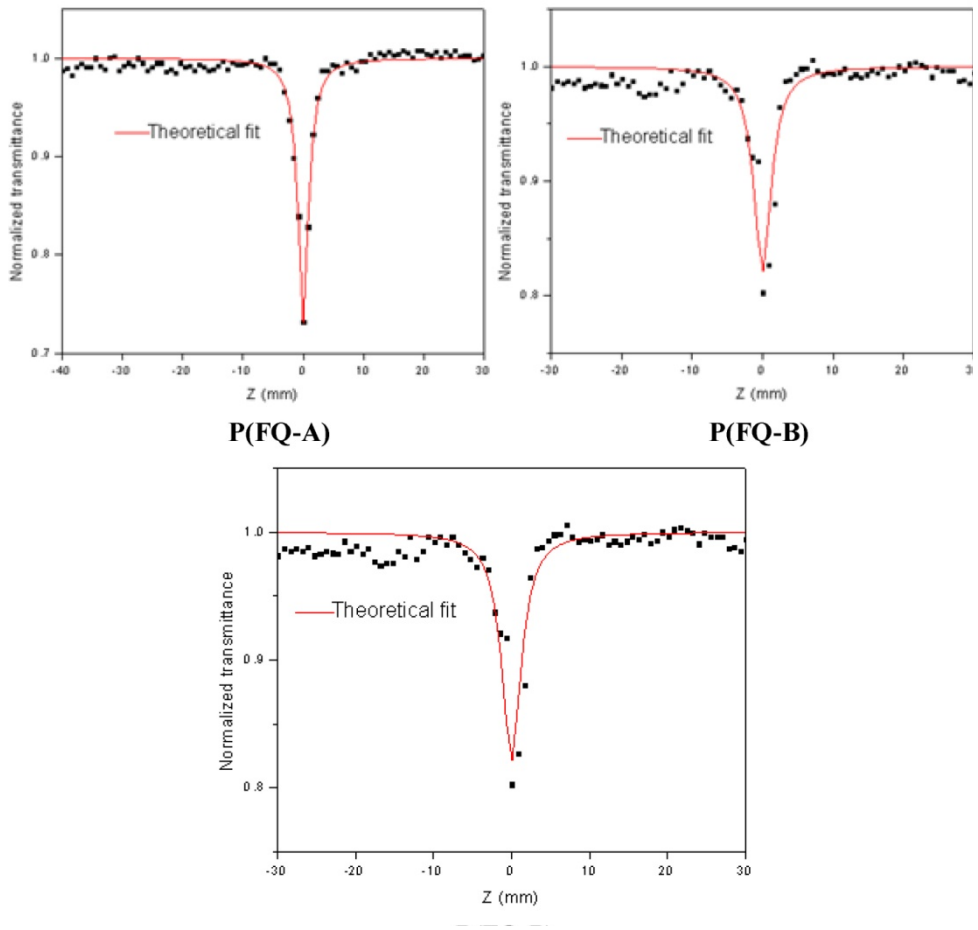

Fig. 5.4: Open aperture z-scan traces of the polymers: a) P(FQ-A), (b) P(FQ-B) and (c) P(FQ-P). (Energy of the laser is 100 µJ)

Here, the three polymers show a normalized transmittance valley, indicating that the polymers behave as reverse saturation absorber (RSA) with a positive NLO absorption coefficient. The nonlinear absorption of the three copolymers were fitting well with two photon absorption (TPA). The calculated values of nonlinear absorption coefficient (β, m/W) and imaginary value of third order nonlinear susceptibility ($\chi^{(3)}$ esu) are given in the

table 5.1. The polymers show large optical nonlinearity due to strong delocalisation of π electrons.

Table 5.1: Nonlinear absorption coefficient (β, m/W), imaginary value of third order nonlinear susceptibility (Im $\chi^{(3)}$ esu) and optical limiting threshold (GW/cm^2) of copolymers

Polymer	β * 10^10 (m/W)	Im $\chi^{(3)}$ * 10 ^ 9 (esu)	Optical limiting threshold (GW/cm^2)
P(FQ-A)	8.32	0.79	0.47
P(FQ-B)	5.32	0.69	0.48
P(FQ-P)	7.86	1.04	0.47

Optical limiting

Recently, Conducting polymers have drawn significant attention as optical limiters for eyes or for sensor protection from laser or laser threats on the battle-field. Optical limiters are devices that transmit light at low input fluences or intensities, but become opaque at high inputs. The optical limiting property occurs mostly due to absorptive nonlinearity, which corresponds to the imaginary part of third-order susceptibility. An important term in the optical limiting measurement is the limiting threshold. It is obvious that the lower the optical limiting threshold, the better the optical limiting material. The nonlinear optical properties of conducting polymers are of great interest for optical switching, pulse power shaping of an OPO (optical parametric oscillator)/OPG (optical parametric generator), and other nonlinear optical applications. However, the great potentials of conducting polymers as optical power limiters have just begun to be recognized. Optical limiting experiment was carried out

at 532 nm using OA z-scan technique. Fig 5.6 shows the transmitted energy of the polymers P(FQ-A), P(FQ-B) and (c) P(FQ-P). Here the three polymers show comparable optical limiting threshold values (Table 5.1).

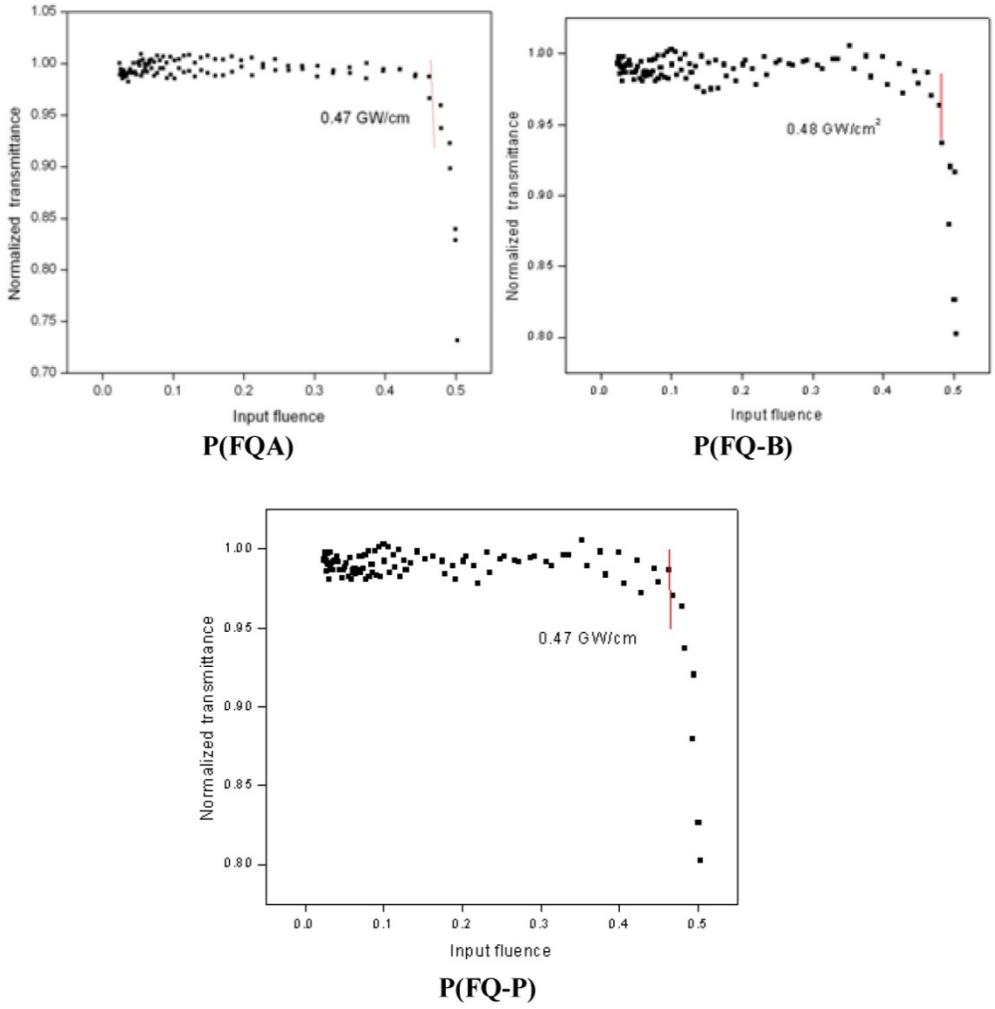

Fig. 5.6: Optical limiting curves of the polymers a) P(FQ-A), (b) P(FQ-B) and (c) P(FQ-P).

b) Fluorene-thiophene copolymer

The open –aperture (OA) and closed aperture z-scan trace of the two polymers P(FMT), and P(EF) in $CHCl_3$ were taken. Fig 5.7 presents the open aperture z-scan traces of the copolymers. The solid curves in the figure are the theoretical fit to the experimental data.

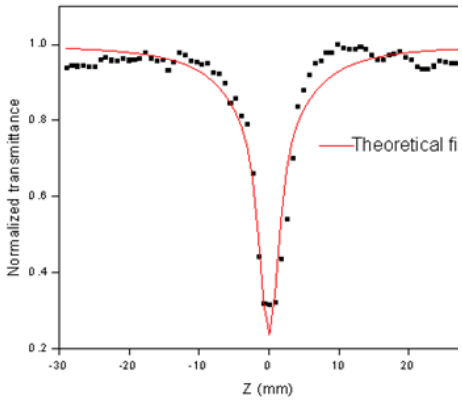

P(FMT) **P(EF)**

Fig. 5.7: Open aperture z-scan traces of the polymers P(FMT) and (c) P(EF). (Energy of the laser is 100 μJ).

Here the open aperture z-scan traces of the polymers show normalized valley, indicating the presence of reverse saturation absorption (RSA) with a positive coefficient. It is seen that the experimental curve is fitted well with two photon absorption theory. The calculated values of nonlinear absorption coefficient (β, m/W) and the imaginary part of third order nonlinear susceptibility ($\chi,^{(3)}$ esu) are given in the table 5.2. From the table it is clear that two polymers show comparable third order nonlinear response. In donor-acceptor polymers nonlinearity is mainly due to strong delocalisation of π electrons.

Table 5.2: Nonlinear absorption coefficient (β, m/W), imaginary value of third order nonlinear susceptibility (Im $\chi^{(3)}$ esu) and optical limiting threshold (GW/cm^2) of copolymers

Polymer	β * 10^10 (m/W)	Im $\chi^{(3)}$ * 10 ^ 9 (esu)	Optical limiting threshold (GW/cm^2)
P(FMT)	12.93	1.72	0.32
P(EF)	12.98	1.86	0.35

The nonlinear refractive (NLR) property of the copolymers were also investigated using closed aperture method. After excluding the nonlinear absorption effects, the pure NLR z-scan curves can be obtained by dividing the closed aperture z-scan data by corresponding open aperture data.

The polymers P(FMT) and P(EF) show the transmittance maximum followed by valley pattern The copolymers show strong self defocussing behaviour and negative nonlinear refraction coefficient, n_2. Here nonlinear refractive index n_2, the real part of $\chi^{(3)}$ and the third order nonlinear susceptibility were also calculated by using the equations 4-6.

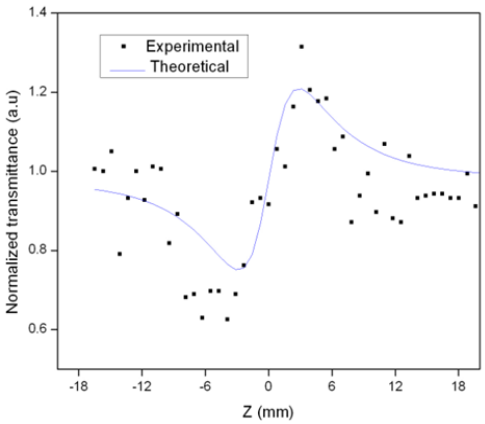

P(FMT) **P(EF)**

Fig. 5.8: Closed aperture z-scan traces of the polymers P(FMT) and (c) P(EF). (Energy of the laser is 100 μJ)

Optical limiting

Optical limiting experiment was carried out at 532 nm for the polymers P(FMT) and P(EF) using OA z-scan technique. The deviation from linearity is taken as the optical limiting threshold. Here the optical limiting threshold values of the polymers P(FMT) and P(EF) are 0.48 GW/cm^2 and 0.35 GW/cm^2 respectively as shown in figure 5.9 and Table 5.2.

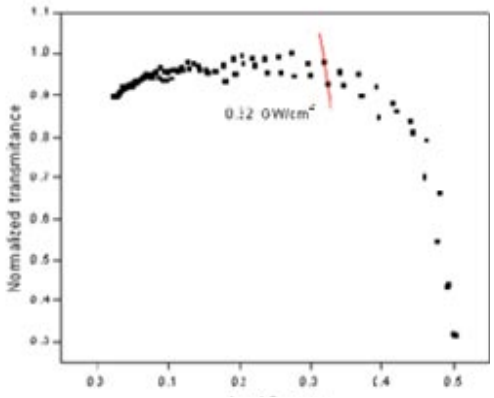

P(FMT) **P(EF)**

Fig. 5.9: Optical limiting curves of the polymers P(FMT) and (c) P(EF).

c) EDOT based polymers

The open –aperture (OA) z-scan trace of P(EHT) and P(EC) in $CHCl_3$ is shown in figure 5.10. Here the copolymers show a normalized transmittance valley, showing reverse saturation type of absorption with positive NLO absorption coefficient. The normalised transmittance for open aperture z-scan was calculated. The theoretical curves obtained with the equation 3 (Section 5.2.2) were fitted with the experimental data for RSA. The nonlinear absorption coefficient (β, m/W) and the imaginary part of third order nonlinear susceptibility ($\chi^{(3)}$ esu) were calculated. The results are given in Table 5.3.

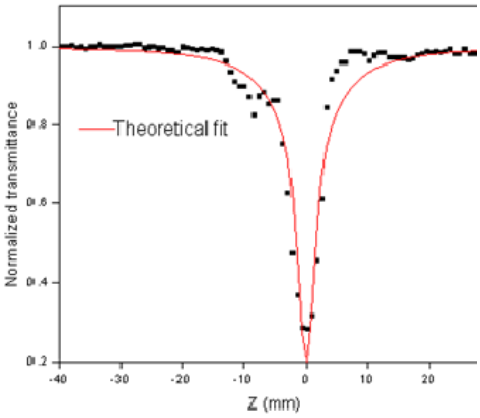

P(EHT) P(EC)

Fig. 5.10: Open aperture z-scan traces of the polymers P(EHT) and (c) P(EC). (Energy of the laser is 100 µJ).

Table 5.3: Nonlinear absorption coefficient (β, m/W), imaginary value of third order nonlinear susceptibility (Im $\chi^{(3)}$ esu) and optical limiting threshold (GW/cm^2) of copolymers

Polymer	β * 10^10 (m/W)	Im $\chi^{(3)}$ * 10 ^9 (esu)	Optical limiting threshold (GW/cm^2)
P(EHT)	13.15	2.73	0.38
P(EC)	12.35	1.62	0.28

In the closed aperture z-scan technique, P(EC) shows the transmittance maximum followed by valley pattern. It exhibits strong self defocussing behaviour and negative nonlinear refraction coefficient, n_2. Here nonlinearity is mainly due to charge transfer from donor to acceptor ie., due to strong delocalisation of π- electrons. The nonlinear refractive index n_2, the real part of $\chi^{(3)}$ and the third order nonlinear susceptibility values were also calculated and is shown in Table 5.6. For the closed aperture z-scan of polymer P(EHT), the signal obtained did not fit well in the theoretical curve.

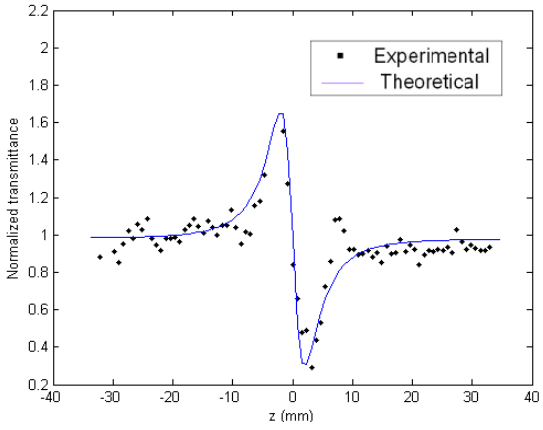

P(EC)

Fig. 5.11: Closed aperture z-scan traces of the polymers P(EC). (Energy of the laser is 100 µJ).

Optical limiting

Figure 5.12 shows the transmitted energy of copolymers as a function of input fluence. The optical limiting process occurs mostly due to nonlinear absorption. When the energy reaches optical limiting threshold, the transmitted energy starts to deviate and exhibits an optical limiting effect. Here the optical limiting threshold values of the polymers P(EHT) and P(EC) are 0.47 GW/cm^2 and 0.48 GW/cm^2 respectively (Table 5.3).

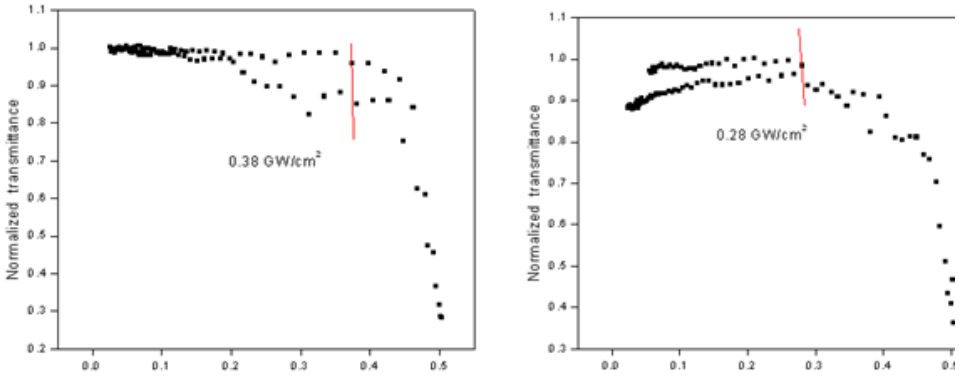

P(EHT) **P(EC)**

Fig. 5.12: Optical limiting curves of the polymers P(EHT) and (c) P(EC).

d) Cyanovinyline based polymers

Here, the three polymers (P(CN1), P(CN2) and P(CN3) show normalized valley in the open aperture z-scan technique , indicating that the polymers are behaving as reverse saturation absorber (RSA) with a positive NLO absorption coefficient (Figure 5.13). The nonlinear absorption of the three copolymers was fitting well with the two photon absorption (TPA). The calculated values of nonlinear absorption coefficient (β, m/W) and imaginary value of third order nonlinear susceptibility (χ, $^{(3)}$ esu) are given in the table 5.4.

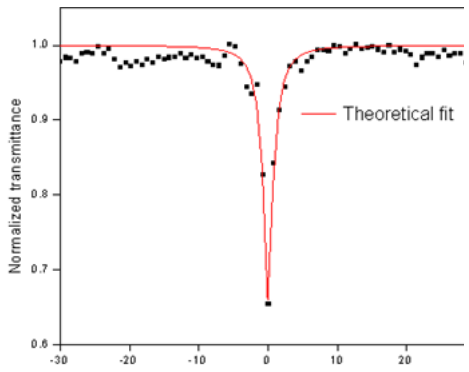

P(CN1) P(CN2)

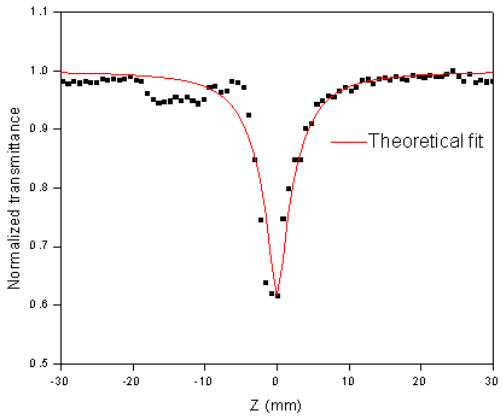

P(CN3)

Fig. 5.13: Open aperture z-scan traces of the polymers P(CN1), P(CN2) and P(CN3). (Energy of the laser is 100 µJ).

Table 5.4: Nonlinear absorption coefficient (β, m/W), imaginary value of third order nonlinear susceptibility (Im $\chi^{(3)}$ esu) and optical limiting threshold (GW/cm^2) of copolymers

Polymer	β * 10^10 (m/W)	Im $\chi^{(3)}$ * 10 ^ 9 (esu)	Optical limiting threshold (GW/cm^2)
P(CN1)	9.47	1.25	0.47
P(CN2)	10.36	1.38	0.37
P(CN3)	2.53	0.34	0.45

The nonlinear refractive (NLR) property of the copolymers were also investigated using closed aperture method. After excluding the nonlinear absorption effects, the pure NLR z-scan curves can be obtained by dividing the closed aperture z-scan data by corresponding open aperture data.

The polymer P(CN1) and P(CN2) show the transmittance maximum followed by valley pattern The copolymers show strong self-focussing behaviour and negative nonlinear refraction coefficient, n_2. Here nonlinear refractive index n_2, the real part of $\chi^{(3)}$ and the third order nonlinear susceptibility were also calculated using the equations. The results show that the polymers show good nonlinear optical response and can be ideal candidates for nonlinear optical devices.

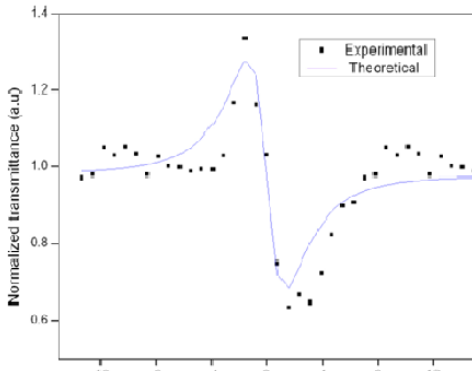

P(CN1) P(CN2)

Fig. 5.14: Closed aperture z-scan traces of the polymers P(CN1) and P(CN2) (Energy of the laser is 100 µJ).

Optical limiting

To investigate the optical limiting threshold of the polymers P(CN1), P(CN2) and P(CN3) open aperture z-scan technique was used. Optical limiting property of a material is mainly due to absorptive nonlinearity, is the result of a combination of factors such as extent of conjugation, donor-acceptor groups, dimensionality, conformation and orientation. As shown in figure 5.15, the optical limiting threshold values for the polymers P(CN1), P(CN2) and P(CN3) are 0.47 GW/cm^2, 0.37 GW/cm^2 and 0.45 GW/cm^2 respectively (Table 5.4). The results show that the polymers can be used for optical power limiting at high laser fluences.

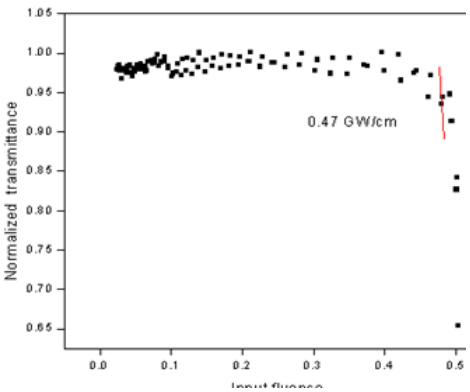

P(CN1)

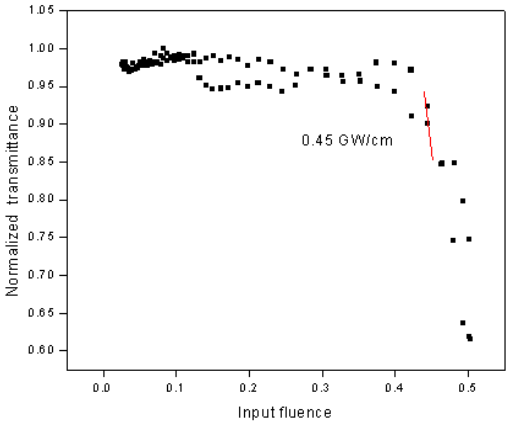

P(CN2)

P(CN3)

Fig. 5.15: Optical limiting curves of the polymers P(CN1), P(CN2) and P(CN3).

e) Phenylene based polymers

The third order NLO properties of phenylene based polymers were also investigated using z-scan technique. The open aperture z-scan traces of the three polymers in chloroform is given in the fig 5.16. From the plot it is clear that the three polymers show reverse saturable absorption. The nonlinear absorption coefficient (β, m/W) is obtained by fitting the experimental data using the equation 1 and imaginary value of third order nonlinear susceptibility ($\chi^{(3)}$ esu) is also calculated and is shown in Table 5.5.

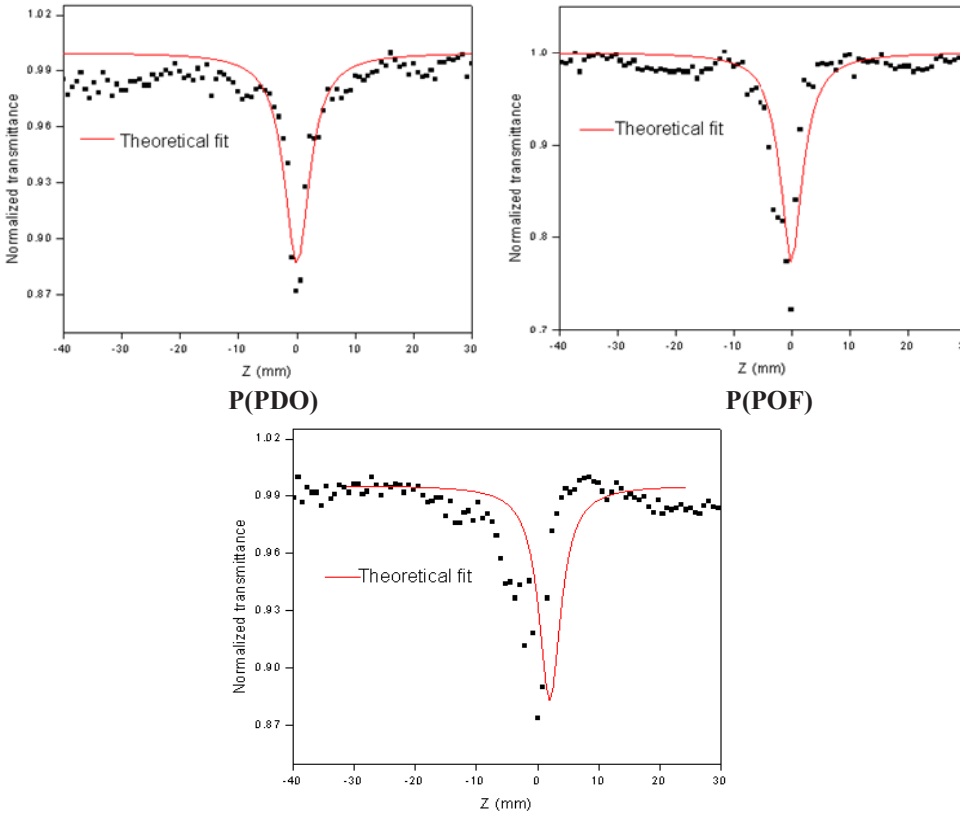

Fig. 5.16: Open aperture z-scan traces of the polymers P(PDO), P(POF) and P(PF). (Energy of the laser is 100 µJ).

Table 5.5: Nonlinear absorption coefficient (β, m/W), imaginary value of third order nonlinear susceptibility (Im $\chi^{(3)}$ esu) and optical limiting threshold (GW/cm^2) of copolymers

Polymer	β * 10^10 (m/W)	Im $\chi^{(3)}$ * 10 ^9 (esu)	Optical limiting threshold (GW/cm^2)
P(POD)	3.0	0.50	0.40
P(POF)	6.93	9.24	0.43
P(PF)	8.02	1.06	0.43

Optical limiting

Optical limiters are devices designed to have high transmittance for low level inputs, while blocking the transmittance for high intensity laser beams.

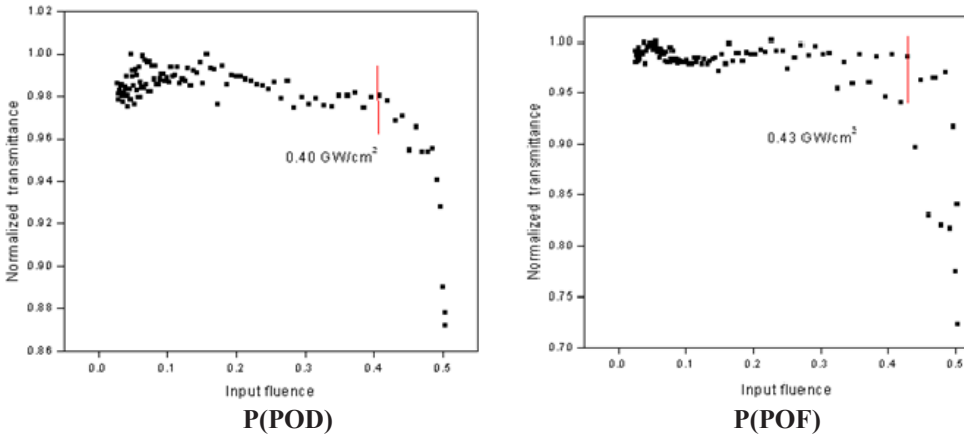

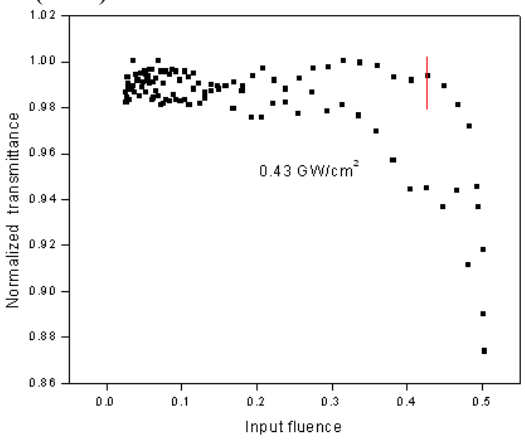

Fig. 5.17: Optical limiting curves of the polymers P(PDO), P(POF) and P(PF)

Molecules that exhibit reverse saturable absorption (RSA) show strong limiting behavior. Here the optical limiting property of the polymers P(PDO), P(POF) and P(PF) were studied and is shown in figure 5.17 and Table 5.5. All the polymers show comparable optical limiting property and are promising candidates for future optical limiters.

In closed aperture z-scan, only five polymers exhibited peak-valley characteristics, indicating the negative NLR index due to self defocussing. The nonlinear refraction coefficient (n_2) and the real value of third order nonlinear susceptibility ($\chi^{(3)}$) of these polymers were calculated and are given in table 5.6.

Table 5.6: Nonlinear refractive index n_2 (esu), imaginary value of third order nonlinear susceptibility (Im$\chi^{(3)}$ esu), real part nonlinear susceptibility Re $\chi^{(3)}$(esu) and Nonlinear susceptibility $\chi^{(3)}$ (esu) of copolymers

Polymer	Nonlinear refractive index n_2*10^9 (esu)	Imaginary part of nonlinear Susceptibility Im$\chi^{(3)}$*10^9 (esu)	Real part of nonlinear susceptibility Re $\chi^{(3)}$*10^9 (esu)	Nonlinear susceptibility $\chi^{(3)}$ *10^9 (esu)
P(CN1)	-0.11	1.25	-0.02	1.56
P(CN2)	-0.12	1.38	-0.02	1.37
P(EC)	-0.27	1.62	-0.04	1.62
P(EF)	-0.14	1.86	-0.02	1.86
P(FMT)	-0.25	1.72	-0.04	1.72

5.3 Conclusion

Photovoltaic and NLO properties of all the synthesized copolymers were evaluated. Of these polymers, P(FMT) showed good photovoltaic activity with device structure of ITO/In_2S_3/P(FMT)/Ag. Third order nonlinear optical studies were also conducted for all the thirteen polymers. It was found that all the synthesised donor-acceptor conjugated polymers showed good third order nonlinear optical properties because of the strong intramolecular charge transfer between the donor and the acceptor units. All

the copolymers showed optical power limiting behaviour at 532 nm. Thus all the synthesised polymers can be used as ideal candidates in nonlinear optical applications.

References

[1] U. Lange, N. V. Roznyatovskaya, V. M. Mirsky, Anal. Chim Acta, 2008, 614, 1.

[2] J. J. M. Halls, C. A. Walsh, N. C. Greenham, E. A. Marseglia, R. H. Friend, S. C. Moratti, A. B. Holmes, Nature, 1995, 376, 498.

[3] A. Kraft, A. C. Grimsdale, A. B. Holmes, Angew. Chem. Int. Edn., 1998, 37, 402.

[4] A. R. Hepburn, J. M Marshall, J. M. Maud, Synth. Met., 1991, 43 , 2935.

[5] J. C. Dubois, O. Sagnes, F. Henry, Synth. Met., 1989, 28, 871.

[6] J. Roncali, R. Garreau, D. Delabouglise, F. Garnier, M. Lemaire, J. Chem. Soc., Chem. Commun., 1989, 11, 679.

[7] A. Burke, J. Power Sources, 2000, 91, 37.

[8] G. Sonmez, H. Meng, Q. Zhang, F. Wudl. Adv. Funct. Mater., 2003, 13, 726.

[9] K. Gurunathan, A. V. Murugan, R. Marimuthu, U. P. Mulik, D. P. Amalnerkar, Mater. Chem. Phys., 1999, 173, 191.

[10] K. Kaneto, K. Yoshino, Y. Inuishi, Jpn. J. Appl. Phys., 1983, 22, L157.

[11] F. Garnier, G. Tourillon, M. Gazard, J. C. Dubois, J. Electroanal. Chem., 1983, 148, 299.

[12] A. L. Dyer, J. R. Reynolds, ''Handbook of Conducting Polymers'', 3rd edition, CRC Press, Boca Raton, 2007.

[13] T. A. Skotheim, L. E. Ronald, J. R. Reynolds, Handbook of Conducting Polymers, 2nd ed, Marcel Dekker Inc., New York, 1997.

[14] L. Groenendaal, F. Jonas, D. Freitag, H. Pielartzik, J. R. Reynolds, Adv. Mater. 2000, 12, 481.

[15] S. Kirchmeyer, K. Reuter, J. Mater. Chem. 2005, 15, 2077.

[16] A. Eftekhari, Nanostructured Conductive Polymers, Wiley, UK, 2010.

[17] L. Kong, Int. J. Electrochem. Sci., 2015, 10, 982.

[18] M. S. AlSalhi, J. Alam, L. A. Dass, M. Raja, Int J Mol Sci., 2011, 12, 2036.

[19] J. C. Carlberg, O. Inganas, J. Electrochem. Soc.,1997, 144, L61.

[20] P. A. Basnayaka, M. K. Ram, L. Stefanakos, A. Kumar, J. Sci. Res., 2013, 2, 81.

[21] M. A. Rahman, P. Kumar, D. S. Park, Y. B. Shim, Sensors, 2008, 8, 118.

[22] H. Bai, G. Q. Shi, Sensors, 2007, *7*, 267.

[23] H. Yoon, J.Nano Mat., 2013, 3, 524.

[24] H. A. Carlos, A. Esteves, B. Iglesias, W. C. Rosamaria, Li, T. Ogawac, K. Araki, J. Gruber, Sensors and Actuators, 2014, B193, 136.

[25] C. K. Chiang, S. C. Gau, C. R. Fincher Jr., Y. W. Park, M. Diarmid, A. J. Heeger, Appl. Phys. Lett., 1978, 33, 18.

[26] N. S. Saricifitci, A. J. Heeger, H.S. Nalwa, Handbook of Organic Conductive Molecules and Polymers, vol. 1, Wiley, NewYork, 1991.

[27] S. L. Lai, M. Y. Chan, C. S. Lee, S. T. Lee, J. Appl. Phys., 2003, 94, 7297.

[28] C. K. Frederik, A. G Suren, A. Jan, J. Mater. Chem., 2009, 19, 5442.

[29] T. J. Teny, M. C. Meril, C. S. Kartha, K. P. Vijayakumar, T. Abe, Y. Kashiwaba, Sol. Energy Mater. Sol. Cells, 2005, 89, 27.

[30] C. W. Spangler, J. Mater. Chem., 1999, 9, 2013.

[31] P. N. Prasad, B. A. Reinhardt, Chem. Mater., 1990, 2, 660.

[32] B. L. Davies, M. Samoc, Curr. Opin. Solid State Mater. Sci., 1997, 2, 213.

[33] A. Mathy, K. Ueberhofen, R. Schenk, H. Gregorius, R. Garay, K. Mullen, C. Bubeck, Phys. Rev. B, 1996, 53, 4367.

[34] M. Albota, D. Beljonne, J. L. Bredas, J. E. Ehrlich, J. Y. Fu, A. A. Heikal, S. E. Hess, T Kogej, M. D. Levin, S. R. Marder, D. McCord-Maughon, J. W. Perry, H. Rockel, M Rumi, G. Subramaniam, W. W. Webb, X. L. Wu, C. Xu, Science, 1998, 281, 1653.

[35] N. Ooba, S. Tomaru, T. Kurihara, T. Kaino, W. Yamada, M. Takagi, T. Yamamoto, Jpn. J. Appl. Phys., 1995, 34, 3139.

[36] J. E. Ehrlich, X. L. Wu, I. Y. S. Lee, Z. Y. Hu, H. Rockel, S. R. Marder, J. W. Perry, Optics Letters**,** 1997**,** 22, 1843.

[37] H. M. Gibbs, Optical bistability : Controlling Light with Light, Acadamic Press, Orlando, FL, 1985.

[38] P. N. Prasad, D. J. Williams, Introduction to Nonlinear Optical Effects in Molecules and Polymers, Wiley, New York, 1991.

[39] Y. R. Shen, Nonlinear Optics, Wiley, New York, 1984.

[40] M. S. Bahae, A. A. Said, T. H. Wei, D. J. Hagan, E. W.V. Stryland, IEEE Journal of Quantum Electronics, 1990, 26, 760.

[41] D. L. Wise, G. E. Wnek, D. J. Trantolo, T. M. Cooper, J. D. Gresser, Electrical and Optical Polymer Systems, Dekker, New York, 1998.

[42] S. Mathew, A. D. Saran, S. A. Joseph, B. S. Joseph, B. S.Bharadwaj, D. Punj, P. Radhakrishnan, V. P. N. Nampoori, C. P. G. Vallabhan, J. R. Bellare, J Mater Sci : Mater Electron, 2012, 23, 739.

[43] S. Q. Zheng. H. Guang, L. Changgui, P. N. Prasad, J. Mat. Chem., 2005, 15, 3488.

[44] J. L. Bredas, C. Adant, P. Tackx, A. Persoons, M. Pierce, Chem. Rev., 1994, 94, 243.

[45] P. Audebert, K. Kamada, K. Matsunaga, K. Ohta, Chem. Phys. Lett., 2003, 367, 62.

[46] M. S. Bahae, A. A. Said, E. W. Van Stryland, Opt. Lett., 1989, 14, 955

[47] S. Pramodini, Y. N Sudhakar, M. SelvaKumar, P. Poornesh, Laser Phys., 2014, 24 045408

[48] G. S. He, G. C. Xu, P. N. Prasad, B. A. Reinhardt, J. C. Bhatt, A. G. Dillard, Opt. L ett., 1995, 20, 35.

[49] N. K. M. N. Srinivas, S. V. Rao, D. N. Rao, J. Opt. Soc. Am.B, 2003, 20, 2470.

[50] R. L. Sutherland, Handbook of Nonlinear Optics, New York, Dekker, 1996.

[51] M. S. Bahae, A. A. Said, T. H. Wei, D. J. Hagan, E. W. V. Stryland, IEEE Journal of Quantum Electronics, 1990, 26, 760.

.....ൠ.....

Chapter 6

SUMMARY AND OUTLOOK

Conducting polymers play a vital role in advanced communications, computation, guidance, and robotic systems as well as in other high technology systems such as in the area of nonlinear optical devices, solar energy collection and storage etc. In the present work, the aim was to develop polymers which are suitable in optoelectronics. One well-established approach to obtain conjugated polymers with desired optoelectronic properties is based on the strategy of donor–acceptor polymers, which could tune the electronic structure of conjugated polymers. Polymers with a desired energy gap can be obtained by incorporating an electron donating and/or withdrawing unit into the polymer backbone. We have used computational design combined with chemical intuition to predict electronic properties of the donor -acceptor polymers.

We have designed thirteen low band gap donor -acceptor polymers composed of fluorene, thiophene, EDOT and quinoxaline as the core units, with the help of PBC/DFT methods. We have also computed the oscillator strength and activation energy of the designed polymers by employing the Time Dependent- Density Functional Theory (TD-DFT). It is possible to find the polymers with high absorption coefficient by this method, which is an

important factor governing the performance of the polymers. All the designed polymers were synthesised by means of direct arylation polymerisation and Suzuki polycondensation reaction. The theoretical studies prior to synthesis helps to eliminate the unwanted materials before synthesis and also it saves time and cost and can reduce the number of steps involved in the reaction. All the designed polymers were characterised by analytical and spectral methods. Most of the polymers showed very good solubility in common organic solvents like Chloroform, THF and Chlorobenzene. The band gap calculated by means of theoretical methods were in good agreeement with the experimental results.

Table 6.1: Theoretical and Experimental band gap of copolymers

Polymer	Eg (theoretical) eV	Eg (Electrochemical) eV	Eg (Optical) eV
P(FQ-A)	2.57	2.9	2.62
P(FQ-B)	2.6	2.66	2.63
P(FQ-P)	2.43	2.2	2.32
P(FMT)	2.42	2.2	2.11
P(EF)	2.6	2.63	2.63
P(EHT)	2.2	2.5	2.12
P(EC)	2.86	2.25	2.16
P(CN1)	2.62	2.71	2.71
P(CN2)	2.25	2.70	2.28
P(CN3)	2.15	2.0	1.97
P(PDO)	2.86	2.68	2.68
P(POF)	2.73	2.8	2.91
P(PF)	2.68	2.2	2.0

Bilayer heterojunction devices with device structure ITO/In_2S_3/P(FMT)/ Ag were also fabricated. (Figure 6.1). Under white light illumination, the device of P(FMT) exhibited a short circuit current density (Jsc) of 0.69 mA/cm^2 and open circuit voltage (Voc) of 463 mV. The fill factor (FF) and efficiency for P(FMT) were calculated to be 30 and 0.09% respectively. The data suggest that the polymer P(FMT) showed good photovoltaic activity. Other polymers also showed diodic character. But the J-V characteristics were not well resolved.

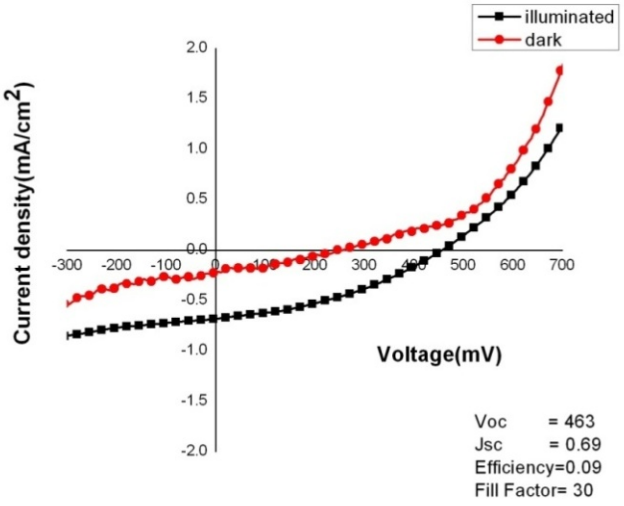

Figure 6.1: J-V characteristics of ITO/In_2S_3/polymer/Ag heterojunctions of P(FMT)

The third order nonlinear optical properties of the copolymers were also investigated by z-scan technique. From the open aperture z-scan it is clear that all the copolymers show reverse saturable absorption. Nonlinear absorption coefficient (β, m/W) and imaginary value of third order nonlinear susceptibility ($\chi^{(3)}$ esu) of all the synthesised polymers were calculated and are given in table 6.2.

Table 6.2: Nonlinear absorption coefficient (β, m/W), imaginary value of third order nonlinear susceptibility (Im $\chi^{(3)}$ esu) and optical limiting threshold (GW/cm^2) of copolymers

Polymer	β * 10^10 (m/W)	Im $\chi^{(3)}$ * 10 ^ 9 (esu)	Optical limiting threshold (GW/cm^2)
P(FQ-A)	8.32	0.79	0.47
P(FQ-B)	5.32	0.69	0.48
P(FQ-P)	7.86	1.04	0.47
P(FMT)	12.93	1.72	0.32
P(EF)	12.98	1.86	0.35
P(EHT)	13.15	2.73	0.38
P(EC)	12.35	1.62	0.28
P(CN1)	9.47	1.25	0.47
P(CN2)	10.36	1.38	0.37
P(CN3)	2.53	0.34	0.45
P(POD)	3.0	0.50	0.40
P(POF)	6.93	9.24	0.43
P(PF)	8.02	1.06	0.43

In closed aperture z-scan, only five polymers exhibited peak-valley characteristics, indicating the negative NLR index due to self defocussing. The nonlinear refraction coefficient (n_2) and the real value of third order nonlinear susceptibility ($\chi^{(3)}$) were calculated and are given in table 6.3.

Table 6.3: Nonlinear refractive index n_2 (esu), imaginary value of third order nonlinear susceptibility (Im $\chi^{(3)}$ esu), real part nonlinear susceptibility (Re $\chi^{(3)}$ esu) and Nonlinear susceptibility ($\chi^{(3)}$ esu) of copolymers

Polymer	Nonlinear refractive index n_2*10^9 (esu)	Imaginary part of nonlinear susceptibility Im$\chi^{(3)}$ *10^9 (esu)	Real part of nonlinear susceptibility Re $\chi^{(3)}$ *10^9 (esu)	Nonlinear susceptibility $\chi^{(3)}$ *10^9 (esu)
P(CN1)	0.11	1.25	0.02	1.56
P(CN2)	0.12	1.38	0.02	1.37
P(EC)	0.27	1.62	0.04	1.62
P(EF)	0.14	1.86	0.02	1.86
P(FMT)	0.25	1.72	0.04	1.72

All the donor-acceptor conjugated polymers show good third order nonlinear optical properties, because of the strong intramolecular charge transfer betwen the donor and the acceptor units. So all the synthesised polymers can be used as ideal candidates in nonlinear optical applications

In short, thirteen copolymers were synthesised and characterised for photovoltaic and NLO applications. Of these polymers P(FMT) showed good photovoltaic activity with device structure of ITO/In_2S_3/P(FMT)/Ag. Third order optical studies were also conducted for all the thirteen polymers and was found that all the copolymers show optical power limiting behaviour at 532 nm. From the studies it is clear that all the synthesised copolymers seems to be ideal candidates for optical applications.